

University of Kentucky

UKnowledge

---

Theses and Dissertations--Physiology

Physiology

---


2022

## EVALUATING THE RELATIONSHIP BETWEEN PLASMA BIOMARKERS AND DEMENTIA USING HIERARCHICAL CLUSTERING ANALYSIS AND LINEAR MODELING

Zachary Winder

University of Kentucky, winder.zachary@uky.edu

Author ORCID Identifier:

 <https://orcid.org/0000-0001-9412-9697>

Digital Object Identifier: <https://doi.org/10.13023/etd.2022.324>

[Right click to open a feedback form in a new tab to let us know how this document benefits you.](#)

### Recommended Citation

Winder, Zachary, "EVALUATING THE RELATIONSHIP BETWEEN PLASMA BIOMARKERS AND DEMENTIA USING HIERARCHICAL CLUSTERING ANALYSIS AND LINEAR MODELING" (2022). *Theses and Dissertations--Physiology*. 59.

[https://uknowledge.uky.edu/physiology\\_etds/59](https://uknowledge.uky.edu/physiology_etds/59)

This Doctoral Dissertation is brought to you for free and open access by the Physiology at UKnowledge. It has been accepted for inclusion in Theses and Dissertations--Physiology by an authorized administrator of UKnowledge. For more information, please contact [UKnowledge@lsv.uky.edu](mailto:UKnowledge@lsv.uky.edu).

## **STUDENT AGREEMENT:**

I represent that my thesis or dissertation and abstract are my original work. Proper attribution has been given to all outside sources. I understand that I am solely responsible for obtaining any needed copyright permissions. I have obtained needed written permission statement(s) from the owner(s) of each third-party copyrighted matter to be included in my work, allowing electronic distribution (if such use is not permitted by the fair use doctrine) which will be submitted to UKnowledge as Additional File.

I hereby grant to The University of Kentucky and its agents the irrevocable, non-exclusive, and royalty-free license to archive and make accessible my work in whole or in part in all forms of media, now or hereafter known. I agree that the document mentioned above may be made available immediately for worldwide access unless an embargo applies.

I retain all other ownership rights to the copyright of my work. I also retain the right to use in future works (such as articles or books) all or part of my work. I understand that I am free to register the copyright to my work.

## **REVIEW, APPROVAL AND ACCEPTANCE**

The document mentioned above has been reviewed and accepted by the student's advisor, on behalf of the advisory committee, and by the Director of Graduate Studies (DGS), on behalf of the program; we verify that this is the final, approved version of the student's thesis including all changes required by the advisory committee. The undersigned agree to abide by the statements above.

Zachary Winder, Student

Dr. Donna M. Wilcock, Major Professor

Dr. Ken Campbell, Director of Graduate Studies

EVALUATING THE RELATIONSHIP BETWEEN PLASMA BIOMARKERS AND DEMENTIA  
USING HIERARCHICAL CLUSTERING ANALYSIS AND LINEAR MODELING

---

DISSERTATION

---

A dissertation submitted in partial fulfillment of the  
requirements for the degree of Doctor of Philosophy in the  
College of Medicine  
at the University of Kentucky

By  
Zachary S. Winder  
Lexington, Kentucky  
Director: Dr. Donna M. Wilcock, Professor of Physiology  
Lexington, Kentucky  
2022

Copyright © Zachary S. Winder 2022  
<https://orcid.org/0000-0001-9412-9697>

## ABSTRACT OF DISSERTATION

### EVALUATING THE RELATIONSHIP BETWEEN PLASMA BIOMARKERS AND DEMENTIA USING HIERARCHICAL CLUSTERING ANALYSIS AND LINEAR MODELING

Alzheimer's disease (AD) and vascular contributions to cognitive impairment and dementia (VCID) are the two leading causes of dementia, and have pathologies which can be evaluated using MRI and protein quantification from cerebral spinal fluid (CSF). However, the high costs of MRIs and the invasiveness of CSF draws limit their utility as screening tools for dementia. Therefore, we must look toward a more cost effective and less invasive screening tool, which leads us to plasma-based biomarkers.

In the first experiment, we compared two models of hierarchical clustering analysis to create plasma profiles of participants with mild cognitive impairment due to VCID. Both models identified a profile consisting of elevated VEGF-A, MMP1, MMP9, and IL-8, which suggests patients with this profile have an increased angiogenic and inflammatory state potentially coinciding with pathological progression. In the second experiment, we evaluated the association between plasma biomarkers and various dementia neuropathologies in an autopsy cohort of participants. In this study, we found that increased angiogenic markers are positively associated with worsening AD neuropathology. Lastly, we evaluated the relationship between plasma biomarkers and cognitive impairment in a longitudinal cohort of participants and found that 6-years post-baseline GFAP and NfL were associated with a decline in verbal memory and verbal fluency, respectively. Interestingly, the anti-inflammatory cytokine, IL-10, was found to be positively associated with both verbal memory and verbal fluency at both 3- and 6-years post-baseline.

Overall, we show how angiogenic and inflammatory plasma biomarkers have the potential to be used as prognostic indicators of both pathology and cognitive impairment. The goal for these markers will be to use them in the clinic to facilitate the diagnosis of dementia and help physicians make more informed predictions about the progression of the disease.

KEYWORDS: Plasma Biomarkers, Alzheimer's Disease, Vascular Cognitive Impairment  
and Dementia, Hierarchical Clustering Analysis, Linear Modeling

Zachary S. Winder

---

05/14/2022

---

Date

EVALUATING THE RELATIONSHIP BETWEEN PLASMA BIOMARKERS AND DEMENTIA  
USING HIERARCHICAL CLUSTERING ANALYSIS AND LINEAR MODELING

By  
Zachary S. Winder

Dr. Donna M. Wilcock

---

Director of Dissertation

Dr. Ken Campbell

---

Director of Graduate Studies

05/14/2022

---

Date

## DEDICATION

To all of those who participate in medical research, who help to cure the many diseases of humanity.

.

## ACKNOWLEDGMENTS

First and foremost, I would like to thank all my teachers and mentors from kindergarten to graduate school, who have helped nurture my passion for learning. I simply do not know where I would be without each one of you. I would also like to thank several people who were instrumental in my graduate school success.

Donna, beginning with our first conversation on my interview day for the MD/PhD program, you made me feel right at home. Every chat and meeting we've had since then has always lifted my spirits no matter the situation and kept me motivated to keep pursuing my goals. Thank you for introducing me to the study of biomarkers and providing me with incredible opportunities to meet with and present my research to other leaders in the field. I am incredibly lucky to have learned from you not only laboratory techniques but also how to work in a larger science team to conduct clinical trials. The experiences I have had under your training are without compare and I am forever thankful for your guidance in helping me down my path to becoming a physician-scientist.

Tiffany, thank you for helping me stay organized and for running all the plasma assays I used in my analyses. Without your help, I would have never been able to complete any of my experiments. Finding someone like you to work with for the rest of my career will be next to impossible and I sincerely appreciate all the help you have given me throughout my time in the lab.



Erica, I'm unbelievably happy you decided to come back to Lexington. I can safely say that all of us graduate students look up to you immensely. Your willingness to help us through any problem (which we know there were many) whether big or small makes you a great mentor to us and we all thank you for it. Thank you for sharing my love of bourbon and trying mellow corn with Charles and I (even though it didn't live up to the hype), and for organizing lab game night despite me still never winning with Pete. You have been an instrumental part in making this graduate experience enjoyable and I cannot thank you enough for that.

Courtney, Charles, and Alex, thank you all for being the best graduate student family I could ask for. Thanks for indulging all my inquiries, scientific and not, and for being there to bounce ideas off. There are far too many memories to list here but I am happy that we got to share them all together and I'm thankful that I was able to make such great friends during graduate school. I could not have asked for a better group of people to hang out with, and I hope that every graduate student finds a family like the one we have.

To the rest of the Wilcock Lab, thank you for putting up with all my shenanigans and for continuing to provide a great working environment necessary to foster our scientific contributions.

To the MD/PhD program, you have all been invaluable in the support you provide to me through our monthly meetings and annual retreat. Being able to learn from the experiences of others who are going down the same path has been extremely helpful for my success.

Chelsey, thank you for being so supportive of me and my chosen career. Since I've met you, you've always been understanding of what I have to do to achieve my goals and you've not only encouraged me to continue to pursue them but also helped me stay organized and focused and pushed me to be the best person that I can possibly be. I love you more than you know, and I can't wait to see what our future has in store.

Sami, Syd, Mom, and Dad, I love you all so much. Words cannot explain how much you all mean to me. You always saw the potential that I had and never stopped believing in what I could accomplish. You are my rocks and are always there to support me through tough times and celebrate with me in my successes. Everything that I achieve, I attribute to all of you.

## TABLE OF CONTENTS

|   |     |
|---|-----|
| ACKNOWLEDGMENTS.....  | iii |
| LIST OF TABLES .....  | ix  |
| LIST OF FIGURES .....   | x   |
| 1 Introduction.....   | 1   |
| 1.1 Overview .....  | 1   |
| 1.2 Alzheimer’s Disease .....   | 2   |
| 1.2.1 Neuropathological Findings .....  | 2   |
| 1.2.2 Biomarkers of Alzheimer’s Disease.....  | 5   |
| 1.2.3 Course of Alzheimer’s Disease.....  | 11  |
| 1.3 Vascular Cognitive Impairment and Dementia.....   | 13  |
| 1.3.1 Clinical Assessment of VCID .....   | 13  |
| 1.3.2 Neuropathological Findings .....  | 15  |
| 1.3.3 Neuroimaging of VCID.....   | 17  |
| 1.3.4 Fluid Biomarkers of VCID .....  | 18  |
| 1.4 Current Research Efforts.....   | 20  |
| 2 Hierarchical Clustering Analyses of Plasma Proteins in Subjects with Cardiovascular Risk Factors Identifies Informative Subsets Based on Differential Levels of Angiogenic and Inflammatory Biomarkers..... | 23  |
| 2.1 Abstract.....   | 23  |
| 2.2 Introduction .....  | 24  |
| 2.3 Methods.....  | 26  |
| 2.3.1 Participants .....  | 26  |
| 2.3.2 Plasma Collection and Quantification.....   | 26  |
| 2.3.3 Plasma Sample Analysis .....  | 29  |
| 2.3.4 Hierarchical Clustering Analysis .....  | 30  |
| 2.3.5 Simulated Data Generation and Analysis .....  | 32  |
| 2.3.6 Statistical Analysis.....   | 33  |
| 2.4 Results.....  | 33  |
| 2.4.1 Study Population Description .....  | 33  |
| 2.4.2 Simulated Data Analysis.....  | 34  |
| 2.4.3 Predicted Distribution Analysis.....  | 35  |
| 2.4.4 Application of Models to Dataset .....  | 36  |
| 2.4.5 Characterizing Cluster Differences .....  | 36  |
| 2.5 Discussion.....   | 37  |

|       |  |     |
|-------|--|-----|
| 3     | Examining the association between blood-based biomarkers and human post-mortem neuropathology in the University of Kentucky Alzheimer’s Disease Research Center autopsy cohort ..... | 52  |
| 3.1   | Abstract .....   | 52  |
| 3.2   | Introduction .....   | 53  |
| 3.3   | Methods .....  | 56  |
| 3.3.1 | Participant Selection and Plasma Collection .....  | 56  |
| 3.3.2 | Plasma Sample Analysis .....   | 56  |
| 3.3.3 | Neuropathology .....   | 57  |
| 3.3.4 | Statistical Analysis .....   | 58  |
| 3.4   | Results .....  | 59  |
| 3.4.1 | Study Participant Characterization .....   | 59  |
| 3.4.2 | Biomarkers for Pathological Hallmarks of Alzheimer’s Disease .....   | 60  |
| 3.4.3 | Biomarkers for Pathological Cerebral Small Vessel Disease .....  | 62  |
| 3.5   | Discussion .....   | 64  |
| 4     | Longitudinal effects of blood based neurodegenerative and inflammatory biomarkers on cognition in the University of Kentucky Alzheimer’s Disease Research Center cohort .....        | 78  |
| 4.1   | Abstract .....   | 78  |
| 4.2   | Introduction .....   | 79  |
| 4.3   | Methods .....  | 81  |
| 4.3.1 | Participant Selection and Plasma Collection .....  | 81  |
| 4.3.2 | Plasma Sample Analysis .....   | 82  |
| 4.3.3 | Cognitive Assessments .....  | 83  |
| 4.3.4 | Statistical Analysis .....   | 83  |
| 4.4   | Results .....  | 84  |
| 4.4.1 | Study Participant Characterization .....   | 84  |
| 4.4.2 | GFAP and NfL are Inversely Associated with Cognition at Six-Years Post-Baseline .....  | 84  |
| 4.4.3 | IL-10 is Positively Associated with Verbal Memory and Verbal Fluency at Three- and Six-Years Post-Baseline .....   | 85  |
| 4.4.4 | Discussion .....   | 86  |
| 5     | Discussion .....   | 96  |
| 5.1   | Overview .....   | 96  |
| 5.2   | Chapter 2 Review .....   | 96  |
| 5.3   | Chapter 3 Review .....   | 99  |
| 5.4   | Chapter 4 Review .....   | 103 |

|     |                              |     |
|-----|------------------------------|-----|
| 5.5 | Limitations.....             | 107 |
| 5.6 | Current Research Focus ..... | 107 |
|     | REFERENCES .....             | 110 |
|     | VITA.....                    | 126 |

## LIST OF TABLES

|   |    |
|---|----|
| Table 1.1 AD Neuropathologic Change Scoring .....   | 22 |
| Table 2.1 MCI-CVD Cohort Demographics and Clinical History .....                                | 40 |
| Table 2.2 Combined HCA Model Cluster Differences .....  | 41 |
| Table 2.3 Euclidean Distance Model Cluster Differences .....                                    | 42 |
| Table 3.1 Sample Size For Each Pathology.....   | 68 |
| Table 3.2 Simoa Biomarker Dilutions.....  | 69 |
| Table 3.3 Participant Characteristics .....   | 70 |
| Table 3.4 Neuropathological Lesion Distribution .....   | 71 |
| Table 3.5 p-Values and Adjusted p-Values for Plasma Biomarkers and AD<br>Neuropathology .....   | 72 |
| Table 3.6 p-Values and Adjusted p-Values for Plasma Biomarkers and cSVD<br>Neuropathology ..... | 74 |
| Table 4.1 Simoa Biomarker Dilutions.....  | 90 |
| Table 4.2 Cognitive Tests Evaluating Cognitive Domains .....                                    | 91 |
| Table 4.3 Participant Characteristics .....   | 92 |

## LIST OF FIGURES

|  |    |
|--|----|
| Figure 2.1 Comparison of HCA Models in Multiple Simulated Datasets .....                           | 43 |
| Figure 2.2 Comparison of HCA Models in Predicted Distributions .....                               | 44 |
| Figure 2.3 Dimensionality Reduction Plots of Clustered Data .....                                  | 45 |
| Figure 2.4 Combined HCA Model Cluster Comparison .....   | 46 |
| Figure 2.5 Euclidean Distance Model Cluster Comparison .....                                       | 47 |
| Figure 2.6 3-D Cluster Comparison .....  | 48 |
| Figure 3.1 Associations of Plasma Biomarkers with Pathological Hallmarks of AD.....                | 76 |
| Figure 3.2 Associations of Plasma Biomarkers with Pathological Hallmarks of cSVD .....             | 77 |
| Figure 4.1 Baseline Plasma GFAP Association with Future Verbal Memory .....                        | 93 |
| Figure 4.2 Baseline Plasma NfL Association with Future Verbal Fluency .....                        | 94 |
| Figure 4.3 Baseline Plasma IL-10 Association with Future Verbal Memory and Verbal<br>Fluency ..... | 95 |

## 1 Introduction

### 1.1 Overview

Dementia is clinically described by the Diagnostic and Statistical Manual of Mental Disorders (DSM-5) as a major cognitive disorder with a significant cognitive decline from a previous level of performance in one or more cognitive domains, which interferes with independent everyday activities[1]. Dementia can be further classified based on both the type of cognitive symptoms seen clinically and the type of neuropathology seen on imaging and at autopsy[2]. While it is widely accepted that the neuropathology seen in dementia patients contributes to the cognitive symptoms seen in clinic, their exact relationship is still unknown[3, 4]. Therefore, it is vital to further study this relationship, especially in the preclinical and prodromal phases of the disease[4]. Biomarkers are increasingly being studied to help clinicians identify in-vivo neuropathology and create criteria for preclinical/prodromal phases of dementia and will ultimately play a major role in the future clinical management of dementia[5, 6]. The leading types of dementia are Alzheimer's Disease (AD) and Vascular Cognitive Impairment and Dementia (VCID) with recent studies suggesting that the majority of dementia patients actually have multiple pathologies occurring simultaneously contributing to their dementia[7, 8]. Patients with multiple brain pathologies have been shown to have an increased likelihood of developing dementia, however the mechanism that underlies this potential synergistic effect is not well understood[9-12]. In this dissertation, I will be focusing on pathologies that underlie the two leading causes of dementia, AD and VCID independently of each other.



## 1.2 Alzheimer's Disease

AD was first described in 1907 by Dr. Alois Alzheimer studying Auguste Deter, a patient suffering from severe memory impairment[5]. On autopsy Dr. Alzheimer found the hallmark pathologies now associated with AD; amyloid plaques and neurofibrillary tangles[5]. Since 1907 these pathologic hallmarks have been extensively studied in the field to advance our understanding, however, our understanding about their initiation remains a mystery[13]. Currently, AD neuropathology can be characterized according to three different evaluation methods (Thal, Braak, and CERAD), each focusing on a different neuropathological finding (amyloid plaques, neurofibrillary tangles, and neuritic plaques – described in more detail below)[14].

### 1.2.1 Neuropathological Findings

#### 1.2.1.1 Amyloid Plaques

Amyloid plaques are extracellular deposits of a fibrillary protein called beta-amyloid (A $\beta$ )[2, 15]. Plaques are composed of aggregated A $\beta$ 1-42, which is more likely to aggregate and form plaque than the more prevalent A $\beta$ 1-40[16, 17]. Excess accumulation of A $\beta$ 1-42 can occur sporadically or as a result of genetic mutations in the amyloid precursor protein (APP) from which the A $\beta$  peptide is cleaved, or presenilin 1 or 2 (PSEN1/2), a component of the  $\gamma$ -secretase complex that cleaves the amyloid precursor protein (APP)[18-22]. Amyloid plaques are scored using the Thal scale which uses the density and location of amyloid plaques to determine disease progression. Thal is scored on a scale of 1-5 where a score of 1 indicates amyloid plaques in the neocortical region, 2 indicates additional amyloid plaques in the allocortical region, 3

indicates additional amyloid plaques in the diencephalic nuclei and the striatum, 4 indicates additional amyloid plaques in distinct brainstem nuclei, and 5 indicates additional amyloid plaques in the cerebellum and additional brainstem nuclei[23]. Thal scoring can also be transformed using the NIA-AA guidelines to a scale of 0 – 3 for meaningful differences in classifications[14]. A $\beta$  deposition as plaques are believed to be the initial step in the amyloid cascade hypothesis which posits that amyloid plaques cause the formation of neurofibrillary tangles and neurodegeneration ultimately leading to cognitive decline[24]. Multiple clinical trials have targeted the formation and removal of A $\beta$  to treat AD, however most of these treatments have failed to show any improvement in their primary cognitive outcome measure[25].

#### 1.2.1.2 Neurofibrillary Tangles

Neurofibrillary tangles are intracellular aggregates of misfolded, abnormally phosphorylated tau protein found within neurons[26-28]. These intracellular tangles have been shown to precede neuronal death and have been linked to cognitive decline in humans[14, 28-30]. Neurofibrillary tangles are evaluated using Braak scoring which uses density and location of tangles to determine staging. Braak scoring is also on a scale of 1 – 6 where stage 1 indicates lesions in the transentorhinal region, stage 2 indicates lesions extending into the entorhinal region, stage 3 indicates lesions that have extended into the neocortex of the fusiform and lingual gyri, stage 4 indicates that the disease process progresses more widely into neocortical association areas, stage 5 indicates that the neocortical pathology extends fanlike in frontal, superolateral, and occipital directions, and reaches the peristriate region, and lastly stage 6 indicates that

the pathology reaches the secondary and primary neocortical areas and, in the occipital lobe, extends into the striate area[31, 32]. NIA-AA guidelines also allow for a transformation to a 0 – 3 scale of disease[14]. Tangles have been targeted in many clinical trials including removal of tau using immunotherapy or inhibition of aggregation using methylene blue, but these trials have also not yet demonstrated any clinical improvement[33].

#### 1.2.1.3 Neuritic Plaques

Neuritic plaques are a combination of amyloid plaques surrounded by dystrophic neurites containing intracellular tau formations[34]. Neuritic plaques are thought to form during a later stage of neurodegeneration and have also been shown to be associated with cognitive decline[14, 35, 36]. Consortium to Establish a Registry for Alzheimer's Disease (CERAD) provides the guidelines for classifying neuritic plaques using a semiquantitative scale of none, sparse, moderate, or frequent[14, 37].

#### 1.2.1.4 AD Neuropathologic Change

Together these three pathologic criteria of amyloid plaques, neurofibrillary tangles, and neuritic plaques, can be combined using the NIA-AA guidelines to determine AD neuropathologic change, consisting of four tiers (Table 1.1). Tiers range from “not” AD neuropathologic change to “high” AD neuropathologic changes. Individuals with cognitive impairment along with “high” or “intermediate” AD neuropathologic change are found to have their impairment sufficiently explained by AD. Patients with cognitive impairment and with “not” or “low” AD neuropathologic change are likely to have an additional pathology resulting in their cognitive decline[14].

## 1.2.2 Biomarkers of Alzheimer's Disease

### 1.2.2.1 Neuroimaging

Antemortem clinical evaluation of AD neuropathology currently relies on neuroimaging and cerebrospinal fluid (CSF)[38-40]. The two main modalities of neuroimaging are magnetic resonance imaging (MRI) and positron emission tomography (PET)[41]. MRI's primary utility is identifying regions of atrophy which, in the case of AD, is often primarily in hippocampus and medial-temporal lobe, along with expanded ventricles[42-44]. These findings although associated with cognitive decline do not have a high specificity for AD[45, 46].

PET imaging is more useful at evaluating specific AD pathologies, predominantly amyloid plaques and neurofibrillary tangles[38]. Specific radioligands were created to evaluate amyloid plaques in 2004; first described by Klunk and colleagues[47], PET amyloid tracers have now been refined and are utilized frequently in research studies and clinical trials[48-51]. Tangle PET ligands were developed later, and at the current time are undergoing refinement for specificity and sensitivity[52]. These tracers have now progressed sufficiently for use in research studies and clinical trials, although not as widely utilized as the amyloid ligands at this point[53-56]. FDG-PET imaging is a third type of PET imaging tool used to evaluate brain health by looking at glucose uptake in the brain. Researchers have found that a reduction in glucose uptake in the posterior cingulate cortex and temporoparietal is associated with cognitive decline, although this is not necessarily specific for AD[41, 44, 57, 58].

Though both MRI and PET remain the gold standard of in-vivo neuropathology, they carry a substantial price tag, especially PET due to the high cost of the radioligands, and they lack accessibility for patients living in medically underserved areas. MRI and PET are primarily used for research purposes, however, there is a growing need for a more inexpensive and accessible tool used for screening individuals at a high risk of developing AD[59].

#### 1.2.2.2 Fluid Biomarkers

Cerebral spinal fluid (CSF) and plasma are two inexpensive and widely accessible samples to collect, which are currently being evaluated to assist physicians in evaluating in-vivo neuropathology in order to both diagnosis and prognosticate a patient's disease[59]. CSF biomarkers are currently the only fluid biomarkers which have been recommended for usage in a clinical setting. While the first plasma biomarker was recently approved for A $\beta$ , p-Tau biomarkers are still in testing phases [40, 60]. In this dissertation, we will focus on three broad groups of fluid biomarkers:

Neurodegenerative, Inflammatory, and Angiogenic.

##### 1.2.2.2.1 Neurodegenerative

The most widely studied group of fluid biomarkers in their association with AD are the neurodegenerative biomarkers. CSF biomarkers for amyloid and tau pathology are currently used clinically to rule in or out AD as the cause of dementia in a patient[61-63]. The ratio of A $\beta$ 42 to A $\beta$ 40 is hypothesized to be the earliest indicator of AD neuropathology[64]. A $\beta$ 42 and 40 are derived from APP which is normally expressed in neurons for normal cellular functions such as neuronal plasticity and response to acute

injury[65]. APP can be cleaved by both  $\alpha$ - and  $\beta$ -secretase to produce non-amyloidogenic fragments, however  $\beta$ - and  $\gamma$ - secretases function to cleave APP into two fragments of varying lengths, especially A $\beta$  42 or A $\beta$  40[65]. A $\beta$  42 has been found to accumulate within amyloid plaques while A $\beta$  40 appears in the vasculature in cerebral amyloid angiopathy[17, 66, 67]. When A $\beta$  42 is measured in CSF it has been found to be decreased in patients with AD due to the inability to remove it from the parenchyma as it has formed dense plaques[68-71]. Plasma A $\beta$  42, on the other hand appears to have mixed results for its relationship to CSF A $\beta$  42 while the ratio of A $\beta$  42/ A $\beta$  40 demonstrates more consistency in having a significant positive relationship between plasma and CSF findings[72-75]. These findings show that plasma quantification of these proteins may provide similar information to that which can be obtained from CSF measurements. The ratio of A $\beta$  42/ A $\beta$  40 in plasma has already been shown to differentiate patients with AD from cognitively normal and non-AD dementia controls, with AD patients with having a significantly lower ratio of A $\beta$  42/ A $\beta$  40 compared with controls across multiple cohorts of patients, which was similarly observed in CSF A $\beta$  42/ A $\beta$  40 ratios[73, 74].

Tau biomarkers measure either phosphorylation independent or dependent tau proteins[59]. Tau is an intraneuronal protein involved in the stabilization of the neuronal cytoskeleton along the axon[27, 76]. Phosphorylation of tau causes conformational changes in tau and detachment from the axon, therefore allowing for cytoskeleton remodeling in normal conditions[27, 77, 78]. In AD, and other tauopathies, neurofibrillary tangles form when tau is hyperphosphorylated and more permanently

detaches from the microtubules, aggregating in the cell body[76]. CSF based phosphorylation independent tau (Total-Tau) has been shown to positively correlate with neurodegeneration, while phosphorylation dependent tau (pTau) is hypothesized to be more disease specific and correlate with different stages of disease depending on the specific tau phospho-epitope[69, 79-81]. Plasma levels of p-tau-181, for example, is significantly increased in patients with AD compared with controls and one study found that it is significantly correlated with levels in the CSF[82]. Such use provides another alternative to the more invasive and expensive CSF protein quantifications at use presently.

Neurofilament light (NfL) is a component of the neurofilament protein, which is found in the axonal cytoskeleton[83]. When neurons are damaged, as in AD, neurofilament is released into the blood and CSF, where it can be quantified and used as a biomarker for evaluating neuronal damage[83]. Studies have been conducted measuring NfL in plasma, serum, and CSF, where NfL levels appeared to be correlated for plasma and CSF as well as serum and CSF[84, 85]. Plasma NfL levels were shown significantly elevated not only in AD compared with controls but also in patients with MCI compared with controls and in AD compared with MCI[83, 84, 86]. Serum NfL also has shown effectiveness as a biomarker in evaluating conversion of asymptomatic AD in autosomal dominant mutation carriers to symptomatic AD based on the rate of serum NfL change. Converters from asymptomatic to symptomatic AD had increased serum NfL change compared with those who remained asymptomatic from baseline to follow-up testing[87]. These studies provide evidence for the continued evaluation of NfL as a

biomarker to both evaluate and monitor disease progression in individuals at risk of developing AD in both the presymptomatic and MCI phases of the disease. NfL, however, is a nonspecific biomarker of accelerated neuronal death and degeneration, so may lack specificity for the AD disease state despite the strong data supporting its use in tracking disease progression[88, 89].

#### 1.2.2.2.2 Inflammatory

Gliosis in the form of activated microglia and astrocytes are prominent pathologic findings in patients with AD, as well as other pathological findings of dementia[90-92]. These activated microglia and reactive astrocytes stimulate an inflammatory phenotype throughout the brain, which has been evaluated in the CSF and plasma[62]. Unlike traditional biomarkers associated with AD, some inflammatory biomarkers have been shown to differentiate patients at different stages of AD and may serve to monitor the progression of the disease. These markers are interesting for their ability to track disease progression but remain in a preliminary stage of study.

TNF $\alpha$  is a protein involved in various inflammatory pathways, often resulting in the upregulation of more downstream cytokines[93-95]. Multiple mouse models of AD have been observed to have increased TNF $\alpha$  expression in the brain, which has also been found to occur in humans as well[93-95]. Early human plasma studies found an increase in TNF $\alpha$  in patients with AD and although this hasn't been fully validated it is hypothesized that TNF $\alpha$  is increased in the plasma of patients with MCI and AD compared to cognitive controls[96]. Interestingly, SNPs in the promoter region of the



TNF $\alpha$  gene that are hypothesized to upregulate TNF $\alpha$  have been found to be associated with an increased risk of developing AD and an earlier age of onset of AD[97, 98].

Reactive astrogliosis is a pathological finding which has been associated with amyloid plaques on human post-mortem tissue[91, 92]. Glial fibrillary acidic protein (GFAP) is a histological marker for reactive astrogliosis and has been found to be upregulated in human brain tissue of patients with AD[99, 100]. Higher levels of GFAP have also been found in the CSF, plasma, and serum of patient with AD[101-103]. Additionally, increased blood-based levels of GFAP have been found to positively associate with amyloid PET burden, inversely associate with MMSE scores, and predict conversion to AD dementia in a longitudinal cohort[104-107]. As a result of the association of GFAP and A $\beta$  pathology, plasma GFAP can potentially be used as an early screening tool for AD along with other more specific plasma biomarkers.

Anti-inflammatory cytokines like IL-10 have also been hypothesized to play a role in reducing the inflammatory response in the development of AD[108]. SNPs in the promoter region of IL-10 have been evaluated for their association with AD, with low-producing SNPs associated with a higher risk of AD[109]. Three SNPs have been evaluated in a meta-analysis independently and as haplotypes and demonstrated that two of the three SNPs have a significant positive association with AD [110]. Haplotype analysis also showed that having all three high-producing IL-10 SNPs resulted in a decreased risk of AD[110, 111]. IL-10 levels in the CSF were also found to be associated with rates of cognitive memory decline, with IL-10 having a significant interaction with time and a positive association with memory z-score adjusted for age, sex, race, and

education[112]. These findings suggest that there is a balance between inflammatory and anti-inflammatory cytokines that can be evaluated using fluid biomarkers.

#### 1.2.2.2.3 Angiogenic

Lastly, angiogenic biomarkers have been studied to determine their association with AD. The results have not been straight forward, some studies have found that vascular endothelial growth factor A (VEGFA) was increased in the CSF of patients with AD, while other studies have found that higher levels of VEGFA decrease hippocampal atrophy, increase FDG-PET SUVR and benefit patient cognition longitudinally who are positive for A $\beta$  and Tau[113-115]. VEGFA belongs to the vascular endothelial growth factor family of proteins which includes other growth factors including placental growth factor (PlGF), as well as their receptors, which are responsible for the growth and management of the vasculature throughout the body[116]. In evaluating gene expression of cognitive controls and patients with MCI and AD, increased expression of PlGF was associated with longitudinal cognitive decline and increased tau burden and neuritic plaques at autopsy[117]. Overall, the VEGF family of protein's role in the development of AD remains elusive but offers multiple potential biomarkers to help physicians better predict the cognitive future of the patient.

#### 1.2.3 Course of Alzheimer's Disease

AD is categorized into three phases of clinical disease: preclinical, mild cognitive impairment, and dementia[118]. The preclinical phase is of substantial interest as it represents patients who are positive for biomarkers of AD yet show no clinical symptoms of cognitive impairment[118]. Criteria for preclinical AD requires a positive

biomarker for amyloid beta pathology and/or neurofibrillary tau tangles while having no cognitive deficits[38]. Individuals in the preclinical AD phase are at an increased risk of developing dementia but some estimate that only between 5% to 42% of amyloid positive individuals in this phase progress to MCI or dementia[119, 120].

MCI is classified as an intermediate step in the development of dementia due to AD. Patients are diagnosed with MCI if they suffer from a cognitive decline from a previous level of cognition while at the same time are able to maintain their social or occupational functioning[38, 121]. In MCI due to AD cognitive decline is often seen through evaluations of episodic memory however the domains affected in MCI are variable[121]. While not recommended cognitive decline can also be evaluated through subjective complaints detailed by an informant on behalf of the patient or through observation by the clinician[120]. Evaluating the influence of AD on MCI can be done through biomarkers. For a patient to have a high likelihood of experiencing MCI due to AD a positive biomarker for amyloid beta is required along with a positive biomarker of neuronal injury which includes those associated with neurofibrillary tangles[38, 120]. Patients with negative biomarkers of amyloid beta or neuronal injury are considered to have MCI unlikely due to AD[38, 120].

The dementia phase of AD begins when the cognitive deficits strongly affect multiple cognitive domains and interfere with a patient's ability to independently care for themselves and affects their activities of daily living[38, 120, 122]. Dementia due to AD can often manifest in with different clinical phenotypes, predominantly the amnesic syndrome of the hippocampal type, however other more atypical phenotypes do exist

such as the posterior cortical atrophy or the logopenic primary progressive aphasia variant[120]. Similar to the criteria for MCI, two positive biomarkers are required for a clinical diagnosis of AD, one for amyloid pathology and the other for tau pathology[38, 120].

### 1.3 Vascular Cognitive Impairment and Dementia

VCID is a leading cause of dementia in the world along with AD and encompasses the full spectrum of disease from MCI to dementia including cases of mixed dementia, often comorbid with AD[123-125]. VCID is a relatively new way to describe dementia as a result of cerebrovascular pathology. Older studies referred to dementia as a result of a major vascular insult as multi-infarct dementia, which subsequently became broadened to vascular dementia to incorporate all dementia which was believed to be the result of both chronic and acute vascular disease[125]. Vascular cognitive impairment (VCI) was introduced in the early 2000s as a term to encompass patients who do not meet the clinical criteria for dementia but are still experiencing cognitive impairment[126]. VCID has since followed as the most common terminology to refer to both the mild cognitive impairment and dementia stages of vascular origin[125].

#### 1.3.1 Clinical Assessment of VCID

Classifying cases of VCID has proved challenging given the various pathological causes of VCID, ranging from acute injuries like stroke to more chronic processes such as arteriolosclerosis and cerebral amyloid angiopathy (CAA). Currently, VCID is broken down into two subtypes, mild and major[127]. Mild VCID is defined as “impairment in at least one cognitive domain and mild to no impairment in instrumental activities of daily

living (IADLs)", while major VCID is defined as "clinically significant deficits of sufficient severity in at least one cognitive domain and severe disruption to IADLs"[127]. Core cognitive domains assessed when evaluating a patient for VCID include executive function, attention, memory, language and visuospatial[126, 127]. Impaired executive function, which is used in processes involving planning, decision making, and working memory, is widely considered to be the key clinical finding in a patient with VCID, and evaluation of executive function can differentiate patients with VCID from those with AD[123, 124, 128]. Assessment tools for fluency (semantic and phonemic) have also been shown to differentiate VCID and AD with AD patients demonstrating lower levels of semantic fluency compared to phonemic fluency and patients with VCID demonstrating the opposite phenomena[123, 129, 130].

Major VCID is further broken down into four additional subdivisions: post stroke dementia, subcortical ischemic vascular dementia (SIVaD), multi-infarct (cortical) dementia, and mixed dementias[127]. Post stroke dementia occurs when patients experience cognitive impairment within 6 months of a stroke that persists. This is similar to, and can occur alongside, multi-infarct dementia, a term used when there are multiple large cortical infarcts likely contributing to the dementia[127]. SIVaD encompasses pathologies such as lacunar infarcts and white matter lesions which often occur subcortically[131]. Cerebral small vessel disease (cSVD) is the major cause of SIVaD pathology and is estimated to occur in 40-50% of cases of major VCID[128, 132].

Diagnosis of VCID currently relies on the usage of neuroimaging to evaluate the brain changes in-vivo alongside a cognitive impairment as discussed earlier[127, 133]. A

diagnosis of probable VCID can be made when vascular lesions are identified either through MRI, or CT if MRI is unavailable. A diagnosis of possible VCID is made if all neuroimaging is unavailable and suspicion of vascular lesions is high[127].

### 1.3.2 Neuropathological Findings

VCID neuropathology has been found to affect both the cerebrovasculature and the parenchyma of the brain[123, 131]. Vascular pathologies focus on damage to vessels of all sizes within the brain and includes arteriolosclerosis, cerebral amyloid angiopathy (CAA) and large artery occlusions[123, 128]. Brain parenchymal lesions occur in both gray and white matter regions and range from small silent lesions to large infarctions and bleeds. Types of lesions include white matter lesions, lacunar infarcts, microinfarcts, microbleeds, white/gray matter atrophy, and large cortical infarctions[123, 128].

Cerebral small vessel disease (cSVD) is a disease that affects all the small vessels of the brain (arterioles, capillaries, venules) and encompasses the pathology in the vasculature as well as the resulting parenchymal damage[134]. Two of the most common vascular pathologies in cSVD are arteriolosclerosis and CAA[134-136].

Arteriolosclerosis is characterized by the deposition of fibro-hyaline in the lining of the blood vessel with subsequent loss of smooth muscle cells resulting in a narrowed lumen and thickened vessel[137]. Hypertension has been shown to be a leading risk factor for the development of arteriolosclerosis along with age[137]. Arteriolosclerosis is graded on an ordinal scale of 0-3 with a grade of 0 indicating no arteriolosclerosis, 1 as mild, 2 as moderate, and 3 as severe[135-137]. As severity of arteriolosclerosis increases, the basement membrane thickens, and the vessel lumen begins to reduce. This can cause

cerebral blood flow to become dysregulated, resulting in downstream hypoperfusion causing endothelial cells within capillaries to undergo apoptosis. This resultant loss in capillaries is marked by the observation of string vessels, containing only the remnant basement membrane from the previous capillaries[138, 139]. Additionally, arteriosclerotic changes can cause the vessels to lose elasticity affecting their ability to dilate and constrict, when necessary, in autoregulation of cerebral blood flow[137]. This capillary damage ultimately alters perfusion to regions surrounding the vasculature producing tissue pathology such as microinfarctions, lacunar infarcts, microhemorrhages, and leukoaraiosis[137, 138]. Arteriosclerosis has been found to increase the odds of dementia in older persons even after adjusting for parenchymal pathologies such as microinfarctions and hemorrhages[140, 141]. This demonstrates that the effect of arteriosclerosis on cognitive impairment is still not completely known, with hypotheses of subthreshold parenchymal pathology and reduced cerebral perfusion causing this effect[128].

CAA is another vascular pathology found in cSVD. CAA differs from arteriosclerosis in that it primarily affects small to medium cortical and leptomenigeal arterioles and arteries where amyloid beta is deposited into the vessel wall[123]. CAA can be graded using a similar ordinal scale as arteriosclerosis from 0-3, with 0 indicating no CAA, 1 as mild, 2 as moderate, and 3 as severe[136]. Ultimately, CAA can lead to loss of vessel compliance and decreased cerebral reactivity which is similar to the impact seen of arteriosclerosis. Importantly, CAA has also been

associated with increased cortical microinfarctions, intracerebral and lobar hemorrhages, and cortical microbleeds[123].

Microinfarctions are one of the parenchymal tissue findings in patients with cSVD[123, 131, 142]. As their name implies, microinfarctions are smaller than gross infarctions and generally must be seen using a microscope with sizes often smaller than 1 mm[123, 131, 142]. Microinfarctions can be found cortically and subcortically, and it is hypothesized that different vasculature pathologies contribute to regional differences in microinfarctions, with CAA causing cortical lesions while arteriolosclerosis may play more of a role in subcortical microinfarctions[123, 131, 142-146]. On autopsy, microinfarctions have been found to be ubiquitous in both cognitively normal and patients with dementia, however increased observed quantities of microinfarctions have been associated with increased odds of dementia and cognitive impairment[147-153]. As there are often countless numbers of microinfarctions, a sampling of tissue sections is used to estimate the number of microinfarctions found in the entire brain with it hypothesized that every microinfarction observed represents hundreds of microinfarctions present within the brain[154].

### 1.3.3 Neuroimaging of VCID

Cerebral microbleeds and white matter lesions (WMLs) are two pathologies that result from cSVD that are most visible using MRI[132]. Cerebral microbleeds are small hypointense foci on T2\* weighted scans[155]. They are hypothesized to form as a result of broken-down iron deposits from erythrocyte derived hemosiderin which leaked from the vasculature[156-158]. Cerebral microbleeds have been shown to have a positive



association with CAA and it was widely hypothesized that there is a causal relationship between the two[156-158]. Studies have also shown that patients with more microbleeds are at an increased risk of not only having dementia but also of future cognitive decline.

WMLs or white matter hyperintensities (WMHs) are hyperintense regions within the white matter on T2 weighted MRI, and are lesions predominantly associated with reduced cerebral blood flow and vascular pathology[155, 156, 159]. The pathogenesis of WMHs is still unknown, but WMH regions have been shown to have increased blood brain barrier breakdown, demyelination, axon loss, and gliosis and may be the initial evidence of tissue breakdown in patients with SVD[156, 159-164]. WMHs are also associated with cognitive decline and an increased risk of dementia, although the findings of WMHs are not specific for VCID as cognitively normal and patients with AD may also have WMHs on MRI[159, 164-168].

#### 1.3.4 Fluid Biomarkers of VCID

In comparison to AD, VCID is lacking in fluid-based biomarkers, likely due to the many different pathologies which underlie VCID[169]. However, fluid-based biomarkers have still been studied and leverage two pathological processes that underlie most VCID pathologies: endothelial dysfunction and inflammation.

Hypoperfusion resulting from cSVD-related endothelial dysfunction induces a local hypoxic environment in the parenchyma triggering an angiogenic response[170, 171]. Angiogenesis begins when the hypoxic environment inhibits the breakdown of hypoxia inducible factor 1-alpha (HIF1 $\alpha$ ), allowing HIF1 $\alpha$  to bind hypoxia response

elements in the DNA, ultimately upregulating vascular growth factors such as placental growth factor (PlGF) and VEGFA[172, 173]. PlGF serves to facilitate angiogenesis by acting through vascular endothelial growth factor receptor 1 (VEGFR1)[116]. This mechanism that involves PlGF is active in both physiologic and pathologic cases of hypoxia, appearing in the former role during placental growth and in the latter role in cases of tumor angiogenesis and cerebral ischemia[174]. Interestingly, low levels of free PlGF have predictive value in assessing pre-eclampsia, a disorder characterized by hypertension likely as a result of decreased uterine perfusion pressure in pregnant woman[175, 176]. Further, mouse models of pre-eclampsia have demonstrated that matrix metalloproteinases (MMPs) 2 and 9 are significantly decreased when free levels of PlGF are decreased as well but can be rescued via a supplementation of PlGF[176]. This provides evidence for PlGF's role in upregulation of matrix metalloproteinases (MMPs) MMP2 and MMP9, which have also been implicated in development of microhemorrhages in a mouse model of SVD[177]. In the context of cognitive impairment, increased RNA expression of PlGF and VEGFA in the brain correlated to decreases in longitudinal cognition and increased odds of having AD and VCID[117].

Inflammatory fluid biomarkers have also been hypothesized to be associated with VCID pathology, particularly IL-6, which has been shown to have a positive association with WMHs[169, 178]. IL-6 is a pro-inflammatory cytokine produced by microglia and the tunica muscularis cells of the blood vessels[169, 179, 180]. It is hypothesized that one mechanism for IL-6 to exert its effect on VCID is through the upregulation of c-reactive protein (CRP) in the liver, which increases blood brain barrier

permeability[169, 181]. In CSF studies of IL-6 in patients with VCID and AD, IL-6 levels were higher in patients with vascular dementia compared to AD and VCI, and in plasma studies higher levels of IL-6 were associated with decreased functional ability in patients with dementia[182-184]. Additionally, in a hyperhomocysteinemia induced mouse model of VCID, increased expression of IL-6 was seen in brain tissue[177].

#### 1.4 Current Research Efforts

One of the biggest hurdles in developing novel treatments for dementia is in identifying patients who are at risk of developing dementia to prevent further cognitive impairment[4, 6]. Neuropsychological exams allow clinicians to evaluate the current level of cognitive impairment a patient may have[2, 38, 128]. Physicians can also visualize a patient's AD and VCID neuropathology using in-vivo PET imaging and MRI assessments[2, 38, 128]. However, both of these tools are expensive and require specialized facilities to perform the assessments which limits accessibility to many patients[40, 59]. While CSF is a more cost-efficient alternative for AD evaluations it is still invasive to patients and not suitable as a tool for annual screenings for large demographics of patients[40, 59]. This presents an opportunity for the usage of a low-cost, less invasive, and easily accessible tool which may be used in the early stages of AD and VCID to screen patients for future disease progression. Plasma biomarkers fill this niche and are widely used in other fields of medicine to assess risk of disease[59, 169]. Given the small concentration of proteins used in the assessment of AD and VCID it is vital to have technology that can match the required sensitivity necessary for the clinical usefulness of these biomarkers. Electrochemical immunoassays have emerged as one of

the primary tools that can achieve the picogram per mL level of quantification necessary to evaluate these blood-based biomarkers[185, 186].

In this dissertation, I will discuss three studies that focus on the different aspects of evaluating blood-based biomarkers. The second chapter asks the question of whether there are identifiable blood-based biomarker profiles in a cohort of patients with MCI due to cerebrovascular disease. In that study I use hierarchical clustering to identify groups of patients with similar angiogenic and inflammatory plasma biomarker levels to evaluate which proteins are able to differentiate patient biomarker profiles. The third chapter evaluates the cross-sectional association of plasma biomarkers with AD and VCID neuropathology using linear modeling. In this study, I looked at biomarkers from plasma within two years of a patient's autopsy related to AD and neurodegeneration, angiogenesis, and inflammation and determined their association with neuropathological findings at autopsy. Finally, in the fourth chapter I determined the relationship between plasma biomarkers at baseline and cognitive levels at 3 and 6 years postbaseline. Here I also used linear modeling to evaluate neurodegenerative, inflammatory, and anti-inflammatory markers and assessed their relationship with age, sex, and education adjusted cognitive domain scores. Overall, I aim to demonstrate the utility of plasma biomarkers in their in-vivo assessment of AD and VCID.

Table 1.1 AD Neuropathologic Change Scoring

|                                    |                              | B: NFT score               |                |              |
|------------------------------------|------------------------------|----------------------------|----------------|--------------|
| A: A $\beta$ /amyloid plaque score | C: Neuritic plaque score     | B0 or B1<br>(None or I/II) | B2<br>(III/IV) | B3<br>(V/VI) |
| A0 (0)                             | C0 (none)                    | Not                        | Not            | Not          |
| A1 (1/2)                           | C0 or C1<br>(none to sparse) | Low                        | Low            | Low          |
|                                    | C2 or C3<br>(mod. to freq.)  | Low                        | Intermediate   | Intermediate |
| A2 (3)                             | Any C                        | Low                        | Intermediate   | Intermediate |
| A3 (4/5)                           | C0 or C1<br>(none to sparse) | Low                        | Intermediate   | Intermediate |
|                                    | C2 or C3<br>(mod. to freq.)  | Low                        | Intermediate   | High         |

AD neuropathologic change is evaluated using an “ABC” score that derives from three separate four-point scales: A $\beta$ /amyloid plaques (A) by the method of Thal phases, NFT stage by the method of Braak (B), and neuritic plaque score by the method of CERAD (C). The combination of A, B, and C scores receive a descriptor of “Not”, “Low”, “Intermediate” or “High” AD neuropathologic change. “Intermediate” or “High” AD neuropathologic change is considered sufficient explanation for dementia. Adapted from Hyman, B.T., et al., *National Institute on Aging-Alzheimer's Association guidelines for the neuropathologic assessment of Alzheimer's disease*. *Alzheimers Dement*, 2012. **8**(1): p. 1-13.

## 2 Hierarchical Clustering Analyses of Plasma Proteins in Subjects with Cardiovascular Risk Factors Identifies Informative Subsets Based on Differential Levels of Angiogenic and Inflammatory Biomarkers

Zachary Winder, Tiffany L Sudduth, David Fardo, Qiang Cheng, Larry B Goldstein, Peter T Nelson, Frederick A Schmitt, Gregory A Jicha, Donna M Wilcock

### 2.1 Abstract

Agglomerative hierarchical clustering analysis (HCA) is a commonly used unsupervised machine learning approach for identifying informative natural clusters of observations. HCA is performed by calculating a pairwise dissimilarity matrix, and then clustering similar observations until all observations are grouped within a cluster. Verifying the empirical clusters produced by HCA is complex and not well studied in biomedical applications. Here, we demonstrate the comparability of a novel HCA technique with one that was used in previous biomedical applications while applying both techniques to plasma angiogenic (FGF, FLT, PIGF, Tie-2, VEGF, VEGF-D) and inflammatory (MMP1, MMP3, MMP9, IL8, TNF $\alpha$ ) protein data to identify informative subsets of individuals. Study subjects were diagnosed with mild cognitive impairment (MCI) due to cerebrovascular disease (CVD). Through comparison of the two HCA techniques, we were able to identify subsets of individuals, based on differences in VEGF ( $p < 0.001$ ), MMP1 ( $p < 0.001$ ), and IL8 ( $p < 0.001$ ) levels. These profiles provide novel insights into angiogenic and inflammatory pathologies that may contribute to VCID.

## 2.2 Introduction

Vascular Cognitive Impairment and Dementia (VCID) is an active area in dementia research[187] and is described as “encompassing all the cognitive disorders associated with cerebrovascular disease, from dementia to mild cognitive deficits”[125]. VCID is estimated to occur in roughly 20% of the cases of dementia, however the exact prevalence in the population is unknown with varying estimates in the literature[188, 189]. Much of the uncertainty in assessing the prevalence of VCID is due to varied diagnostic criteria[190]. In addition, there is substantial overlap in cognitive manifestations of cerebrovascular and neurodegenerative pathologies (such as Alzheimer’s disease, AD) that can culminate in clinical dementia[191], which further complicates our understanding of VCID. Further, both pathologies commonly co-exist in the same individual, yet some autopsy studies suggest that there is a significant increase in dementia risk due to vascular factors when Alzheimer pathology is low[192, 193].

Currently, magnetic resonance imaging (MRI) and cerebrospinal fluid (CSF) biomarkers are used to differentiate VCID from AD and monitor the progression of VCID[169, 170]. Plasma biomarkers are currently being investigated as a lower cost and less invasive alternative approach. The current study is focused on exploring the potential clustering of plasma biomarkers using HCA in participants with VCID who have mild cognitive impairment due to cerebrovascular disease (MCI-CVD) to identify unique plasma profiles of disease[194]. Persons with MCI-CVD are of particular interest as they are at an increased risk of developing dementia and already have cognitive decline[195].

We evaluated angiogenic (FGF, FLT, PIGF, Tie-2, VEGF, VEGF-D) and inflammatory (MMP1, MMP3, MMP9, IL8, TNF $\alpha$ ) protein plasma biomarkers in these participants using the highly sensitive meso-scale discoveries (MSD) platform. Angiogenic and inflammatory markers are of particular interest due to their roles in endothelial dysfunction, which has been shown to play a role in the pathogenesis of cerebrovascular disease[171, 196]. Presently, studies have demonstrated mixed results in the association of angiogenic and inflammatory biomarkers with VCID, however it is suspected that this is due to the inconsistency in both the patient populations and the analytical measures[169].

Agglomerative hierarchical clustering analysis (HCA) is an unsupervised machine learning technique commonly used to determine similar subsets within a larger population[197]. HCA can be used to identify subsets within a variety of different patient populations. The accuracy of this technique is difficult to quantify, as most studies rely on post-hoc analysis of the clusters produced by HCA to determine their validity. We propose a unique methodology for validating clusters produced by HCA. This method relies on using two unique HCA models on the same dataset and evaluates congruencies between the two models by comparing a novel HCA model to one that is widely used[198-201]. Before applying both HCA models to our dataset, we tested the accuracy of each model on various distributions of data and compared them to each other using the adjusted rand index. After demonstrating the interchangeability of the two HCA models in the simulated data distribution comparable to our dataset, we



tested both models on our dataset and compared the underlying components of each cluster produced by the HCA models.

## 2.3 Methods

### 2.3.1 Participants

Plasma samples were collected from a cohort of adult research volunteers enrolled in a randomized behavioral intervention study for MCI-CVD (N = 80, NCT01924312). Inclusion criteria for the parent study include age older than 55-years, Montreal Cognitive Assessment score < 29, and at least one uncontrolled vascular risk factor. Risk factors included poorly controlled hypertension, poorly controlled cholesterol, cardiomyopathy/CHF, diabetes with a fasting glucose > 110 or HbA1c > 7%, homocysteine > 12, history of transient ischemic attack, tobacco use > 30 pack-years, and BMI >30. Potential subjects were excluded from this cohort if they had dementia, evidence of a non-CVD cause of cognitive decline, evidence of a non-CVD neurologic disease, or any focal motor, sensory, visual, or auditory deficits. For the current study, participants were also excluded if they had an incomplete panel of markers as measured via MSD assays as described below (n = 7).

### 2.3.2 Plasma Collection and Quantification

Plasma samples were collected by venous puncture using 10ml EDTA Vacutainer tubes. Plasma was aliquot into cryo-tubes at 500µl volumes. Quantification of plasma samples was accomplished using MSD Multi-Spot V-PLEX assays (Angiogenesis Panel 1 (human) and Proinflammatory Panel 1 (human)) and Ultra-Sensitive assays (MMP 2-Plex and MMP 3-Plex). Plasma did not undergo any freeze-thaw cycles after the initial

thawing of the aliquot. Assays were performed using plate specific protocols as followed with analysis performed in the MSD Discovery Workbench 4.0 software:

#### 2.3.2.1 MMP 2-Plex and MMP 3-Plex

MMP plates were brought to room temperature for approximately 30 minutes and then loaded with 25 $\mu$ l of diluent, covered (protect from light), and incubated at room temperature for 30 minutes while shaking at 600 rpm. After incubation, plates were removed from the shaker and 25 $\mu$ l of calibrator was added to the assigned wells in duplicate with 5 $\mu$ l of undiluted sample and 20 $\mu$ l of diluent. Plates were covered and incubated at room temperature while shaking at 600 rpm. After incubation, plates were removed from the shaker and washed three times with 300 $\mu$ l of wash buffer. Plates were turned upside down and tapped against paper towels to ensure the removal of all wash buffer from the wells. 25 $\mu$ l of the antibody mix was loaded into each well, covered (protect from light), and incubated at room temperature for two hours shaking at 600 rpm. After incubation, plates were removed from the shaker and the wash steps were repeated from above. 150 $\mu$ l of read buffer was loaded into each well and read on the MSD Quickplex SQ 120 machine.

#### 2.3.2.2 Proinflammatory Panel 1

Proinflammatory plates were brought to room temperature for approximately 30 minutes and washed three times with 300 $\mu$ l of wash buffer. Plates were turned upside down and tapped against paper towels to ensure the removal of all wash buffer from the wells. 50 $\mu$ l of calibrator was added to the assigned wells in duplicate with 50 $\mu$ l of undiluted sample and covered (protect from light). Plates were incubated at 4°C

overnight while shaking at 600 rpm. In the morning plates were removed from 4°C and incubated at room temperature for one hour while shaking at 600 rpm. After incubation, plates were removed from the shaker and the wash steps were repeated from above. 25µl of the antibody mix was added into each well, covered (protect from light), and incubated at room temperature for two hours shaking at 600 rpm. After incubation, plates were removed from the shaker and wash steps were repeated from above. 150µl of read buffer was loaded into each well and read on the MSD Quickplex SQ 120 machine.

#### 2.3.2.3 Angiogenesis Panel 1

Angiogenesis plates were brought to room temperature for approximately 30 minutes and then loaded with 150µl of diluent, covered (protect from light), and incubated at room temperature for one hour while shaking at 600 rpm. After incubation, plates were removed from the shaker and washed three times with 300µl of wash buffer. Plates were turned upside down and tapped against paper towels to ensure the removal of all wash buffer from the wells. 50µl of calibrator was added to the assigned wells in duplicate with 25µl of undiluted sample and 25µl of diluent. Plates were covered (protect from light) and incubated at 4°C overnight while shaking at 600 rpm. In the morning, plates were removed from 4°C and incubated at room temperature for one hour while shaking at 600 rpm. After incubation, plates were removed from the shaker and wash steps were repeated from above. 25µl of the antibody mix was added into each well, covered (protect from light), and incubated at room temperature for two hours shaking at 600 rpm. After incubation, plates were

removed from the shaker and wash steps were repeated from above. 150µl of read buffer was loaded into each well and read on the MSD Quickplex SQ 120 machine.

Samples were run in duplicate and three pooled control samples were run on each plate to measure inter- and intra-plate variability. MSD quantification was performed on a table stabilizer in order to reduce error in MSD plate readings.

### 2.3.3 Plasma Sample Analysis

Protein markers measured through MSD assays were subjected to intra- and inter-plate variability tests. Intra-plate variability was assessed through two distinct methods. The first method calculated the percentage of samples for each marker that had a coefficient of variation, as determined by the duplicate runs for each sample, greater than or equal to 0.25. Markers that contained 20% of samples above this threshold were removed from further analysis. The second method ran three pooled control sample twice on the same plate (two samples each run in duplicate) to ensure consistency in final quantifications. The coefficient of variation for each of the three controls measured for each marker were then averaged together. Markers with an average coefficient of variation greater than 0.25 were excluded from the analysis. Markers that passed both criteria were included in the final analysis. Inter-plate variability was accounted for using the three pooled control samples run on each plate. Each plate control value was divided by the control mean and all three of these values for each marker were averaged together to provide a plate-scaling factor. Each value was then divided by this factor to adjust for inter-plate variability. The resulting measures were log-transformed to scale each marker to a common order of magnitude,

which is required in clustering algorithms to provide equal weighting of markers.

Grubb's test was lastly applied to the data to remove outliers[202]. Individual samples containing one or more outliers in the measured markers were excluded from further analysis (n = 7) due to their effects on clustering techniques. The final dataset consisted of 66 patient plasma samples, which were quantified for 11 plasma markers (FGF, FLT, PLGF, Tie-2, VEGF, VEGFD, MMP1, MMP3, MMP9, IL8, TNF $\alpha$ ).

#### 2.3.4 Hierarchical Clustering Analysis

All HCA were performed using the Matlab Statistics and Machine Learning Toolbox functions pdist, linkage, and cluster. Previously described HCA models were comprised of three different algorithms, distance, linkage, and clustering [198-201]. The conventional HCA model consists of a Euclidean distance algorithm, which calculates the distance between two samples using the Euclidean distance formula (a special case of the generalized Minkowski distance formula), where the distance between observations s and t in a sample with n markers equals  $d_{st}$ :

$$d_{st} = \sqrt{\sum_{j=1}^n |X_{sj} - X_{tj}|^2}$$

The linkage algorithm used was Ward's Linkage, which calculates the incremental increase in within-cluster sum of squares and links samples one at a time until all samples are combined into a single cluster[197]. This method combines similar samples until all samples fall within one cluster (i.e., agglomerative hierarchical clustering). The final algorithm in the conventional HCA model used a standard agglomerative clustering approach [199].

The novel proposed HCA model uses consensus clustering as presented by Fred and Jain [203] to combine HCA models with different distance and clustering algorithms. The distance algorithms used the Minkowski distance formula with  $p$  ranging from 0.1 to 2.0 in increments of 0.1. The distance between observations  $s$  and  $t$  in a sample with  $n$  markers equals  $d_{st}$ :

$$d_{st} = \sqrt{\sum_{j=1}^n |X_{sj} - X_{tj}|^2}$$

Each distance algorithm's data was then used with the weighted average linkage algorithm, which combines samples into clusters that have the smallest distance between them and determines that distance using a recursive function which treats the subset of linkages equally[197].

Lastly, data from each linkage algorithm was clustered using an inconsistency clustering algorithm. This algorithm calculates an inconsistency coefficient of a new linkage using the mean and standard deviation of the linkage heights for a specified depth ( $dep$ ) of sub linkages within each new linkage. Clusters were formed when the inconsistency coefficient for each linkage and all sub linkages were less than a specified cutoff ( $cut$ ) value. Each linkage algorithm output was run through multiple iterations of the inconsistency clustering algorithm with values for depth ( $dep$ ) from 2 to 6 in increments of 1, whereas cutoff ( $cut$ ) values were adjusted from 1.0 to 3.0 in increments of 0.1. All iterations of depth and cutoff were evaluated, and if only one cluster was formed then that iteration was not used in the consensus clustering model. Once each

clustering model was established, distances between samples were calculated based on the percentage of models in which two samples shared a cluster. Samples that shared no clusters were given a distance of 1 and, samples that were paired in the same cluster in each model were given a distance of 0. Plots of each clustering model were created using the dimensionality reduction function, t-Distributed Stochastic Neighbor Embedding (t-sne), with a random number generation seed of 10 to maintain reproducibility[204]. Clinical data was excluded from the clustering algorithm to avoid clusters based on clinical findings as this study sought to identify clusters of participants based on a differential level of fluid biomarkers.

#### 2.3.5 Simulated Data Generation and Analysis

Simulated data generation was performed using the Matlab Statistics and Machine Learning Toolbox function *mvnrnd*. Each simulated data experiment was run with 35 trials and each trial was initiated with a unique random number generation seed to maintain reproducibility. Generated data contained 11 variables and 100 samples per group, obtained from known distributions with the mean and sigma of each distribution differing depending on the experiment. Supplementary Tables 2.1, 2.2, and 2.3 detail the mean and sigma for each group within each experiment. The adjusted rand index (ARI) was used to evaluate the accuracy of each clustering model by comparing each clustering result to the known cluster assignment. The ARI has a maximum value of 1 indicating that the clustering result matches perfectly to the known cluster assignment. An ARI of 0 indicates that the clustering model assigns observations to the correct cluster assignment with an equal probability as random chance. An ARI below 0

demonstrates that the clustering model is less effective than random chance at assigning observations to the correct cluster assignment[205].

### 2.3.6 Statistical Analysis

Statistical analysis was performed using the Matlab Statistics and Machine Learning Toolbox and SPSS. A two-sample t-test using the Matlab function *ttest2* was conducted to compare the ARI means of the two HCA models for all simulated data experiments. SPSS was used for the remaining statistical tests to determine differences between clusters for each log-transformed protein marker. Levene's test for equality of variances was performed before each two-sample t-test, and Satterthwaite's t-test was used for any marker found to have significantly different variances. Levene's test for homogeneity of variances based on the mean was also conducted before performing an ANOVA test for each marker and a Welch's test for equality of means was performed for markers with nonhomogeneous variances. Post-hoc analysis was then conducted on markers which had a significant p-value for an ANOVA or Welch's test. Tukey's HSD was used for significant ANOVA tests and Dunnett T3 was used for significant Welch's Test.

## 2.4 Results

### 2.4.1 Study Population Description

Demographic and neurocognitive evaluations were obtained in 65/66 participants within our MCI-CVD cohort (Table 2.1). The mean age of the participants was  $75.07 \pm 8.14$  with a female population of 47%. MMSE scores ranged from 18-30 with a mean of  $26.86 \pm 2.95$ , while MoCA scores ranged from 11-28 with a mean of  $22.11 \pm 3.74$ . Vascular risk factors including systolic blood pressure, hemoglobin A1C,



and LDL cholesterol were also evaluated in our cohort (Table 2.1). Mean systolic blood pressure was found to be  $141.33 \pm 15.31$  mmHg, hemoglobin A1c  $6.18 \pm 1.31$  %, and LDL cholesterol  $97.44 \pm 42.63$  mg/dL.

#### 2.4.2 Simulated Data Analysis

To test the applicability of the novel combined HCA model we tested its accuracy in eight unique simulated datasets (detailed in Supplementary Table 2.1). We tested the novel model against an established HCA model using the adjusted rand index (ARI) to measure the accuracy of each model (Figure 2.1). In our first experiment, we studied the accuracy of both models in a dataset with two distant uniform clusters (Figure 2.1a). The established HCA model using Euclidean distance showed no difference in ARI compared to the novel combined HCA model (Euclidean:  $0.9892 \pm 0.0029$ , Novel:  $0.9920 \pm 0.0019$ ,  $p = 0.413$ ). A similar result was found in a dataset with two distant variable clusters (Euclidean:  $0.9920 \pm 0.0023$ , Novel:  $0.9926 \pm 0.0020$ ,  $p = 0.857$ ) (Figure 2.1e). These results demonstrate that both models were able to assign each distribution to its own cluster. Next, we tested both models on a dataset with three distant uniform clusters (Figure 2.1c) and three distant variable clusters (Figure 2.1g). The established HCA model had a significantly increased ARI over the novel HCA model in both of these experiments (Euclidean:  $0.6186 \pm 0.0139$ , Novel:  $0.4067 \pm 0.0320$ ,  $p < 0.001$ , Figure 2.1c) (Euclidean:  $0.5767 \pm 0.0200$ , Novel:  $0.4393 \pm 0.0092$ ,  $p < 0.001$ , Figure 2.1g). These results show that the established HCA model has a higher accuracy when separating three distant clusters of normally distributed data. We then tested if the models performed differently on distributions that had more overlapping characteristics. The

first experiments of these distributions were with two close uniform clusters (Figure 2.1b) and two close variable clusters (Figure 2.1f). In both experiments the established HCA model had a higher accuracy compared to the novel HCA model (Euclidean:  $0.6579 \pm 0.0150$ , Novel:  $0.5482 \pm 0.0237$ ,  $p < 0.001$ , Figure 2.1b) (Euclidean:  $0.6186 \pm 0.0139$ , Novel:  $0.4067$ ,  $p < 0.001$ , Figure 2.1f). This difference continued in the final set of experiments which used three close uniform clusters (Euclidean:  $0.2477 \pm 0.0087$ , Novel:  $0.2103 \pm 0.0103$ ,  $p < 0.007$ , Figure 2.1d) and three distant variable clusters (Euclidean:  $0.2370 \pm 0.0080$ , Novel:  $0.2023 \pm 0.0078$ ,  $p < 0.003$ , Figure 2.1h). These experiments show that as the distributions progressively overlap the accuracy for both models decrease and the difference between the accuracy of the models decreases as well.

#### 2.4.3 Predicted Distribution Analysis

We hypothesized that clusters, if any, in our empirical dataset would overlap more and thus be more difficult to differentiate than those used in the previous experiments. To test the accuracy of each model in this distribution we generated simulated data from predicted distributions based on analysis from our collaborators (detailed in Supplementary Tables 2.2 and 2.3). The first experiment was based on a two-cluster model within our sample population (Figure 2.2a). This experiment showed no differences between the established Euclidean HCA model and the novel HCA model (Euclidean:  $0.1422 \pm 0.0118$ , Novel:  $0.1270 \pm 0.0181$ ,  $p = 0.486$ , Figure 2.2a). In addition, we tested a three-cluster model for our sample population and found similar results with no differences between the two models in this study (Euclidean:  $0.0902 \pm 0.0092$ ,

Novel:  $0.0895 \pm 0.0105$ ,  $p = 0.962$ , Figure 2.2b). The data from these two experiments demonstrate the interchangeability of these two models when studying datasets with extensive overlapping distributions.

#### 2.4.4 Application of Models to Dataset

After validating the novel combined HCA model using predicted distributions, we applied both HCA models to our 66 patient sample (Figure 2.3). When the Euclidean distance HCA model was applied to our dataset, 4 clusters emerged (Figure 2.3a). Clusters 1, 3, and 4 appear to be more compact in the 2-D t-SNE dimensionality reduction plot, while cluster 2 exists along the periphery of the plot in a more scattered manner. We continued this experiment and applied the novel combined HCA model to the same dataset and uncovered 2 clusters (Figure 2.3b). Cluster 1 contains 14 samples of which 12 also appear in cluster 1 of the Euclidean distance HCA model. The other 52 samples appear in cluster 2, which is comprised of clusters 2-4 from the Euclidean distance HCA model. The similarity of these two results emphasize the underlying distributions within this dataset.

#### 2.4.5 Characterizing Cluster Differences

We proceeded to analyze the differences that drive cluster differentiation. First, we examined the clusters produced by the novel HCA model (Figure 2.4) and found that cluster 1 was increased compared to cluster 2 in FGF ( $p < 0.001$ ), Tie-2 ( $p = 0.013$ ), VEGF ( $p < 0.001$ ), MMP1 ( $p < 0.001$ ), MMP3 ( $p = 0.005$ ), MMP9 ( $p < 0.001$ ), and IL8 ( $p < 0.001$ ) (Table 2.2). When the clusters produced from the Euclidean distance HCA model were analyzed (Figure 2.5), we found a similar pattern of clusters. In this model, cluster 1 was

increased compared to clusters 2-4 in VEGF ( $p = 0.006$ ,  $p < 0.001$ ,  $p = 0.013$ ), MMP1 ( $p = 0.003$ ,  $p < 0.001$ ,  $p = 0.001$ ), and IL8 ( $p < 0.001$ ,  $p < 0.001$ ,  $p < 0.001$ ) respectively (Table 2.3). Cluster 1 was also increased in FGF ( $p = 0.004$ ), Tie-2 ( $p = 0.033$ ), and MMP9 ( $p = 0.003$ ) compared to cluster 3. The elevated level of these proteins in cluster 1 agrees with the characteristics of cluster 1 established previously with both models demonstrating a subset with significant increases in VEGF, MMP1, and IL8 compared to the other subsets (Figure 2.6). However, the Euclidean distance HCA model does show differences between clusters 2-4, which were not seen in the novel HCA model. Cluster 2 and cluster 4 were similar in their makeup, both increased over cluster 3 in MMP1 ( $p < 0.001$  and  $p < 0.001$ ) and VEGF ( $p = 0.032$  and  $p = 0.016$ ) respectively, but different levels of FGF ( $p < 0.001$ ). These differences lead to the possibility of four disease profiles within the MCI-CVD patient population.

## 2.5 Discussion

The results of this study provide evidence supporting the use of the novel combined HCA model in datasets with extensive overlapping distributions. The results of the first set of experiments demonstrate that the Euclidean distance HCA model outperforms the novel combined HCA model in datasets with a moderate amount of overlapping distributions (Figure 2.1(b-d,f-h)). This difference is reduced as the distributions progressively increase in overlap and eventually disappears entirely in our second set of experiments involving the more complex datasets with predicted distributions (Figure 2.2).

It is important to note that the capacity of the two HCA models to accurately cluster data into their known distributions decreases as the datasets become more complex. In our experiments involving two distant distributions of data, both models were able to separate each distribution with an adjusted rand index approximately equal to 1 (Figure 2.1(a,e)). In experiments using our predicted distributions the average adjusted rand index decreased to approximately 0.13 and 0.09 for the two and three cluster models respectively (Figure 2.2). These findings demonstrate the limits of reliability in both HCA models and provide a measure to compare additional HCA models to in future experiments. Accounting for this accuracy is crucial when interpreting HCA results because clusters produced by the HCA model may not correspond to any true unique distribution and may simply be a subset within the normal variation of a larger distribution. Therefore, it is important to compare multiple HCA models on an unknown dataset in order to elucidate which clusters are in fact unique distributions within the dataset. Overall, results from our experiments support the interchangeability of HCA models in datasets similar to those shown in Supplementary Tables 2.2 and 2.3, which allows for the use of both models in assessing clustering distributions within our dataset.

Both the Euclidean distance HCA model and the novel combined HCA model resulted in similar disease profiles within our cohort of MCI-CVD patients (Figure 2.3). In this study both models classified participants into a cluster that had elevated levels of VEGF, MMP1, and IL8 compared to the other clusters (Figures 2.4-2.5). We suspect that this disease profile seen in cluster 1 may be involved in a more active VCID process

resulting in increased pathology due to the increased level of angiogenic and inflammatory markers. Clusters 2-4 in the Euclidean distance HCA model may also be clinically relevant in terms of disease pathology but require future studies to understand how these profiles may contribute to progression of VCID in a population of individuals with MCI-CVD.

In conclusion, the usage of both the novel HCA model and a Euclidean distance HCA model identified a novel subset of patients within the MCI-CVD population. This study provides insight into a potential underlying inflammatory and angiogenic profile of disease in patients with VCID. Defining subsets of patients within this population with different disease profiles continues to be a key research objective. These profiles can provide a more complete understanding of disease progression and allow physicians and researchers to identify patients undergoing different rates of pathologic change in a prospective cohort. In the future, we hope to further clarify these profiles by combining plasma and MRI imaging biomarkers that can also be used in clinical trials as key outcome measures to determine the efficacy of novel therapeutics.

Table 2.1 MCI-CVD Cohort Demographics and Clinical History

|                                       | <b>Mean ± SDev</b> | <b>Range</b>    |
|---------------------------------------|--------------------|-----------------|
| <b>Age (yrs)</b>                      | 75.07 ± 8.14       | (56.99 - 89.22) |
| <b>MMSE</b>                           | 26.86 ± 2.95       | (18 - 30)       |
| <b>MoCA</b>                           | 22.11 ± 3.74       | (11 - 28)       |
| <b>Systolic Blood Pressure (mmHg)</b> | 141.33 ± 15.31     | (102-185)       |
| <b>Hemoglobin A1c (%)</b>             | 6.18 ± 1.31        | (4.3-11.8)      |
| <b>LDL Cholesterol (mg/dL)</b>        | 97.44 ± 42.63      | (22-299)        |
| <b>Sex</b>                            | 47% Female         |                 |

Means ± Standard Deviation for age, MMSE, and MoCA for the MCI-CVD cohort population in addition to percent of female participants.

Table 2.2 Combined HCA Model Cluster Differences

| <b>Biomarker</b> | <b>p-value</b> | <b>Cluster 1 (pg/mL)</b> | <b>Cluster 2 (pg/mL)</b> |
|------------------|----------------|--------------------------|--------------------------|
| FGF              | < 0.001        | 24.56 ± 2.39             | 12.27 ± 1.22             |
| FLT              | 0.568          | 12.92 ± 1.35             | 11.87 ± 0.59             |
| PIGF             | 0.093          | 3.52 ± 0.38              | 2.94 ± 0.11              |
| Tie-2            | 0.013          | 500.55 ± 31.69           | 411.09 ± 14.77           |
| VEGF             | < 0.001        | 98.39 ± 17.46            | 43.55 ± 3.63             |
| VEGFD            | 0.350          | 560.73 ± 52.17           | 515.59 ± 24.35           |
| MMP1             | < 0.001        | 5244.74 ± 700.11         | 2292.86 ± 219.55         |
| MMP3             | 0.005          | 17275.46 ± 3267.49       | 10547.71 ± 856.39        |
| MMP9             | < 0.001        | 43561.18 ± 8177.19       | 19232.98 ± 1851.63       |
| IL8              | < 0.001        | 4.20 ± 0.49              | 2.25 ± 0.11              |
| TNFα             | 0.283          | 1.81 ± 0.15              | 1.63 ± 0.10              |

Means ± SEM for clusters 1 and 2 produced by the Combined HCA model. Statistical significance between groups was determined using the log transform of the data shown in Figure 2.4 in an independent samples t-test (p < 0.05)

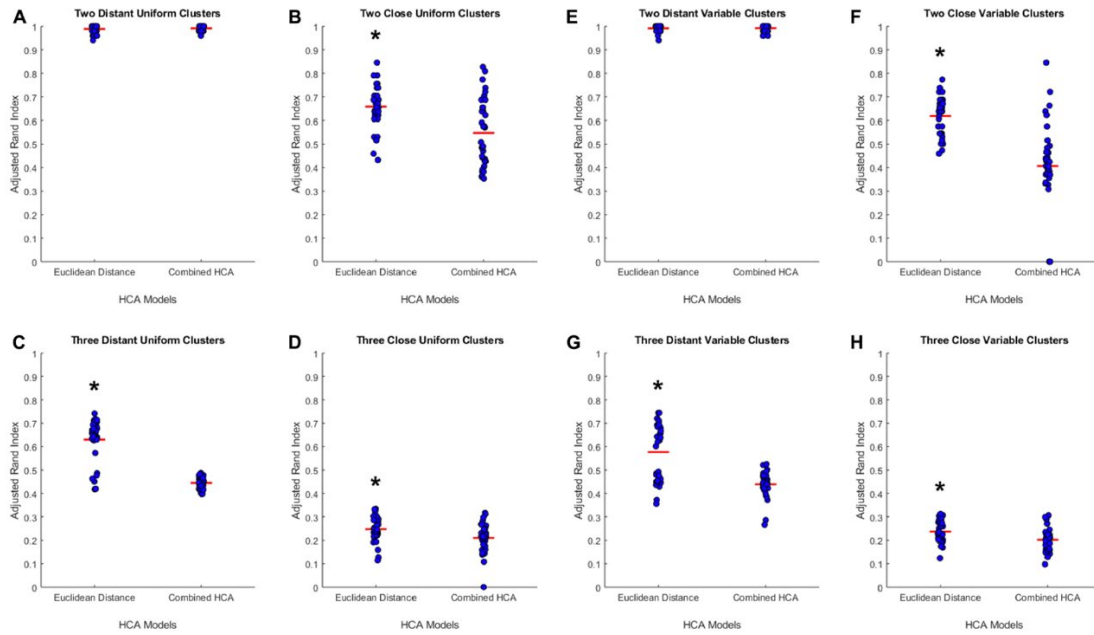


Table 2.3 Euclidean Distance Model Cluster Differences

| <b>Biomarker</b> | <b>p-value</b> | <b>Cluster 1<br/>(pg/mL)</b> | <b>Cluster 2<br/>(pg/mL)</b> | <b>Cluster 3<br/>(pg/mL)</b> | <b>Cluster 4<br/>(pg/mL)</b> |
|------------------|----------------|------------------------------|------------------------------|------------------------------|------------------------------|
| FGF              | < 0.001        | 24.90 ±<br>2.78              | 5.16 ± 0.60                  | 12.70 ± 1.37                 | 20.11 ± 1.97                 |
| FLT              | 0.340          | 12.77 ±<br>1.56              | 13.08 ± 0.82                 | 11.05 ± 1.44                 | 11.42 ± 0.82                 |
| PIGF             | 0.342          | 3.53 ± 0.45                  | 2.94 ± 0.17                  | 2.79 ± 0.28                  | 3.10 ± 0.16                  |
| Tie-2            | 0.040          | 512.42±<br>35.98             | 437.13 ±<br>25.44            | 384.29 ±<br>26.72            | 405.64± 21.72                |
| VEGF             | < 0.001        | 106.97 ±<br>19.29            | 49.97 ± 6.65                 | 27.69 ± 4.39                 | 48.56 ± 5.14                 |
| VEGFD            | 0.258          | 563.88 ±<br>60.58            | 579.18 ±<br>46.39            | 469.25 ±<br>36.56            | 487.25 ±<br>32.33            |
| MMP1             | < 0.001        | 5605.20 ±<br>769.82          | 3061.39 ±<br>356.41          | 736.27 ±<br>71.84            | 2692.85 ±<br>285.62          |
| MMP3             | 0.096          | 17517.09 ±<br>3822.29        | 10666.69 ±<br>1443.84        | 9646.52 ±<br>1192.19         | 11587.35 ±<br>1561.28        |
| MMP9             | < 0.001        | 46055.29 ±<br>9378.94        | 25868.67 ±<br>3771.38        | 17474.83 ±<br>2787.13        | 14764.34 ±<br>1748.47        |
| IL8              | < 0.001        | 4.49 ± 0.52                  | 2.32 ± 0.18                  | 1.78 ± 0.12                  | 2.53 ± 0.18                  |
| TNFα             | 0.362          | 1.86 ± 0.16                  | 1.52 ± 0.16                  | 1.51 ± 0.10                  | 1.83 ± 0.21                  |

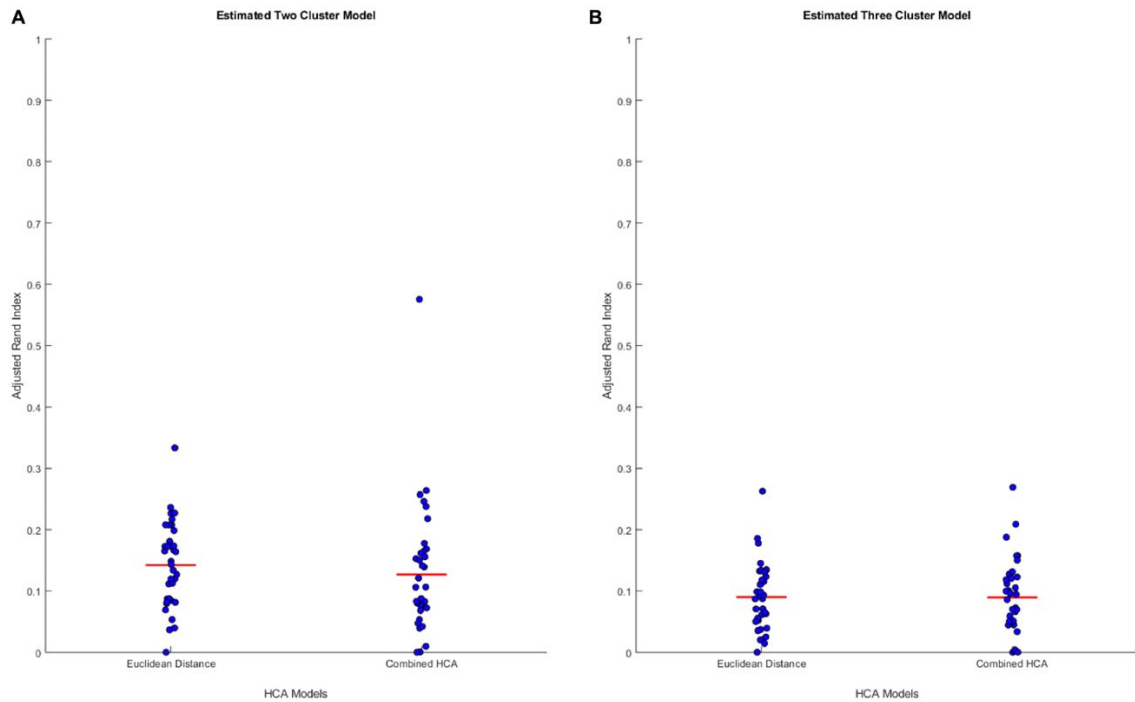
Means ± SEM for clusters 1-4 produced by the Euclidean Distance model. Statistical significance between groups was determined using the log transform of the data shown in Figure 2.5 in an ANOVA followed by Tukey's HSD for post-hoc analysis (p < 0.05). Results of the ANOVA omnibus are shown in p-value.

Figure 2.1 Comparison of HCA Models in Multiple Simulated Datasets



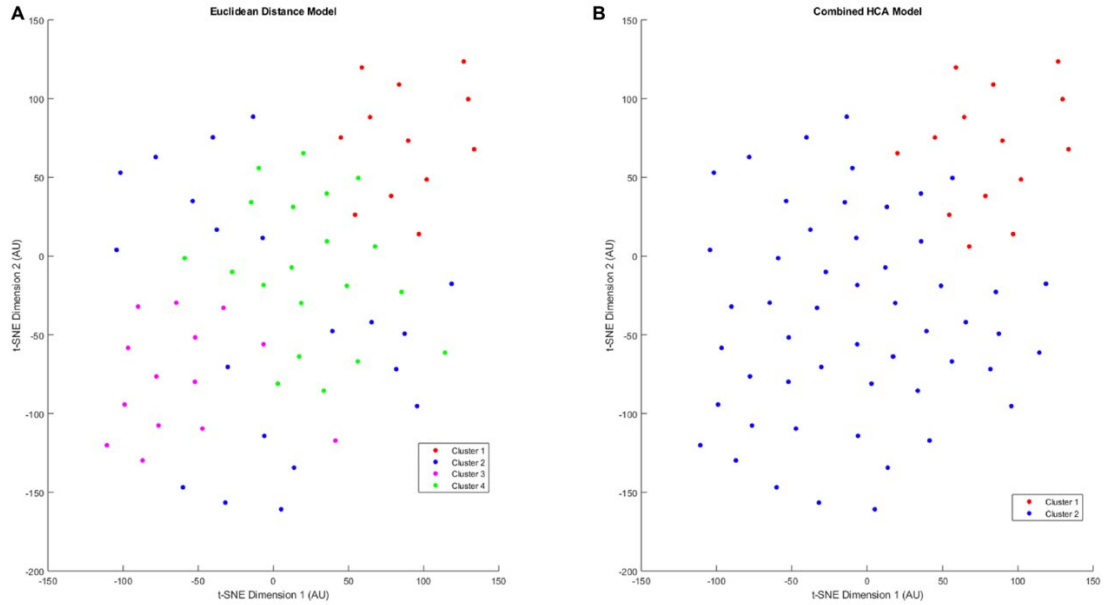
Compares the combined HCA model to the Euclidean distance model in eight different datasets. Each dataset was produced using the *mvnrnd*. The accuracy of each model was assessed using the adjusted rand index (ARI). Datasets used in figures 2.1(a-d) have identical means for each variable in each cluster. Datasets used in figures 2.1(e-h) have the same means for the first 6 variables and means of opposite signs for the other 5 variables. Means and standard deviations for each dataset are shown in Supplementary Table 2.1. Horizontal red lines indicate means for each model. Stars (\*) indicate statistical significance between groups using an independent samples t-test ( $p < 0.05$ ).

Figure 2.2 Comparison of HCA Models in Predicted Distributions



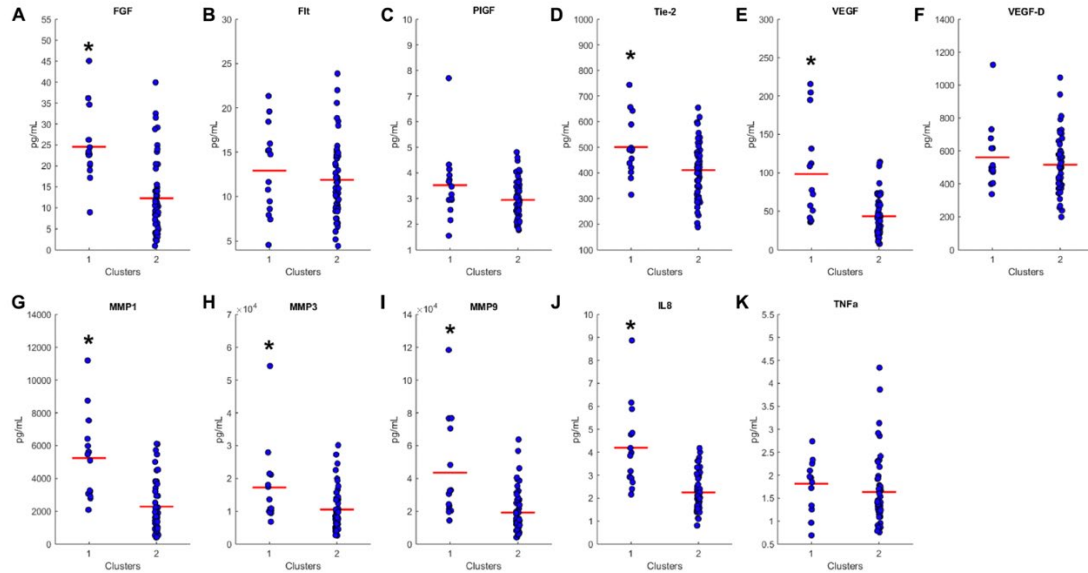
Compares the combined HCA model to the Euclidean distance model in two predicted distributions. Each dataset was produced using *mvnrnd*. The accuracy of each model was assessed using the adjusted rand index (ARI). Means and covariance matrix for each dataset are shown in Supplementary Tables 2.2 and 2.3. Horizontal red lines indicate means for each model. Stars (\*) indicate statistical significance between groups using an independent samples t-test ( $p < 0.05$ ).

Figure 2.3 Dimensionality Reduction Plots of Clustered Data



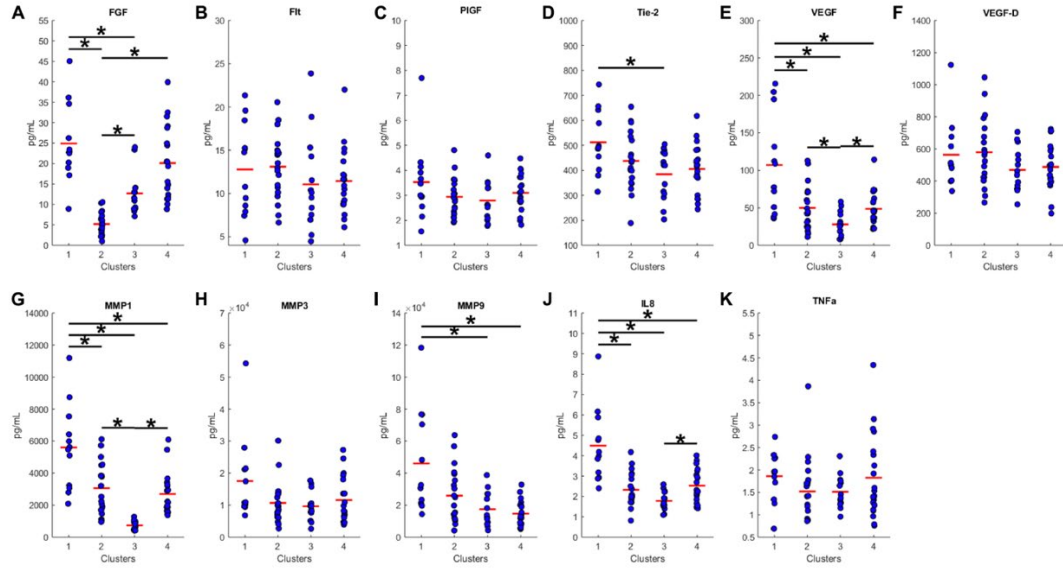
T-SNE dimensionality reduction plot of clustered data. Data was clustered using the Euclidean Distance Model (a) and the Combined HCA model (b). The dataset was produced by measuring 11 inflammatory (MMP1, MMP3, MMP9, IL8, TNF $\alpha$ ) and angiogenic proteins of interest (FGF, FLT, PIGF, Tie-2, VEGF, VEGF-D) from 66 participant plasma samples.

Figure 2.4 Combined HCA Model Cluster Comparison



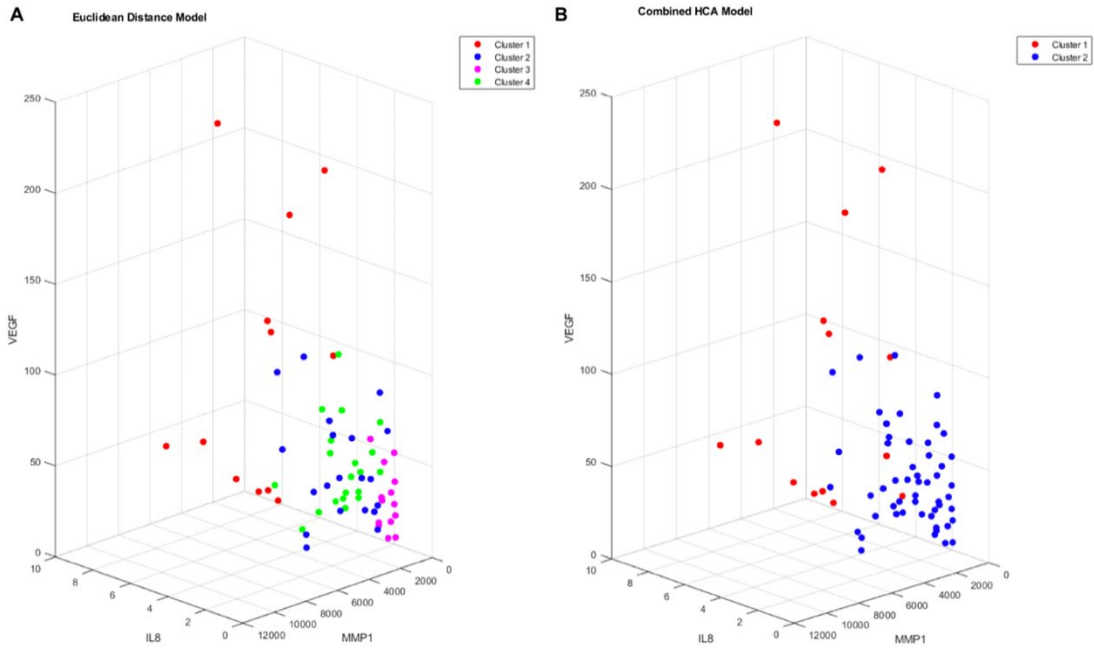
Compares cluster 1 and 2 produced from the Combined HCA model in each inflammatory and angiogenic protein measured. Horizontal red lines indicate the means for each cluster. Stars (\*) indicate statistical significance between groups as calculated by the log transform of the data shown using an independent samples t-test ( $p < 0.05$ ). Means  $\pm$  SEM are shown in Table 2.2.

Figure 2.5 Euclidean Distance Model Cluster Comparison



Compares clusters 1-4 produced from the Euclidean Distance model in each inflammatory and angiogenic protein measured. Horizontal red lines indicate the means for each cluster. Stars (\*) indicate statistical significance between groups as calculated by the log transform of the data shown using ANOVA followed by Tukey's HSD for post-hoc analysis (p < 0.05). Means ± SEM are shown in Table 2.3.

Figure 2.6 3-D Cluster Comparison



Cluster comparison of VEGF (pg/mL), MMP1 (pg/mL), and IL8 (pg/mL) for data clustered using the Euclidean Distance Model (a) and the Combined HCA model (b) from 66 participant plasma samples.

Supplementary Table 2.1

| Experiment Name                 | Cluster | Means   | Sigma                   |
|---------------------------------|---------|---|-------------------------|
| Two Distant Uniform Clusters    | 1       | [1 1 1 1 1 1 1 1 1 1 1]                       | [1 1 1 1 1 1 1 1 1 1 1] |
|                                 | 2       | [-1 -1 -1 -1 -1 -1 -1 -1 -1 -1 -1]            | [1 1 1 1 1 1 1 1 1 1 1] |
| Two Close Uniform Clusters      | 1       | [.5 .5 .5 .5 .5 .5 .5 .5 .5 .5 .5]            | [1 1 1 1 1 1 1 1 1 1 1] |
|                                 | 2       | [-.5 -.5 -.5 -.5 -.5 -.5 -.5 -.5 -.5 -.5 -.5] | [1 1 1 1 1 1 1 1 1 1 1] |
| Two Distant Variable Clusters   | 1       | [1 1 1 1 1 1 -1 -1 -1 -1 -1]                  | [1 1 1 1 1 1 1 1 1 1 1] |
|                                 | 2       | [-1 -1 -1 -1 -1 -1 1 1 1 1 1]                 | [1 1 1 1 1 1 1 1 1 1 1] |
| Two Close Variable Clusters     | 1       | [.5 .5 .5 .5 .5 .5 -.5 -.5 -.5 -.5 -.5]       | [1 1 1 1 1 1 1 1 1 1 1] |
|                                 | 2       | [-.5 -.5 -.5 -.5 -.5 -.5 .5 .5 .5 .5 .5]      | [1 1 1 1 1 1 1 1 1 1 1] |
| Three Distant Uniform Clusters  | 1       | [1 1 1 1 1 1 1 1 1 1 1]                       | [1 1 1 1 1 1 1 1 1 1 1] |
|                                 | 2       | [-1 -1 -1 -1 -1 -1 -1 -1 -1 -1 -1]            | [1 1 1 1 1 1 1 1 1 1 1] |
|                                 | 3       | [0 0 0 0 0 0 0 0 0 0 0]                       | [1 1 1 1 1 1 1 1 1 1 1] |
| Three Close Uniform Clusters    | 1       | [.5 .5 .5 .5 .5 .5 .5 .5 .5 .5 .5]            | [1 1 1 1 1 1 1 1 1 1 1] |
|                                 | 2       | [-.5 -.5 -.5 -.5 -.5 -.5 -.5 -.5 -.5 -.5 -.5] | [1 1 1 1 1 1 1 1 1 1 1] |
|                                 | 3       | [0 0 0 0 0 0 0 0 0 0 0]                       | [1 1 1 1 1 1 1 1 1 1 1] |
| Three Distant Variable Clusters | 1       | [1 1 1 1 1 1 -1 -1 -1 -1 -1]                  | [1 1 1 1 1 1 1 1 1 1 1] |
|                                 | 2       | [-1 -1 -1 -1 -1 -1 1 1 1 1 1]                 | [1 1 1 1 1 1 1 1 1 1 1] |
|                                 | 3       | [0 0 0 0 0 0 0 0 0 0 0]                       | [1 1 1 1 1 1 1 1 1 1 1] |
| Three Close Variable Clusters   | 1       | [.5 .5 .5 .5 .5 .5 .5 .5 .5 .5 .5]            | [1 1 1 1 1 1 1 1 1 1 1] |
|                                 | 2       | [-.5 -.5 -.5 -.5 -.5 -.5 -.5 -.5 -.5 -.5 -.5] | [1 1 1 1 1 1 1 1 1 1 1] |
|                                 | 3       | [0 0 0 0 0 0 0 0 0 0 0]                       | [1 1 1 1 1 1 1 1 1 1 1] |

Means and standard deviations for each cluster generated in each experiment.

Distributions were generated using a multivariate normal random number generator consisting of 11 variables. The means and standard deviations for each variable are listed under Means and Sigma respectively.



Supplementary Table 2.2

| Estimated Two Cluster Model |          |          |         |         |         |         |         |         |         |         |         |         |
|-----------------------------|----------|----------|---------|---------|---------|---------|---------|---------|---------|---------|---------|---------|
| Means                       |          | Variable |         |         |         |         |         |         |         |         |         |         |
|                             |          | 1        | 2       | 3       | 4       | 5       | 6       | 7       | 8       | 9       | 10      | 11      |
| Cluster                     | 1        | 2.41276  | 2.4264  | 1.05602 | 6.02993 | 3.82545 | 6.17825 | 7.83046 | 9.14212 | 9.81959 | 0.92351 | 0.42968 |
|                             | 2        | 2.15408  | 2.20339 | 1.05094 | 5.87152 | 3.12812 | 6.13141 | 7.30849 | 9.21008 | 9.37979 | 0.63249 | 0.26084 |
| Covariance                  | Variable | 1        | 2       | 3       | 4       | 5       | 6       | 7       | 8       | 9       | 10      | 11      |
| Cluster 1                   | 1        | 0.87866  | -0.0651 | 0.05276 | 0.04614 | 0.08183 | -0.0553 | 0.1445  | -0.0399 | 0.06146 | 0.12042 | 0.12095 |
|                             | 2        | -0.0651  | 0.12048 | 0.00538 | 0.01383 | 0.02846 | 0.03183 | -0.1008 | 0.00634 | 0.07139 | -0.0268 | -0.0343 |
|                             | 3        | 0.05276  | 0.00538 | 0.05599 | 0.00359 | 0.03583 | 0.01867 | -0.0094 | 0.0072  | 0.03135 | -0.0005 | 0.01021 |
|                             | 4        | 0.04614  | 0.01383 | 0.00359 | 0.06156 | 0.03994 | 0.02873 | 0.02253 | 0.03366 | 0.04254 | 0.04244 | 0.01608 |
|                             | 5        | 0.08183  | 0.02846 | 0.03583 | 0.03994 | 0.34416 | -0.0086 | 0.02522 | 0.13695 | 0.04196 | 0.04953 | -0.035  |
|                             | 6        | -0.0553  | 0.03183 | 0.01867 | 0.02873 | -0.0086 | 0.11702 | 0.03837 | 0.03402 | -0.0015 | 0.01459 | 0.00156 |
|                             | 7        | 0.1445   | -0.1008 | -0.0094 | 0.02253 | 0.02522 | 0.03837 | 0.64788 | 0.14002 | -0.0933 | 0.13159 | -0.0034 |
|                             | 8        | -0.0399  | 0.00634 | 0.0072  | 0.03366 | 0.13695 | 0.03402 | 0.14002 | 0.35036 | 0.07319 | 0.05201 | -0.0469 |
|                             | 9        | 0.06146  | 0.07139 | 0.03135 | 0.04254 | 0.04196 | -0.0015 | -0.0933 | 0.07319 | 0.42658 | 0.02485 | 0.02224 |
|                             | 10       | 0.12042  | -0.0268 | -0.0005 | 0.04244 | 0.04953 | 0.01459 | 0.13159 | 0.05201 | 0.02485 | 0.15123 | 0.0791  |
|                             | 11       | 0.12095  | -0.0343 | 0.01021 | 0.01608 | -0.035  | 0.00156 | -0.0034 | -0.0469 | 0.02224 | 0.0791  | 0.19611 |
| Covariance                  | Variable | 1        | 2       | 3       | 4       | 5       | 6       | 7       | 8       | 9       | 10      | 11      |
| Cluster 2                   | 1        | 0.29432  | -0.0239 | 0.03014 | 0.06766 | 0.10269 | -0.0378 | 0.02776 | -0.0334 | -0.0488 | -0.0314 | 0.14848 |
|                             | 2        | -0.0239  | 0.13127 | -0.0015 | 0.00689 | -0.0398 | 0.0716  | 0.03279 | -0.0919 | 0.02203 | 0.01503 | 0.02645 |
|                             | 3        | 0.03014  | -0.0015 | 0.07576 | 0.03497 | 0.15223 | -0.0008 | 0.13279 | -0.0132 | -0.0242 | 0.00894 | -0.0131 |
|                             | 4        | 0.06766  | 0.00689 | 0.03497 | 0.15692 | 0.16669 | -0.0214 | 0.0743  | -0.0896 | -0.0866 | 0.02748 | -0.0099 |
|                             | 5        | 0.10269  | -0.0398 | 0.15223 | 0.16669 | 0.68923 | -0.0974 | 0.47091 | -0.1791 | -0.041  | 0.07102 | -0.0335 |
|                             | 6        | -0.0378  | 0.0716  | -0.0008 | -0.0214 | -0.0974 | 0.13077 | 0.01574 | -0.0852 | -0.0053 | 0.05371 | 0.03473 |
|                             | 7        | 0.02776  | 0.03279 | 0.13279 | 0.0743  | 0.47091 | 0.01574 | 0.48734 | -0.1808 | 0.0926  | 0.07875 | 0.01983 |
|                             | 8        | -0.0334  | -0.0919 | -0.0132 | -0.0896 | -0.1791 | -0.0852 | -0.1808 | 0.46144 | -0.0346 | -0.0149 | 0.02419 |
|                             | 9        | -0.0488  | 0.02203 | -0.0242 | -0.0866 | -0.041  | -0.0053 | 0.0926  | -0.0346 | 0.2354  | -0.0328 | 0.01535 |
|                             | 10       | -0.0314  | 0.01503 | 0.00894 | 0.02748 | 0.07102 | 0.05371 | 0.07875 | -0.0149 | -0.0328 | 0.09629 | 0.00637 |
|                             | 11       | 0.14848  | 0.02645 | -0.0131 | -0.0099 | -0.0335 | 0.03473 | 0.01983 | 0.02419 | 0.01535 | 0.00637 | 0.23125 |

Means and covariance matrix for each cluster generated in the Estimated Two Cluster model. The means for each of the 11 variables within each cluster are listed above the covariance matrices used to generate the data using multivariate normal random number generators.

Supplementary Table 2.3

| Estimated Three Cluster Model |          |          |         |         |         |         |         |         |         |         |         |         |
|-------------------------------|----------|----------|---------|---------|---------|---------|---------|---------|---------|---------|---------|---------|
| Means                         |          | Variable |         |         |         |         |         |         |         |         |         |         |
| Cluster                       |          | 1        | 2       | 3       | 4       | 5       | 6       | 7       | 8       | 9       | 10      | 11      |
|                               | 1        | 2.58006  | 2.46903 | 1.05126 | 6.07113 | 3.81232 | 6.20695 | 7.91822 | 9.10489 | 9.89962 | 0.96325 | 0.52826 |
|                               | 2        | 2.0921   | 2.3447  | 1.06516 | 5.95098 | 3.85062 | 6.12323 | 7.66225 | 9.21349 | 9.66618 | 0.84734 | 0.24075 |
|                               | 3        | 2.15408  | 2.20339 | 1.05094 | 5.87152 | 3.12812 | 6.13141 | 7.30849 | 9.21008 | 9.37979 | 0.63249 | 0.26084 |
| Covariance                    | Variable | 1        | 2       | 3       | 4       | 5       | 6       | 7       | 8       | 9       | 10      | 11      |
| Cluster 1                     | 1        | 0.72923  | -0.0599 | -0.0254 | 0.02776 | 0.09885 | -0.0845 | 0.00855 | -0.04   | -0.0736 | 0.10091 | 0.11139 |
|                               | 2        | -0.0599  | 0.09333 | 0.01431 | 0.01225 | 0.03817 | 0.02212 | -0.0622 | 0.01042 | 0.09915 | -0.0183 | -0.0353 |
|                               | 3        | -0.0254  | 0.01431 | 0.05121 | 0.01365 | 0.0444  | 0.02786 | -0.0245 | 0.02771 | 0.02918 | 0.01514 | 0.01952 |
|                               | 4        | 0.02776  | 0.01225 | 0.01365 | 0.05857 | 0.06756 | 0.03975 | -0.0134 | 0.03444 | 0.03935 | 0.02669 | 0.02364 |
|                               | 5        | 0.09885  | 0.03817 | 0.0444  | 0.06756 | 0.47158 | 0.01604 | 0.07334 | 0.1683  | 0.03001 | 0.10498 | -0.0304 |
|                               | 6        | -0.0845  | 0.02212 | 0.02786 | 0.03975 | 0.01604 | 0.1398  | 0.05691 | 0.06559 | 0.02986 | 0.00701 | -0.0108 |
|                               | 7        | 0.00855  | -0.0622 | -0.0245 | -0.0134 | 0.07334 | 0.05691 | 0.65972 | 0.20798 | -0.1576 | 0.12552 | -0.0046 |
|                               | 8        | -0.04    | 0.01042 | 0.02771 | 0.03444 | 0.1683  | 0.06559 | 0.20798 | 0.43466 | 0.10547 | 0.06139 | -0.039  |
|                               | 9        | -0.0736  | 0.09915 | 0.02918 | 0.03935 | 0.03001 | 0.02986 | -0.1576 | 0.10547 | 0.4701  | 0.01007 | 0.00096 |
|                               | 10       | 0.10091  | -0.0183 | 0.01514 | 0.02669 | 0.10498 | 0.00701 | 0.12552 | 0.06139 | 0.01007 | 0.10393 | 0.0386  |
|                               | 11       | 0.11139  | -0.0353 | 0.01952 | 0.02364 | -0.0304 | -0.0108 | -0.0046 | -0.039  | 0.00096 | 0.0386  | 0.15638 |
| Covariance                    | Variable | 1        | 2       | 3       | 4       | 5       | 6       | 7       | 8       | 9       | 10      | 11      |
| Cluster 2                     | 1        | 1.08671  | -0.1247 | 0.2188  | 0.04506 | 0.06861 | -0.0312 | 0.34    | -0.0054 | 0.25544 | 0.12985 | 0.0505  |
|                               | 2        | -0.1247  | 0.17467 | -0.0108 | 0.00754 | 0.01503 | 0.0467  | -0.2099 | 0.00843 | 0.00155 | -0.0566 | -0.0612 |
|                               | 3        | 0.2188   | -0.0108 | 0.07049 | -0.015  | 0.02157 | 0.00283 | 0.02244 | -0.0343 | 0.04085 | -0.0308 | -0.0046 |
|                               | 4        | 0.04506  | 0.00754 | -0.015  | 0.06278 | -0.0084 | 0.00209 | 0.07443 | 0.0445  | 0.03267 | 0.06782 | -0.0224 |
|                               | 5        | 0.06861  | 0.01503 | 0.02157 | -0.0084 | 0.11957 | -0.0565 | -0.0617 | 0.08372 | 0.07609 | -0.0537 | -0.0395 |
|                               | 6        | -0.0312  | 0.0467  | 0.00283 | 0.00209 | -0.0565 | 0.07708 | -0.0106 | -0.0195 | -0.0784 | 0.02413 | 0.0092  |
|                               | 7        | 0.34     | -0.2099 | 0.02244 | 0.07443 | -0.0617 | -0.0106 | 0.63612 | 0.03675 | -0.016  | 0.13443 | -0.0539 |
|                               | 8        | -0.0054  | 0.00843 | -0.0343 | 0.0445  | 0.08372 | -0.0195 | 0.03675 | 0.20516 | 0.03345 | 0.047   | -0.0445 |
|                               | 9        | 0.25544  | 0.00155 | 0.04085 | 0.03267 | 0.07609 | -0.0784 | -0.016  | 0.03345 | 0.33927 | 0.03727 | 0.0187  |
|                               | 10       | 0.12985  | -0.0566 | -0.0308 | 0.06782 | -0.0537 | 0.02413 | 0.13443 | 0.047   | 0.03727 | 0.24997 | 0.14341 |
|                               | 11       | 0.0505   | -0.0612 | -0.0046 | -0.0224 | -0.0395 | 0.0092  | -0.0539 | -0.0445 | 0.0187  | 0.14341 | 0.23413 |
| Covariance                    | Variable | 1        | 2       | 3       | 4       | 5       | 6       | 7       | 8       | 9       | 10      | 11      |
| Cluster 3                     | 1        | 0.29432  | -0.0239 | 0.03014 | 0.06766 | 0.10269 | -0.0378 | 0.02776 | -0.0334 | -0.0488 | -0.0314 | 0.14848 |
|                               | 2        | -0.0239  | 0.13127 | -0.0015 | 0.00689 | -0.0398 | 0.0716  | 0.03279 | -0.0919 | 0.02203 | 0.01503 | 0.02645 |
|                               | 3        | 0.03014  | -0.0015 | 0.07576 | 0.03497 | 0.15223 | -0.0008 | 0.13279 | -0.0132 | -0.0242 | 0.00894 | -0.0131 |
|                               | 4        | 0.06766  | 0.00689 | 0.03497 | 0.15692 | 0.16669 | -0.0214 | 0.0743  | -0.0896 | -0.0866 | 0.02748 | -0.0099 |
|                               | 5        | 0.10269  | -0.0398 | 0.15223 | 0.16669 | 0.68923 | -0.0974 | 0.47091 | -0.1791 | -0.041  | 0.07102 | -0.0335 |
|                               | 6        | -0.0378  | 0.0716  | -0.0008 | -0.0214 | -0.0974 | 0.13077 | 0.01574 | -0.0852 | -0.0053 | 0.05371 | 0.03473 |
|                               | 7        | 0.02776  | 0.03279 | 0.13279 | 0.0743  | 0.47091 | 0.01574 | 0.48734 | -0.1808 | 0.0926  | 0.07875 | 0.01983 |
|                               | 8        | -0.0334  | -0.0919 | -0.0132 | -0.0896 | -0.1791 | -0.0852 | -0.1808 | 0.46144 | -0.0346 | -0.0149 | 0.02419 |
|                               | 9        | -0.0488  | 0.02203 | -0.0242 | -0.0866 | -0.041  | -0.0053 | 0.0926  | -0.0346 | 0.2354  | -0.0328 | 0.01535 |
|                               | 10       | -0.0314  | 0.01503 | 0.00894 | 0.02748 | 0.07102 | 0.05371 | 0.07875 | -0.0149 | -0.0328 | 0.09629 | 0.00637 |
|                               | 11       | 0.14848  | 0.02645 | -0.0131 | -0.0099 | -0.0335 | 0.03473 | 0.01983 | 0.02419 | 0.01535 | 0.00637 | 0.23125 |

Means and covariance matrix for each cluster generated in the Estimated Three Cluster model. The means for each of the 11 variables within each cluster are listed above the covariance matrices used to generate the data using multivariate normal random number generators.

### 3 Examining the association between blood-based biomarkers and human post-mortem neuropathology in the University of Kentucky Alzheimer's Disease Research Center autopsy cohort

Zachary Winder<sup>1,2</sup>, Tiffany L. Sudduth<sup>1</sup>, Sonya Anderson<sup>1</sup>, Ela Patel<sup>1</sup>, Janna Neltner<sup>1,3</sup>, Barbara J. Martin<sup>1</sup>, Katherine E. Snyder<sup>1</sup>, Erin L. Abner<sup>5</sup>, Gregory A. Jicha<sup>1,4</sup>, Peter T. Nelson<sup>1,3</sup>, Donna M. Wilcock<sup>1,2\*</sup>

University of Kentucky, <sup>1</sup>Sanders-Brown Center on Aging, College of Medicine, Departments of <sup>2</sup>Physiology, <sup>3</sup>Pathology and Laboratory Medicine, <sup>4</sup>Neurology, College of Public Health, <sup>5</sup>Department of Epidemiology, Lexington KY 40536, USA.

#### 3.1 Abstract

**INTRODUCTION:** Clinically, detection of disease-causing pathology associated with AD and VCID is limited to MRI and PET scans, which are expensive and not widely accessible. Here, we assess angiogenic, inflammatory, and AD-related plasma biomarkers to determine their relationships with human post-mortem neuropathology.

**METHOD:** Plasma samples were analyzed using a digital immunoassay and pathological evaluation was performed by UK-ADRC neuropathologists. The association of plasma markers with neuropathology was estimated via proportional odds and logistic regressions adjusted for age.

**RESULTS:** Included cases (N = 90) showed increased Tau/A $\beta$  42 ratio, GFAP, VEGF-A, and PIGF were positively associated with higher level of AD neuropathological change, while higher A $\beta$ 42/A $\beta$ 40 ratio was inversely associated. Higher PIGF, VEGF-A and IL-6 were

inversely associated with chronic cerebrovascular disease, while A $\beta$ 42/A $\beta$ 40 ratio was positively associated.

DISCUSSION: Our results provide support for the continued study of plasma biomarkers as a clinical screening tool for AD and VCID pathology.

### 3.2 Introduction

Alzheimer's Disease (AD) and Vascular Contributions to Cognitive Impairment and Dementia (VCID) are often co-morbid in patients with dementia[8, 206]. Currently, these conditions are diagnosed using cognitive evaluations and neuroimaging studies[122, 128]. Diagnosis typically comes well into the course of the disease as patients do not often show cognitive decline until years after amyloid pathology begins to develop[207]. Blood-based biomarkers of disease have only been possible in recent years because we previously lacked the necessary sensitivity to measure relevant biomarkers accurately[208]. Recently, technological developments have made measuring picogram per mL concentrations more reliable using Single-molecule enzyme-linked immunosorbent assays (SiMoAs)[185, 186]. However, the relation between these new blood-based biomarkers and neuropathologically evaluated disease remains unclear.

The current standard for neuropathological evaluation of AD is the 2012 National Institute on Aging-Alzheimer's Association ("ABC") guidelines, which include three measures of pathology[14]. The "A" component, Thal staging, evaluates distribution of amyloid beta plaques, noting progression from the neocortical brain region to the brainstem and cerebellum[23]. The "B" component, Braak staging, evaluates the distribution of neurofibrillary tangles as they progress from the entorhinal cortex to the

neocortex[209]. The “C” component, Consortium to Establish a Registry in Alzheimer’s Disease (CERAD) scores, evaluates the density of neuritic plaques in the neocortex[37]. Together, these scores describe the degree to which AD neuropathological changes (ADNC) have occurred[14]. Clinically, more severe neuritic plaque (“C”) and neurofibrillary tangle ratings (“B”) have been shown repeatedly to correlate with cognitive impairment and dementia[14]. While PET neuroimaging has been shown to identify brain amyloid and tau *in vivo*, it remains costly and inaccessible for most of the population[41, 210].

VCID encompasses multiple cerebrovascular pathologies that affect cognition, such as arteriolosclerosis, cerebral amyloid angiopathy (CAA), and microinfarctions[206]. Clinically, cerebral small vessel disease (cSVD), a subtype of VCID characterized by arteriolosclerosis and microinfarctions, is diagnosed based on white matter hyperintensities (WMH) seen on MRI[127, 134]. These pathologies may be evaluated on autopsy by a neuropathologist and are scored in different ways. Arteriolosclerosis and CAA, for example, may be rated from none to severe, while infarctions are often counted in multiple sampled sections throughout the brain[126, 211].

Fluid biomarkers can be used as both diagnostic and prognostic indicators to assist the physician in their decision-making process and are vital to the rapidly developing treatment of dementia[38, 40]. Currently, several CSF biomarkers are available for clinical evaluation of A $\beta$ 42, A $\beta$ 40, and tau levels, which correlate well with observed AD neuropathology[62]. However, the procedure for collecting CSF, a lumbar puncture, remains invasive and frightening for many patients.

Plasma and serum biomarkers, such as A $\beta$ 42 to A $\beta$ 40 ratio; pTau181, a phospho-epitope of tau; and GFAP have been studied using SiMoAs and ultrasensitive immunoassays. These studies show positive correlations between biomarker levels in the plasma and the CSF, and distinct differences between AD patients and controls[40, 104, 212]. Specifically, the ratio of A $\beta$ 42 to A $\beta$ 40 has been shown to be reduced in the plasma of patients with AD compared to controls[72-75]. GFAP, as measured in serum, has also been shown to differentiate AD patients from cognitively normal controls[104]. Studies have also demonstrated that plasma pTau181 is both positively and significantly associated with tau PET entorhinal cortex SUVR in patients with A $\beta$  PET positivity based on SUVR[213]. Plasma biomarker development for VCID is less developed than for AD but is rapidly catching up, in large part due to the MarkVCID consortium founded in 2016. MarkVCID aims to identify and validate both fluid and neuroimaging biomarkers for VCID in a multi-center cohort[214].

Plasma biomarkers are much less expensive than neuroimaging, more easily accessible to patients, and they are minimally invasive. In the current study, we evaluated the relationship between a set of plasma-based angiogenic, inflammatory, and neurodegenerative biomarkers measured during the last two years of life and neuropathological hallmarks of AD and VCID observed at autopsy. Study participants were drawn from the longitudinal cohort study at the University of Kentucky Alzheimer's Disease Research Center.

### 3.3 Methods

#### 3.3.1 Participant Selection and Plasma Collection

Participants in this study were selected from the cohort enrolled at the University of Kentucky Alzheimer's Disease Research Center (UK-ARDC) who had died and come to brain autopsy (N = 916). The UK-ADRC recruitment procedures and other methods have been previously described[215]. Briefly, participants consented to approximately annual study visits that included cognitive testing, physical examination, neurological examination, medical history, and other measures, and brain autopsy upon death. All participants provided written informed consent for their participation in UK-ADRC research activities, which were approved by the University of Kentucky Institutional Review Board.

Beginning in 2012, plasma samples were collected during annual study visits by venous puncture using 10 mL EDTA Vacutainer tubes; prior to 2012 only heparinized vacutainer tubes were used. Participants were selected for the current study if they had a banked plasma sample that was collected in an EDTA tube and within the two years prior to death (N = 90). One sample per participant, closest to death, was retrieved for this study.

#### 3.3.2 Plasma Sample Analysis

Plasma samples were stored at -80°C until retrieved and thawed on ice. Samples were then centrifuged at 4°C for 10 minutes at maximum speed (approx. 21,000 x g). Samples were then plated at room temperature using the dilutions listed (Table 3.1) and run on the Quanterix Simoa HD-X in duplicate[186]. Simoa immunoassays for

phosphorylated threonine-181 tau (pTau181), neurofilament light (NfL), total Tau (Tau), amyloid beta 42 (A $\beta$ 42), amyloid beta 40 (A $\beta$ 40), tumor necrosis factor alpha (TNF $\alpha$ ), glial fibrillary acidic protein (GFAP), transforming growth factor beta (TGF $\beta$ ), interleukin 10 (IL10), interleukin 6 (IL6), interleukin 8 (IL8), matrix metalloproteinase 9 (MMP9), vascular endothelial growth factor A (VEGF-A), and placental growth factor (PlGF) were run. Due to limited quantities of plasma from some participants, sample size was reduced for pTau181 and TNF $\alpha$  assessments (Table 3.2).

After the run completed, data were retrieved, and the results were multiplied by the dilution factor. All biomarkers were log transformed and outliers from each biomarker set were removed using the generalized extreme studentized deviate test: VEGF-A (N = 1), MMP9 (N = 1), TGF $\beta$  (N = 1), A $\beta$  42 (N = 1), Tau (N = 3), A $\beta$  42/ A $\beta$  40 Ratio (N = 1), Tau/ A $\beta$  42 Ratio (N = 3), TNF $\alpha$  (N = 4).

### 3.3.3 Neuropathology

#### 3.3.3.1 Assessments

All assessments were performed blind to clinical and biomarker information. Neuropathological assessments for AD were conducted using the National Institute on Aging–Alzheimer’s Association (NIA-AA) guidelines (i.e., Thal phase, Braak Stage, and CERAD plaque ratings)[211].

#### 3.3.3.2 Data Operationalizations

Thal phase, Braak Stage, and CERAD ratings were converted to the scoring of the NIA-AA guidelines (each on a 0-3 scale), and AD neuropathologic change (ADNC) was categorized according to the guidelines[211]. For analysis of the individual components,



Braak stage and CERAD ratings were dichotomized, such that the lowest two scores (0 and 1) were combined as well as the highest two scores (2 and 3), due to small numbers of cases with the highest and lowest ratings. Assessments of CAA and global arteriolosclerosis utilized the ordinal rating scales from the NACC Neuropathology Data Element Dictionary (v10) with responses (scored as 0–3) to designate ‘none’, ‘mild’, ‘moderate’ or ‘severe’, respectively. Due to small cell sizes, ‘moderate’ and ‘severe’ categories were combined for both CAA and global arteriolosclerosis.

Chronic vascular grade was determined using a novel ordinal rating system to assess global level of cSVD. Brains were graded by a neuropathologist on a scale from 0-3, where 0 indicated no signs of arteriolosclerosis, atherosclerosis, other small vessel changes, or infarctions. A score of 1 denotes arteriolosclerosis, atherosclerosis, or other small vessel changes but with no infarctions, while a score of 2 indicates small vessel changes with chronic microinfarctions. A score of 3 represents small vessel changes with chronic gross infarcts. Analysis of chronic vascular grade excluded participants with a score of 3 as this model focused on the relationship between small vessel disease and plasma biomarkers.

#### 3.3.4 Statistical Analysis

Proportional odds and binary logistic regression models were used to evaluate the relationship between plasma biomarkers (independent variable) and different vascular and AD neuropathologies (dependent variable). Proportional odds logistic models were used for neuropathologies with ordinal measurements, i.e., CAA, arteriolosclerosis, chronic vascular grade, and A $\beta$  plaque score. Binary logistic models

were for binary outcome measurements, i.e., dichotomized Braak stage and neuritic plaque score. All models were adjusted for age of the participant at autopsy, and separate models were estimated for each pathology and biomarker; sample size for each model is reported in table 2. Odds ratios obtained from the model results indicate the relative change in age-adjusted odds of more severe pathology for a 1-unit increase in the log-transformed plasma biomarker level.

Sensitivity analysis was conducted to assess the robustness of the results to the inclusion of sex, hypertension (yes vs. no), diabetes (yes vs. no), and *APOE*ε4 allele status (any vs. none) as additional covariates. All data analysis was performed with MATLAB. Statistical significance was set at 0.05. False discovery rate for multiple comparison testing was conducted for each neuropathology analysis independently using the Benjamini-Hochberg method.[216]

### 3.4 Results

#### 3.4.1 Study Participant Characterization

Participants from the UK-ADRC autopsy cohort with banked plasma samples within two years of death were included in this study (N = 90). The sample was mean age 82.0±9.2 years at autopsy and comprised 46.7% female participants (Table 3.3). This sub-population is comparable in age at death, 82.8±9.3 years, but with a smaller percentage of females (58.9% female) than the larger autopsy cohort. A self-reported history of hypertension and diabetes, both risk factors for vascular dementia, was found in 72.2% and 21.4% of the study population, respectively (Table 3.3); both were greater than the observed proportions in the larger autopsy cohort of 65.8% and 17.7%, respectively[217,

218]. A relatively high proportion of the study sample, 37.5%, carried at least one *APOEε4* allele (Table 3.3), which is comparable to the larger autopsy cohort at 43.0%. Clinically, 46.1% of participants were cognitively normal at their last clinical visit, 38.2% were diagnosed with dementia, while 12.8% had a final diagnosis of mild cognitive impairment (MCI). A small number (3.4%) were mildly impaired on cognitive testing but did not meet criteria for MCI. This contrasts with the larger autopsy cohort which had a 52.1% dementia diagnosis, 33.6% cognitively normal, 8.1% mild cognitively impaired, and 6.2% were mildly impaired on cognitive testing but did not meet the criteria for MCI.

CERAD neuritic plaque scores of 0 or 1 were found in 58% of included cases (Table 3.4). NFT stage had a similar distribution, with B scores of 0 and 1 observed in 49% of the sample (Table 3.4). More severe stages of arteriolosclerosis and CAA were less common, with moderate or severe stages showing 27% for cerebral arteriolosclerosis, and 16% in cerebral amyloid angiopathy (Table 3.4). Lastly, higher levels of A $\beta$  plaque score were commonly seen in this cohort at 24% for a score 2 and 51% for a score of 3.

#### 3.4.2 Biomarkers for Pathological Hallmarks of Alzheimer's Disease

We hypothesized that pTau181 would be positively correlated with more severe AD pathology, while A $\beta$ 42/40 ratio would be inversely correlated with more severe AD pathology. Additionally, we sought to determine whether there are novel candidate plasma biomarkers that may have relationships with AD pathology.

Consistent with our hypothesis, age-adjusted odds ratios (OR) for a 1-unit increase in log-transformed pTau181 (OR: 1.11; 95% CI: 0.81-1.51;  $p = 0.51$ ) and A $\beta$ 42/40 ratio (OR: 0.55; 95% CI: 0.17-1.79;  $p = 0.32$ ) were positively and inversely

correlated with higher Thal A $\beta$  plaque score, respectively (Figure 3.1A), though the associations were not statistically significant. Tau/A $\beta$ 42 ratio (OR: 1.89; 95% CI: 0.86-4.19;  $p = 0.11$ ) was also associated with higher Thal A $\beta$  plaque score (Figure 3.1A). The age-adjusted OR for GFAP (OR: 1.77; 95% CI: 0.94-3.33;  $p = 0.08$ ) and IL-6 (OR: 1.25; 95% CI: 0.80-1.94;  $p = 0.33$ ) showed a positive relationship with Thal A $\beta$  plaque score, while the age-adjusted ORs for VEGF-A (OR: 1.36; 95% CI: 1.05-1.76;  $p = 0.02$ ) and PIGF (OR: 1.22; 95% CI: 0.91-1.64;  $p = 0.17$ ) were also positively associated with higher Thal A $\beta$  plaque score, with the VEGF-A association having statistical significance (Figure 3.1A), which was subsequently reduced to non-statistical significance after multiple comparison testing (Adj.  $p = 0.34$ , Table 3.5).

Using a binary logistic regression model, we saw that Braak NFT stage had similar relationships with our tested biomarkers compared to the other AD pathologies: Tau/A $\beta$ 42 ratio (OR: 1.39; 95% CI: 0.61-3.15;  $p = 0.43$ ) and NfL (OR: 1.64; 95% CI: 0.82-3.25;  $p = 0.16$ ), were positively associated with Braak NFT stage, while A $\beta$ 42/40 ratio (OR: 0.46; 95% CI: 0.12-1.69;  $p = 0.24$ ) showed an inverse relationship (Figure 3.1B). Unexpectedly, pTau181 (OR: 0.86; 95% CI: 0.62-1.19;  $p = 0.37$ ) also showed an inverse relationship with Braak NFT stage. GFAP (OR: 1.42; 95% CI: 0.71-2.82;  $p = 0.32$ ), IL-6 (OR: 1.37; 95% CI: 0.83-2.28;  $p = 0.22$ ), VEGF-A (OR: 1.20; 95% CI: 0.91-1.59;  $p = 0.20$ ), and PIGF (OR: 1.19; 95% CI: 0.85-1.65;  $p = 0.32$ ) all had positive age-adjusted associations with Braak NFT stage (Figure 3.1B).

For neuritic plaques, the age-adjusted OR for pTau181 (OR: 1.08; 95% CI: 0.79-1.48;  $p = 0.62$ ), Tau/A $\beta$ 42 ratio (OR: 1.96; 95% CI: 0.85-4.52;  $p = 0.12$ ), and Tau (OR:

2.16; 95% CI: 1.04-4.49;  $p = 0.04$ ) were positively associated with higher (worse) plaque scores, while  $A\beta_{42}/40$  ratio (OR: 0.43; 95% CI: 0.12-1.60;  $p = 0.21$ ) was inversely associated (Figure 3.1C). Inflammatory plasma biomarkers GFAP (OR: 2.22; 95% CI: 1.04-4.77;  $p = 0.04$ ) and IL-6 (OR: 1.18; 95% CI: 0.74-1.89;  $p = 0.48$ ), and angiogenic plasma biomarkers VEGF-A (OR: 1.15; 95% CI: 0.87-1.50;  $p = 0.33$ ) PIGF (OR: 1.13; 95% CI: 0.83-1.53;  $p = 0.43$ ), had positive associations with more frequent neuritic plaques (Figure 3.1C).

The magnitudes and directions of the age-adjusted ORs between the biomarkers and ADNC (rather than its individual components) were similar to the individual components (Figure 3.1D). Tau/ $A\beta_{42}$  ratio (OR: 1.84; 95% CI: 0.85-4.01;  $p = 0.12$ ), NfL (OR: 1.79; 95% CI: 0.96-3.36;  $p = 0.07$ ), GFAP (OR: 1.72; 95% CI: 0.92-3.24;  $p = 0.09$ ), IL-6 (OR: 1.46; 95% CI: 0.91-2.33;  $p = 0.11$ ), VEGF-A (OR: 1.21; 95% CI: 0.94-1.56;  $p = 0.15$ ), and PIGF (OR: 1.24; 95% CI: 0.91-1.68;  $p = 0.17$ ) were positively associated with worse ADNC, while  $A\beta_{42}/40$  ratio (OR: 0.31; 95% CI: 0.09-1.04;  $p = 0.06$ ) was inversely associated (Figure 3.1D). Sensitivity analyses including additional covariates sex, hypertension, diabetes, and *APOEε4* allele did not affect the magnitude or direction of the associations described.

### 3.4.3 Biomarkers for Pathological Cerebral Small Vessel Disease

We hypothesized that increased levels of VEGF-A and PIGF would correlate with higher levels of cSVD pathology, and we sought to evaluate the relationship between additional angiogenic, inflammatory, and AD-related plasma biomarkers with cSVD pathology.

Our analysis demonstrated that PIGF (OR: 1.35; 95%CI: 1.00-1.82;  $p < 0.05$ ) had a statistically significant positive age-adjusted association, which was subsequently reduced to non-statistical significance after multiple comparison testing (Adj.  $p = 0.55$ , Table 3.6), while VEGF-A (OR: 1.07; 95% CI: 0.82-1.40;  $p = 0.61$ ) had a positive association with more severe CAA (Figure 3.2A). IL-6 (OR: 1.28; 95% CI: 0.81-2.03;  $p = 0.30$ ) and pTau181 (OR: 1.32; 95% CI: 0.97-1.81;  $p = 0.08$ ) also had positive associations with more severe CAA (Figure 3.2A). MMP9 (OR: 0.64; 95%CI: 0.38-1.09;  $p = 0.10$ ) and Tau/A $\beta$ 42 ratio (OR: 0.63; 95% CI: 0.26-1.51;  $p = 0.29$ ) had inverse associations with CAA severity (Figure 3.2A).

Contrary to our hypothesis, PIGF (OR: 0.81; 95% CI: 0.60-1.09;  $p = 0.16$ ) had an inverse association with more severe cerebral arteriolosclerosis, while VEGF-A (OR: 1.00; 95% CI: 0.78-1.28;  $p = 0.99$ ) had no association. MMP9 (OR: 0.78; 95% CI: 0.47-1.28;  $p = 0.32$ ), IL-6 (OR: 0.68; 95% CI: 0.43-1.07;  $p = 0.10$ ), and Tau/A $\beta$ 42 ratio (OR: 0.71; 95% CI: 0.33-1.52;  $p = 0.38$ ) all had an inverse association with more severe cerebral arteriolosclerosis, while A $\beta$ 42/40 ratio (OR: 1.73; 95% CI: 0.53-5.66;  $p = 0.36$ ) had a positive association (Figure 3.2B).

PIGF (OR: 0.90, 95% CI: 0.67-1.22;  $p = 0.49$ ), VEGF-A (OR: 0.80; 95% CI: 0.60-1.07;  $p = 0.14$ ), and MMP9 (OR: 0.94; 95% CI: 0.53-1.65;  $p = 0.82$ ) all showed an inverse association with more severe chronic cerebrovascular grade, although the magnitude of the relationships was small (Figure 3.2C). IL-6 (OR: 0.43; 95% CI: 0.25-0.75;  $p < 0.01$ ) was the only biomarker to show a statistically significant inverse relationship with more severe chronic vascular grade (Figure 3.2C), which maintained statistical significance after

multiple comparison testing (Adj.  $p = 0.04$ , Table 3.6). The largest magnitude of association was observed between  $A\beta_{42/40}$  ratio (OR: 2.23; 95% CI: 0.63-7.93;  $p = 0.22$ ) and worse chronic vascular grade (Figure 3.2C). Sensitivity analyses did not affect the magnitude or direction of the associations described.

### 3.5 Discussion

In this study, we evaluated whether plasma-based biomarkers correlated to AD neuropathology at autopsy in 90 participants from the UK-ADRC cohort who had a blood draw within two years prior to death. Additionally, we evaluated how these markers correlated with pathology associated with cSVD. Biomarkers that allow clinicians to diagnose and monitor the level of neuropathology in patients is a crucial step towards identifying at-risk but not yet symptomatic populations, who may be more amenable to potential therapeutics. Currently, studies have shown that plasma pTau181 and  $A\beta_{42/40}$  ratio are highly correlated with amyloid and tau PET measures, with the potential to act as a more cost-effective and accessible yearly screening tool to evaluate the progression of AD[62].

As previously reported in the literature[72-75, 104], GFAP had a positive association and  $A\beta_{42/40}$  ratio had an inverse association with Braak NFT stage, CERAD neuritic plaque scores, Thal Ab plaque scores, and combined AD neuropathologic change. While most of our results were not statistically significant, this was not unexpected given our limited sample size. Interestingly, in our sample, Tau/ $A\beta_{42}$  ratio had a positive association with all the AD neuropathologies investigated. In contrast, pTau181 had a smaller magnitude of association with Thal  $A\beta$  plaque scores and CERAD

neuritic plaque scores, and even had an inverse relationship with Braak NFT stage. Due to the small sample size in analyses using pTau 181, additional studies are required to validate the direction and magnitude of these findings.

A novel finding was the relationships between VEGF-A and PIGF with AD neuropathologies. Our data showed that both VEGF-A and PIGF had positive associations with NFT stage, neuritic plaque score, Ab plaque score, and ADNC. We hypothesize that the association between VEGF-A and AD neuropathology may be mediated by increased IL-1b as a result of inflammation.[219, 220] This result suggests further studies are needed to examine the effect of elevated levels of vascular plasma biomarkers on isolated AD pathologies and how this effect is mediated by inflammation.

For cerebrovascular pathologies, our initial hypothesis was that vascular markers such as PIGF and VEGF-A would show a positive association since it has been shown that these proteins play a major role in the development of new blood vessels, which can occur post vascular injury[116, 173, 174]. While PIGF had a positive association with CAA, it had an inverse association with arteriolosclerosis and chronic vascular grade. VEGF-A had similar results as PIGF, where it had a slightly positive association with cerebral amyloid angiopathy, no association with arteriolosclerosis, and an inverse association with chronic vascular grade. These results suggest new questions regarding the role that these vascular markers play in the development of cerebrovascular pathology in individuals close to death. Two novel markers for cSVD that stood out were A $\beta$ 42/40 ratio and IL-6. A $\beta$ 42/40 ratio had a strong positive association with cerebral arteriolosclerosis and chronic vascular grade, while IL-6 showed an inverse relationship



with cerebral arteriolosclerosis and chronic vascular grade. More studies will have to be conducted to validate these results and understand the mechanism of these two plasma markers as biomarkers of cerebrovascular disease.

This study has some limitations. The sample size led to wide 95% confidence intervals for the age-adjusted odds ratios. While we did observe one statistically significant relationship after multiple comparison testing, many of the relationships we observed would require a larger sample size to demonstrate a statistically significant association, should the association truly exist. The cohort used for this study was a convenience sample comprising a heterogeneous mix of clinical diagnoses and neuropathological classification. While this provided us with a wide range of participants from which we could explore the relationships between neuropathologies and plasma biomarkers, we are not able to isolate the influence one pathology has on the expression of one biomarker. For example, when examining associations between A $\beta$ 42/40 ratio and cerebrovascular pathology, we note that those cases also have AD pathology. Cohorts designed specifically to validate biomarker associations with particular pathologies are needed.

While CSF biomarkers of AD pathology have been validated for clinical use, plasma biomarkers still require more studies[40, 62]. This study was one of the first to evaluate the direction and magnitude of the relationships between AD and cerebrovascular pathologies and plasma biomarkers in a community-based cohort. These associations may prove critical in diagnosing and monitoring the progression of

AD and cerebrovascular pathologies, by using a widely accessible and inexpensive routine clinical testing tool that can safely be administered to patients.

Table 3.1 Sample Size For Each Pathology

| Sample Size (N)       | Arteriolosclerosis | CAA | Chronic Vascular Grade | Thal | Braak | CERAD | AD Neuropathologic Change |
|-----------------------|--------------------|-----|------------------------|------|-------|-------|---------------------------|
| <b>PIGF</b>           | 83                 | 83  | 71                     | 83   | 79    | 83    | 79                        |
| <b>VEGF-A</b>         | 89                 | 89  | 75                     | 89   | 85    | 89    | 85                        |
| <b>MMP9</b>           | 89                 | 89  | 75                     | 89   | 85    | 89    | 85                        |
| <b>IL8</b>            | 90                 | 90  | 76                     | 90   | 86    | 90    | 86                        |
| <b>IL6</b>            | 89                 | 89  | 75                     | 89   | 85    | 89    | 85                        |
| <b>IL10</b>           | 88                 | 88  | 74                     | 88   | 85    | 88    | 85                        |
| <b>TGFb</b>           | 65                 | 65  | 52                     | 65   | 63    | 65    | 63                        |
| <b>GFAP</b>           | 84                 | 84  | 72                     | 84   | 81    | 84    | 81                        |
| <b>Aβ40</b>           | 82                 | 82  | 70                     | 82   | 79    | 82    | 79                        |
| <b>Aβ42</b>           | 81                 | 81  | 69                     | 81   | 78    | 81    | 78                        |
| <b>Tau</b>            | 80                 | 80  | 69                     | 80   | 77    | 80    | 77                        |
| <b>NfL</b>            | 83                 | 83  | 71                     | 83   | 80    | 83    | 80                        |
| <b>Aβ4240 Ratio</b>   | 81                 | 81  | 69                     | 81   | 78    | 81    | 78                        |
| <b>Tau/Aβ42 Ratio</b> | 79                 | 79  | 68                     | 79   | 76    | 79    | 76                        |
| <b>TNFa</b>           | 36                 | 36  | 32                     | 36   | 35    | 36    | 35                        |
| <b>pTau-181</b>       | 52                 | 52  | 45                     | 52   | 49    | 52    | 49                        |

Sample size (N) for each model

Table 3.2 Simoa Biomarker Dilutions

| Assay        | Dilution | Catalog Number | LLOQ        | LOD         | Dynamic Range |
|--------------|----------|----------------|-------------|-------------|---------------|
| Neuro3PlexA  | 1:20     | 101995         |             |             |               |
| A $\beta$ 40 |          |                | .675 pg/ml  | .196 pg/ml  | 0-560 pg/ml   |
| A $\beta$ 42 |          |                | .142 pg/ml  | .045 pg/ml  | 0-240 pg/ml   |
| Tau          |          |                | .063 pg/ml  | .019 pg/ml  | 0-400 pg/ml   |
| NfL          | 1:25     | 103186         | .174 pg/ml  | .038 pg/ml  | 0-1800 pg/ml  |
| pTau181 V2   | NEAT     | 103714         | .085 pg/ml  | .028 pg/ml  | 0-424 pg/ml   |
| TNF $\alpha$ | 1:5      | 101580         | .034 pg/ml  | .016 pg/ml  | 0-200 pg/ml   |
| GFAP         | 1:10     | 102336         | .686 pg/ml  | .221 pg/ml  | 0-4000 pg/ml  |
| IL6          | 1:2      | 101622         | .010 pg/ml  | .0055 pg/ml | 0-120 pg/ml   |
| IL8          | NEAT     | 100198         | .0921 pg/ml | .0560 pg/ml | 0-300 pg/ml   |
| IL10         | 1:2      | 101643         | .021 pg/ml  | .0038 pg/ml | 0-120 pg/ml   |
| PLGF         | NEAT     | 102318         | .30 pg/ml   | .064 pg/ml  | 0-960 pg/ml   |
| VEGF         | 1:2      | 102794         | .137 pg/ml  | .041 pg/ml  | 0-800 pg/ml   |
| MMP9         | 1:500    | 102491         | 4.88 pg/ml  | .581 pg/ml  | 0-5000 pg/ml  |
| TGFb         | NEAT     | 101984         | .514 pg/ml  | .137 pg/ml  | 0-24000 pg/ml |

Dilutions required for quantification for Simoa biomarkers. Lower limit of quantification (LLOQ) and limit of detection (LOD) used to determine dilution.

Table 3.3 Participant Characteristics

| Characteristic                  | Summary*     |
|---------------------------------|--------------|
| Age at autopsy, years           | 82.0 ± 9.2   |
| Female sex                      | 46.6%        |
| Ever Hypertension               | 72.2%        |
| Ever Diabetes                   | 21.4%        |
| ≥ 1 APOE e4 allele              | 37.5%        |
| Last clinical diagnosis         |              |
| Normal cognition                | 46.1%        |
| Impaired but not MCI            | 3.4%         |
| Mild Cognitive Impairment (MCI) | 12.4%        |
| Dementia                        | 38.2%        |
| MMSE                            | 24.12 ± 8.40 |

Characteristics of included autopsied participants from the UK-ADRC cohort (N=90)

\*All results are mean±SD or proportion

Table 3.4 Neuropathological Lesion Distribution

| Neuropathology                                       | % of Cohort     |
|--|-----------------|
| A $\beta$ Plaque Score (0/1/2/3)*                    | 12%/13%/24%/51% |
| NFT Stage (0/1/2/3)*                                 | 4%/45%/10%/41%  |
| Neuritic Plaque Score (0/1/2/3)*                     | 55%/3%/9%/33%   |
| AD Neuropathologic Change (No/Low/Intermediate/High) | 13%/36%/13%/38% |
| Amyloid Angiopathy (None/Mild/Moderate/Severe)       | 63%/21%/2%/14%  |
| Arteriolosclerosis (None/Mild/Moderate/Severe)       | 32%/41%/22%/5%  |
| Chronic Vascular Grade (0/1/2)**                     | 22%/53%/25%     |

Distribution of neuropathological lesions in included autopsied participants from UK-ADRC (N=90)

\* NIA-AA guideline scores of 0-3

\*\* Increasing cSVD pathology from 0-2

Table 3.5 p-Values and Adjusted p-Values for Plasma Biomarkers and AD Neuropathology

| Neuropathology              | Biomarker                 | p-value | Adjusted p-value |
|-----------------------------|---------------------------|---------|------------------|
| Thal A $\beta$ Plaque Score | PIGF                      | 0.17    | 0.56             |
| Thal A $\beta$ Plaque Score | VEGF                      | 0.02    | 0.34             |
| Thal A $\beta$ Plaque Score | MMP9                      | 0.75    | 0.86             |
| Thal A $\beta$ Plaque Score | IL8                       | 0.70    | 0.86             |
| Thal A $\beta$ Plaque Score | IL6                       | 0.33    | 0.75             |
| Thal A $\beta$ Plaque Score | IL10                      | 0.59    | 0.86             |
| Thal A $\beta$ Plaque Score | TGF $\beta$               | 1.00    | 1.00             |
| Thal A $\beta$ Plaque Score | GFAP                      | 0.08    | 0.56             |
| Thal A $\beta$ Plaque Score | TNF $\alpha$              | 0.39    | 0.78             |
| Thal A $\beta$ Plaque Score | A $\beta$ 40              | 0.72    | 0.86             |
| Thal A $\beta$ Plaque Score | A $\beta$ 42              | 0.93    | 0.99             |
| Thal A $\beta$ Plaque Score | TotalTau                  | 0.17    | 0.56             |
| Thal A $\beta$ Plaque Score | NfL                       | 0.71    | 0.86             |
| Thal A $\beta$ Plaque Score | A $\beta$ 42/40ratio      | 0.32    | 0.75             |
| Thal A $\beta$ Plaque Score | TotalTauA $\beta$ 42ratio | 0.11    | 0.56             |
| Thal A $\beta$ Plaque Score | pTau 181                  | 0.51    | 0.86             |
| Braak NFT Stage             | PIGF                      | 0.32    | 0.63             |
| Braak NFT Stage             | VEGF                      | 0.20    | 0.63             |
| Braak NFT Stage             | MMP9                      | 0.82    | 0.82             |
| Braak NFT Stage             | IL8                       | 0.59    | 0.73             |
| Braak NFT Stage             | IL6                       | 0.22    | 0.63             |
| Braak NFT Stage             | IL10                      | 0.43    | 0.63             |
| Braak NFT Stage             | TGF $\beta$               | 0.72    | 0.82             |
| Braak NFT Stage             | GFAP                      | 0.32    | 0.63             |
| Braak NFT Stage             | TNF $\alpha$              | 0.28    | 0.63             |
| Braak NFT Stage             | A $\beta$ 40              | 0.47    | 0.63             |
| Braak NFT Stage             | A $\beta$ 42              | 0.80    | 0.82             |
| Braak NFT Stage             | TotalTau                  | 0.28    | 0.63             |
| Braak NFT Stage             | NfL                       | 0.16    | 0.63             |
| Braak NFT Stage             | A $\beta$ 42/40ratio      | 0.24    | 0.63             |
| Braak NFT Stage             | TotalTauA $\beta$ 42ratio | 0.43    | 0.63             |
| Braak NFT Stage             | pTau 181                  | 0.37    | 0.63             |
| CERAD Neuritic Plaque Score | PIGF                      | 0.43    | 0.73             |
| CERAD Neuritic Plaque Score | VEGF                      | 0.33    | 0.70             |
| CERAD Neuritic Plaque Score | MMP9                      | 0.35    | 0.70             |

|                             |                           |      |      |
|-----------------------------|---------------------------|------|------|
| CERAD Neuritic Plaque Score | IL8                       | 0.99 | 0.99 |
| CERAD Neuritic Plaque Score | IL6                       | 0.48 | 0.73 |
| CERAD Neuritic Plaque Score | IL10                      | 0.57 | 0.76 |
| CERAD Neuritic Plaque Score | TGF $\beta$               | 0.74 | 0.79 |
| CERAD Neuritic Plaque Score | GFAP                      | 0.04 | 0.32 |
| CERAD Neuritic Plaque Score | TNF $\alpha$              | 0.70 | 0.79 |
| CERAD Neuritic Plaque Score | A $\beta$ 40              | 0.28 | 0.70 |
| CERAD Neuritic Plaque Score | A $\beta$ 42              | 0.50 | 0.73 |
| CERAD Neuritic Plaque Score | TotalTau                  | 0.04 | 0.32 |
| CERAD Neuritic Plaque Score | NfL                       | 0.08 | 0.41 |
| CERAD Neuritic Plaque Score | A $\beta$ 42/40ratio      | 0.21 | 0.67 |
| CERAD Neuritic Plaque Score | TotalTauA $\beta$ 42ratio | 0.12 | 0.46 |
| CERAD Neuritic Plaque Score | pTau 181                  | 0.62 | 0.76 |
| AD Neuropathologic Change   | PIGF                      | 0.17 | 0.36 |
| AD Neuropathologic Change   | VEGF                      | 0.15 | 0.36 |
| AD Neuropathologic Change   | MMP9                      | 0.57 | 0.82 |
| AD Neuropathologic Change   | IL8                       | 0.65 | 0.82 |
| AD Neuropathologic Change   | IL6                       | 0.11 | 0.36 |
| AD Neuropathologic Change   | IL10                      | 0.67 | 0.82 |
| AD Neuropathologic Change   | TGF $\beta$               | 0.81 | 0.93 |
| AD Neuropathologic Change   | GFAP                      | 0.09 | 0.36 |
| AD Neuropathologic Change   | TNF $\alpha$              | 0.40 | 0.64 |
| AD Neuropathologic Change   | A $\beta$ 40              | 0.32 | 0.57 |
| AD Neuropathologic Change   | A $\beta$ 42              | 0.92 | 0.96 |
| AD Neuropathologic Change   | TotalTau                  | 0.18 | 0.36 |
| AD Neuropathologic Change   | NfL                       | 0.07 | 0.36 |
| AD Neuropathologic Change   | A $\beta$ 42/40ratio      | 0.06 | 0.36 |
| AD Neuropathologic Change   | TotalTauA $\beta$ 42ratio | 0.12 | 0.36 |
| AD Neuropathologic Change   | pTau 181                  | 0.96 | 0.96 |

P-values and adjusted P-values for the association between plasma markers and AD

Neuropathology



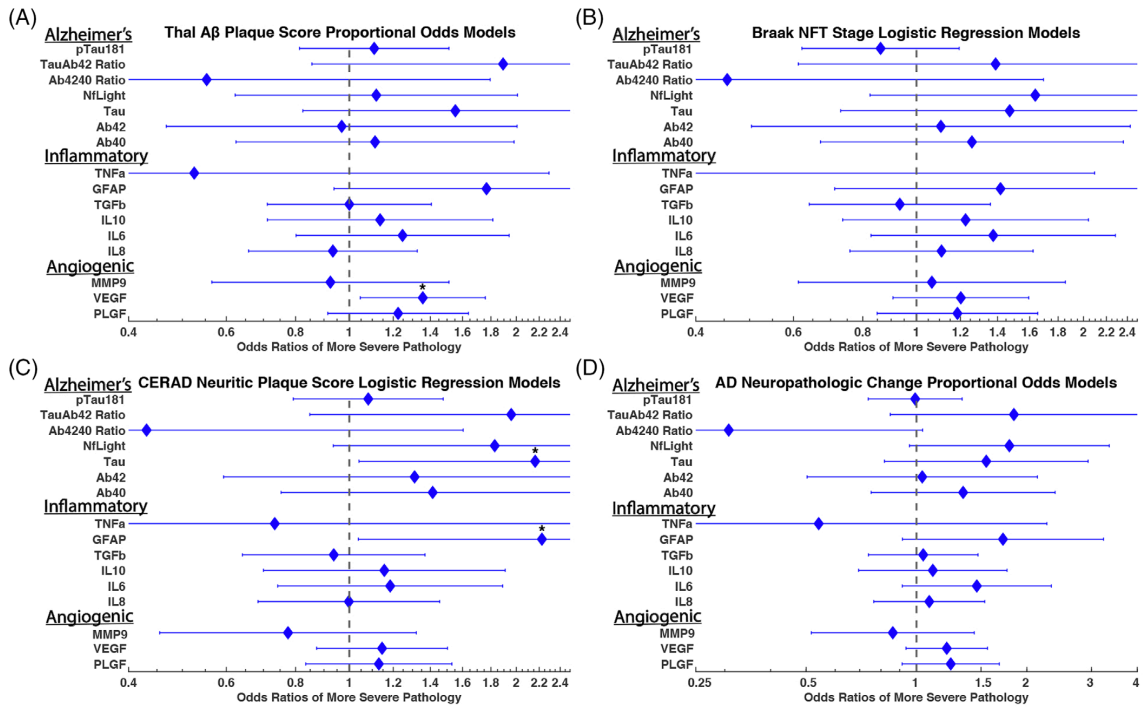
Table 3.6 p-Values and Adjusted p-Values for Plasma Biomarkers and cSVD Neuropathology

| Neuropathology              | Biomarker                 | p-value | Adjusted p-value |
|-----------------------------|---------------------------|---------|------------------|
| Cerebral Amyloid Angiopathy | PIGF                      | 0.05    | 0.55             |
| Cerebral Amyloid Angiopathy | VEGF                      | 0.61    | 0.96             |
| Cerebral Amyloid Angiopathy | MMP9                      | 0.10    | 0.55             |
| Cerebral Amyloid Angiopathy | IL8                       | 0.57    | 0.96             |
| Cerebral Amyloid Angiopathy | IL6                       | 0.30    | 0.82             |
| Cerebral Amyloid Angiopathy | IL10                      | 0.92    | 0.96             |
| Cerebral Amyloid Angiopathy | TGF $\beta$               | 0.75    | 0.96             |
| Cerebral Amyloid Angiopathy | GFAP                      | 0.96    | 0.96             |
| Cerebral Amyloid Angiopathy | TNF $\alpha$              | 0.66    | 0.96             |
| Cerebral Amyloid Angiopathy | A $\beta$ 40              | 0.76    | 0.96             |
| Cerebral Amyloid Angiopathy | A $\beta$ 42              | 0.80    | 0.96             |
| Cerebral Amyloid Angiopathy | TotalTau                  | 0.31    | 0.82             |
| Cerebral Amyloid Angiopathy | NfL                       | 0.91    | 0.96             |
| Cerebral Amyloid Angiopathy | A $\beta$ 42/40ratio      | 0.92    | 0.96             |
| Cerebral Amyloid Angiopathy | TotalTauA $\beta$ 42ratio | 0.29    | 0.82             |
| Cerebral Amyloid Angiopathy | pTau 181                  | 0.08    | 0.55             |
| Arteriolosclerosis          | PIGF                      | 0.16    | 0.99             |
| Arteriolosclerosis          | VEGF                      | 0.99    | 0.99             |
| Arteriolosclerosis          | MMP9                      | 0.32    | 0.99             |
| Arteriolosclerosis          | IL8                       | 0.21    | 0.99             |
| Arteriolosclerosis          | IL6                       | 0.10    | 0.99             |
| Arteriolosclerosis          | IL10                      | 0.76    | 0.99             |
| Arteriolosclerosis          | TGF $\beta$               | 0.95    | 0.99             |
| Arteriolosclerosis          | GFAP                      | 0.64    | 0.99             |
| Arteriolosclerosis          | TNF $\alpha$              | 0.80    | 0.99             |
| Arteriolosclerosis          | A $\beta$ 40              | 0.91    | 0.99             |
| Arteriolosclerosis          | A $\beta$ 42              | 0.62    | 0.99             |
| Arteriolosclerosis          | TotalTau                  | 0.92    | 0.99             |
| Arteriolosclerosis          | NfL                       | 0.70    | 0.99             |
| Arteriolosclerosis          | A $\beta$ 42/40ratio      | 0.36    | 0.99             |
| Arteriolosclerosis          | TotalTauA $\beta$ 42ratio | 0.38    | 0.99             |
| Arteriolosclerosis          | pTau 181                  | 0.46    | 0.99             |
| Chronic Vascular Grade      | PIGF                      | 0.49    | 0.89             |
| Chronic Vascular Grade      | VEGF                      | 0.14    | 0.78             |
| Chronic Vascular Grade      | MMP9                      | 0.82    | 0.89             |
| Chronic Vascular Grade      | IL8                       | 0.83    | 0.89             |

|                        |                            |      |      |
|------------------------|----------------------------|------|------|
| Chronic Vascular Grade | IL6                        | 0.00 | 0.04 |
| Chronic Vascular Grade | IL10                       | 0.40 | 0.89 |
| Chronic Vascular Grade | TGF $\beta$                | 0.75 | 0.89 |
| Chronic Vascular Grade | GFAP                       | 0.16 | 0.78 |
| Chronic Vascular Grade | TNF $\alpha$               | 0.69 | 0.89 |
| Chronic Vascular Grade | A $\beta$ 40               | 0.76 | 0.89 |
| Chronic Vascular Grade | A $\beta$ 42               | 0.24 | 0.78 |
| Chronic Vascular Grade | TotalTau                   | 0.38 | 0.89 |
| Chronic Vascular Grade | NfL                        | 0.53 | 0.89 |
| Chronic Vascular Grade | A $\beta$ 42/40ratio       | 0.22 | 0.78 |
| Chronic Vascular Grade | TotalTau/A $\beta$ 42ratio | 0.91 | 0.91 |
| Chronic Vascular Grade | pTau 181                   | 0.71 | 0.89 |

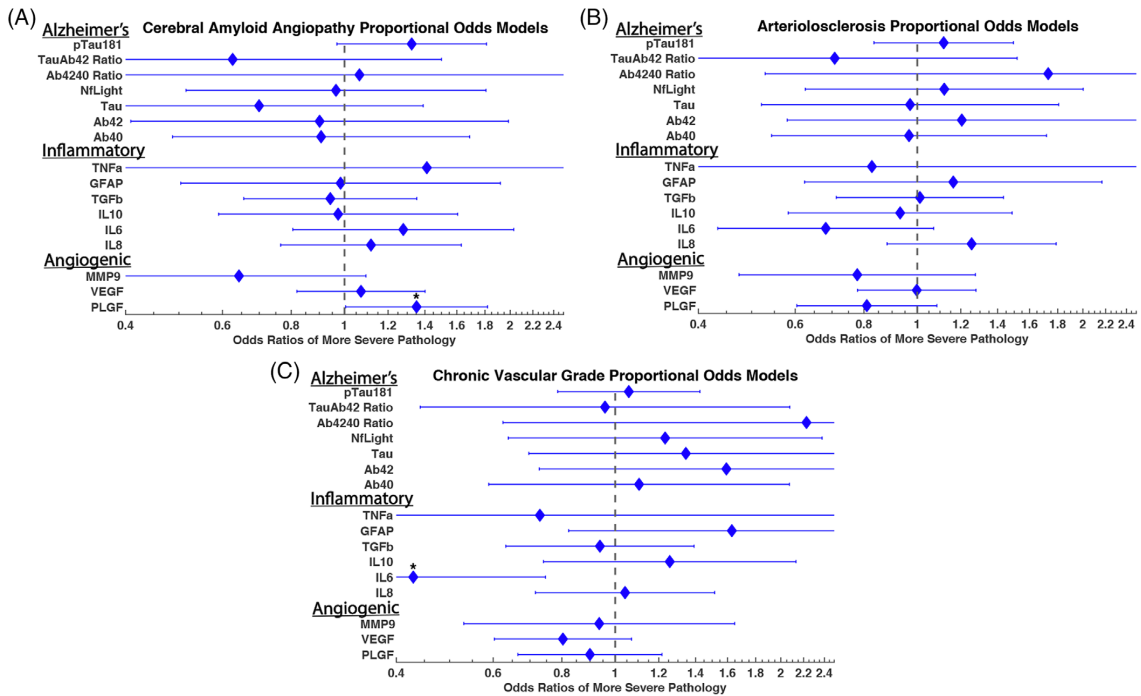
P-values and adjusted P-values for the association between plasma markers and cerebrovascular small vessel neuropathology

Figure 3.1 Associations of Plasma Biomarkers with Pathological Hallmarks of AD



Pathological hallmarks of Alzheimer's disease (AD) are associated with inflammation and angiogenesis biomarkers, as well as the expected AD biomarkers. Odds ratios from proportional odds (A,D) and binary logistic regression (B,C) models for each biomarker. All models were adjusted for age. Biomarkers were log transformed and outliers were removed based on the generalized extreme Studentized deviate test. (B) NFT stage and (C) neuritic plaque score models combined scores 0/1 and 2/3 to create a binary response due to small sample size. (\*) indicates a P-value < .05. A $\beta$ , amyloid beta; GFAP, glial fibrillary acidic protein; IL, interleukin; MMP9, matrix metalloproteinase 9; NfL, neurofilament light; NFT, neurofibrillary tangles; PIGF, placental growth factor; TNF $\alpha$ , tumor necrosis factor alpha; VEGF-A, vascular endothelial growth factor A.

Figure 3.2 Associations of Plasma Biomarkers with Pathological Hallmarks of cSVD



Pathological hallmarks of cerebrovascular small vessel disease are associated with inflammation, angiogenesis, and Alzheimer's disease biomarkers. Odds ratios from proportional odds models for each biomarker. Proportional odds models were adjusted for age. Biomarkers were log transformed and outliers were removed based on the generalized extreme studentized deviate test. Arteriolosclerosis and amyloid angiopathy models combined moderate and severe pathology categories due to small sample size. (\*) indicates a P-value < .05. Aβ, amyloid beta; GFAP, glial fibrillary acidic protein; IL, interleukin; MMP9, matrix metalloproteinase 9; NfL, neurofilament light; NFT, neurofibrillary tangles; PLGF, placental growth factor; TGFβ, transforming growth factor beta; TNFα, tumor necrosis factor alpha; VEGF-A, vascular endothelial growth factor A.

#### 4 Longitudinal effects of blood based neurodegenerative and inflammatory biomarkers on cognition in the University of Kentucky Alzheimer's Disease Research Center cohort

##### 4.1 Abstract

Physicians and researchers have been studying biomarkers for cognitive impairment in predominantly cross-sectional cohorts to determine which biomarkers may be beneficial in diagnosing impairment. Few of these biomarkers have been studied using a longitudinal cohort to evaluate how they may be used in a prognostic role to predict the development of future cognitive decline. In this chapter, we evaluate the relationship between inflammatory and neurodegenerative biomarkers at baseline to both middle- and long-term cognitive impairment. Participants from the UK-ADRC were evaluated at 3-years (N = 278) and 6- years (N = 205) post-baseline in 6 cognitive domains using inflammatory and neurodegenerative plasma biomarkers at baseline. Plasma samples were quantified using the Quanterix SiMoA and ordinary least squares linear regression was used to complete the analysis. GFAP and NfL were found to be significantly associated with verbal memory ( $\beta$ : -0.28; 95% CI: -0.45 – -0.12;  $p = 0.0009$ ) and verbal fluency ( $\beta$ : -0.15; 95% CI: -0.28 – -0.02;  $p = 0.0293$ ) at 6-years post baseline but not at 3 years post-baseline. The anti-inflammatory biomarker, IL-10, was found to have a positive relationship with both verbal memory ( $\beta$ : 0.14; 95% CI: -0.01 – 0.29;  $p = 0.0782$ ); ( $\beta$ : 0.19; 95% CI: 0.06 – 0.31;  $p = 0.0032$ ) and verbal fluency ( $\beta$ : 0.13; 95% CI: 0.01 – 0.25;  $p = 0.0308$ ); ( $\beta$ : 0.12; 95% CI: 0.04 – 0.20;  $p = 0.0024$ ) at both 6- and 3-years postbaseline respectively. Our data suggest that NfL and GFAP levels may represent a

future cognitive decline 6-years postbaseline, while IL-10 appears to act against cognitive impairment at both medium- and long-term future timepoints from baseline.

## 4.2 Introduction

Dementia is a disorder characterized by a significant decline from baseline in one or more cognitive domains that interferes with independence[1] The prevalence of dementia worldwide was estimated to be at 50 million with that number expected to triple by 2030, coming with a cost of roughly \$2 trillion[221, 222]. Deficits can begin as mild cognitive impairments and worsen over time and eventually start to affect an individual's daily living activities[121]. When a patient presents to a physician with symptoms such as loss of memory, the disease has likely been progressing for multiple decades[223]. Currently, clinical practitioners have a battery of different tests at their disposal that they can use to evaluate the domain specific cognitive status of an individual[224]. Cognitive domains that have been annually assessed at Alzheimer's Disease Research Centers (ADRCs) since 2009 using the Uniform Data Set (UDS) include language, verbal fluency, processing speed, executive function, attention, verbal memory; with additional domains being assessed from 2015 onwards[224, 225]. Two domains of particular interest for the study of AD are verbal memory and verbal fluency. Verbal memory refers to the ability to recall information given to an individual both immediately and after a delay[226]. This domain helps to address a common symptom of AD in episodic memory loss[121]. Verbal fluency refers to the ability to retrieve information already known and recite the requested information[227, 228]. One large component of verbal fluency is categorical fluency where individuals are asked to name

as many members of a particular category as possible, such as animals or vegetables[227, 228]. Both verbal memory and verbal fluency have previously been shown to differentiate patients with AD from cognitively normal controls and predict those who may progress from MCI and dementia[121, 227, 229, 230].

While these cognitive evaluations are helpful tools at diagnosing and monitoring the progression of the disease over time, they are also frequently the result of neurodegenerative pathology which is known to accumulate over long periods of time[2]. Therefore, it is vital to evaluate the level of neurodegenerative pathology over time, especially as we consider identifying biomarkers predictive of a future decline. While there are a growing number of biomarkers for AD, including PET scans or CSF protein concentrations of  $\beta$ -amyloid 42 and 40 ( $A\beta$  42/40), both neuroimaging and CSF draws have limitations in their clinical utility[2, 41, 59]. Neuroimaging remains expensive, especially PET imaging where the ligands are costly, and CSF draws are invasive to patients and contraindicated in a number of individuals. Ultimately, an inexpensive and less invasive screening tool is required to evaluate which patients are at risk of developing dementia in the future[40, 41, 59].

Plasma biomarkers fit the clinical need for low cost, minimally invasive biomarkers, and other blood-based biomarkers are already widely used in the clinical management of other diseases[231-234]. Glial fibrillar acidic protein (GFAP) and Neurofilament Light Chain (NfL) are both biomarkers which have been shown to be associated with neuroinflammation and multiple neurodegenerative processes including dementia[59, 169, 235]. GFAP is a filamentous protein expressed in astrocytes that is

found to be upregulated and released during neurodegeneration[99]. NfL is an intermediate filament found in neuronal axons, which is subsequently released after axonal or neuronal damage[83]. Both of these markers have been studied extensively in CSF, and with the introduction of pg/mL level of quantification, they are now beginning to be studied as a blood-based biomarkers as well[83-85, 101-103]. Additionally, anti-inflammatory cytokine, IL-10, has also been implicated in the onset of AD[108, 109]. Previous studies have shown that loss-of-function genotypes of IL-10 are at an increased risk of developing AD[110, 111].

Currently, most studies in the literature evaluate these biomarkers utilizing cross-sectional cohorts to determine the association of the biomarkers to disease. In this study we used a longitudinal cohort to evaluate the association between the baseline levels of plasma-based biomarkers and long-term domain-based cognitive status. We hypothesized that there would be an inverse association between neuro-inflammatory plasma biomarkers at baseline and cognition 6-years post-baseline. Conversely, we hypothesize that anti-inflammatory plasma biomarkers would have a positive association with cognition 6-years post-baseline.

## 4.3 Methods

### 4.3.1 Participant Selection and Plasma Collection

Participants in this study were selected from the cohort enrolled at the University of Kentucky Alzheimer's Disease Research Center (UK-ARDC) who had a baseline plasma sample collected within 3 months of a yearly cognitive evaluation and a follow-up cognitive evaluation 2.5 - 3.5 years (N = 278) or 5.5 – 6.5 years (N = 205) from



baseline cognitive evaluation beginning in 2013 through 2020. The UK-ADRC recruitment procedures and other methods have been previously described[215]. Briefly, participants consented to annual study visits that included cognitive testing, physical examination, neurological examination, medical history, blood collection, and other measures. All participants provided written informed consent for their participation in UK-ADRC research activities, which were approved by the University of Kentucky Institutional Review Board.

#### 4.3.2 Plasma Sample Analysis

Plasma samples were processed within 4 hours of collection and stored at  $-80^{\circ}\text{C}$  within 8 hours of collection until retrieved and thawed on ice. Thawed samples were centrifuged at  $4^{\circ}\text{C}$  for 10 minutes at maximum speed (approx. 21,000 x g) and then plated at room temperature using the dilutions listed (Table 4.1) for analysis on the Quanterix Simoa HD-X[186]. Simoa immunoassays for phosphorylated threonine-181 tau (pTau181), neurofilament light (NfL), total Tau (Tau), amyloid beta 42 ( $\text{A}\beta_{42}$ ), amyloid beta 40 ( $\text{A}\beta_{40}$ ), tumor necrosis factor alpha ( $\text{TNF}\alpha$ ), glial fibrillary acidic protein (GFAP), transforming growth factor beta ( $\text{TGF}\beta$ ), interleukin 10 (IL10), interleukin 6 (IL6), interleukin 8 (IL8), matrix metalloproteinase 9 (MMP9), vascular endothelial growth factor A (VEGF-A), and placental growth factor (PIGF) were assessed.

After the run completed, data were retrieved, and the results were adjusted for the dilution factor. Plasma biomarkers were run in batches based on the year of collection. To adjust for batch variability, plasma protein levels were z-scored after the biomarkers were log transformed and outliers from each biomarker set were removed

using the generalized extreme studentized deviate test: IL-10 (N = 1), GFAP (N = 0), NfL (N = 1).

#### 4.3.3 Cognitive Assessments

Six cognitive domains (verbal memory, verbal fluency, language, attention, executive function, and processing speed) in addition to a global cognitive performance were evaluated in each participant at 6-years post-baseline by a neuropsychiatrist at the UK-ADRC. Cognitive domain scores were calculated by taking the age, sex, and education adjusted z-scores of the cognitive tests listed for each domain and averaging them (Table 4.2). Raw test scores were adjusted using NACC z-score calculator[236]. Evaluations completed before March of 2015 were performed using UDS2 guidelines, while those completed after that date were performed using UDS3 guidelines. Cognitive tests performed only in UDS3 were converted to raw scores of their UDS2 counterpart using the NACC crosswalk[237]. Models evaluating the association of GFAP, NfL, and IL-10 with verbal memory and verbal fluency had larger effect sizes and were further studied at the 3-years post-baseline timepoint.

#### 4.3.4 Statistical Analysis

Ordinary least squares (OLS) regression was used to evaluate the relationship between plasma biomarkers (independent variable) and domain-based cognitive function (dependent variable). Models were adjusted for age at baseline, sex, years of education, and presence of an *APOE* $\epsilon$ 4 allele.  $\beta$  coefficients for each model indicate the mean change of the cognitive domain, in units of standard deviation, for a 1-standard deviation increase in the log of the biomarker.

The association between each plasma biomarker and each cognitive domain at 6 years post-baseline were assessed. Linear models were created by removing points with large delete-1 scaled difference in coefficient estimates of the biomarker to reduce the influence of highly leveraged datapoints.

Due to the large number of models produced, false discovery rate for multiple comparison testing was conducted for each cognitive domain independently using the Benjamini-Hochberg method [216] Models with larger effect sizes and small p-values were further evaluated at 3 years post-baseline, and those results are detailed below. All data analysis was performed with MATLAB. Statistical significance was set at 0.05.

#### **4.4 Results**

##### **4.4.1 Study Participant Characterization**

Participants selected from the UK-ADRC cohort (N = 278, 3 years; N = 205; 6 years) had a mean age of  $75.77 \pm 6.4$  in both the 3- and 6-year post-baseline samples (Table 4.3). Additionally, the baseline MMSE scores, percentage of females, and years of education were nearly identical between the two samples because most of the 6-year individuals were represented in the 3-year samples (Table 4.3). The proportion of individuals with at least one ApoeE4 allele was higher in the 3-year post-baseline sample compared to the 6-year post-baseline sample at 33.5% vs 29.3% respectively (Table 4.3).

##### **4.4.2 GFAP and NfL are Inversely Associated with Cognition at Six-Years Post-Baseline**

We hypothesized that increased inflammatory plasma proteins at baseline would have an inverse association with cognition level at 6-years post-baseline. Consistent with our hypothesis, we found that a one standard deviation increase in log GFAP

corresponds to a statistically significant mean decrease in verbal memory 6-years post-baseline ( $\beta$ : -0.28; 95% CI: -0.45 – -0.12;  $p$  = 0.0009) (Figure 4.1A). However, this effect was not seen in verbal memory 3-years post-baseline ( $\beta$ : -0.03; 95% CI: -0.17 – 0.11;  $p$  = 0.6896) (Figure 4.1B). After correcting for FDR, GFAP still maintained statistical significance ( $q$  = 0.014) 6-years post-baseline (Figure 4.1A). NfL was also found to be inversely associated with verbal fluency with a one standard deviation increase in log NfL corresponding to a statistically significant mean decrease in verbal fluency 6-years post-baseline ( $\beta$ : -0.15; 95% CI: -0.28 – -0.02;  $p$  = 0.0293) (Figure 4.2A). This effect was also not seen at 3-years post-baseline ( $\beta$ : 0.01; 95% CI: -0.07 – 0.01;  $p$  = 0.8132) (Figure 4.2B). After correcting for FDR, NfL did not maintain statistical significance in the 6-year post-baseline ( $q$  = 0.25) (Figure 4.2A).

#### 4.4.3 IL-10 is Positively Associated with Verbal Memory and Verbal Fluency at Three- and Six-Years Post-Baseline

We also hypothesized that increased anti-inflammatory plasma proteins at baseline would have a positive association with cognition level at 6-years post-baseline. Interestingly, we saw that not only was IL-10 positively associated with verbal memory and verbal fluency at 6-years post-baseline, but also at 3-years post-baseline (Figure 4.3 A-D). A one standard deviation increase in log IL-10 was found to have a mean increase in verbal memory 6-years post-baseline ( $\beta$ : 0.14; 95% CI: -0.01 – 0.29;  $p$  = 0.0782) and a statistically significant mean increase in verbal fluency 6-years post-baseline ( $\beta$ : 0.13; 95% CI: 0.01 – 0.25;  $p$  = 0.0308) (Figure 4.3 A,C). At 3-years post-baseline we identified similar effects with a statistically significant mean increase in both verbal memory ( $\beta$ :

0.19; 95% CI: 0.06 – 0.31;  $p = 0.0032$ ) and verbal fluency ( $\beta$ : 0.12; 95% CI: 0.04 – 0.20;  $p = 0.0024$ ) 3-years post-baseline (Figure 4.3 B,D). While this does show that higher IL-10 levels at baseline are associated with higher levels of verbal memory and fluency at 3- and 6-years post-baseline given equal age, sex, education level, and baseline cognitive function, it does not provide any indication on the amount of cognitive change that occurs over post-baseline.

#### 4.4.4 Discussion

In this study, we evaluated the association between plasma-based biomarkers and cognitive status in a longitudinal cohort at the UK-ADRC. We began by analyzing the relationship between baseline plasma levels of neuro-inflammatory and anti-inflammatory markers and evaluating their association with verbal memory and verbal fluency performance 6-years post-baseline. Through this analysis we found that baseline GFAP was inversely associated with 6-years post-baseline verbal memory, while NfL was inversely associated with verbal fluency (Chapter 4.3.2). Interestingly, the anti-inflammatory IL-10 was positively associated with both verbal memory and verbal fluency at 6-years post-baseline (Chapter 4.3.3).

Additionally, the same analyses were conducted using a sample of participants from the UK-ADRC cohort, investigating cognition at 3-years post-baseline. In this secondary analysis, both GFAP and NfL had no significant association with verbal memory or verbal fluency (Chapter 4.3.2). However, IL-10 maintained a positive association with both verbal memory and verbal fluency at this earlier time point (Chapter 4.3.2). These results suggest that increased levels of anti-inflammatory

proteins exert their influence on cognition at an earlier time point compared to inflammatory proteins and maintain the effect over a long period of time. In contrast, the effects of neuroinflammatory proteins like GFAP and NfL do not appear to show until much later in the disease process.

Previous studies have already demonstrated the ability of GFAP and NfL to discriminate cognitively impaired individuals in cross-sectional studies using CSF and recently in plasma as well[59, 83, 84, 100-103]. This study is one of the first to evaluate the effect of these biomarkers on longitudinal cognitive function. The inverse association between verbal memory and verbal fluency with GFAP and NfL, respectively, support what has been previously observed.

GFAP is a protein typically found in astrocytes, and in the brain, GFAP immunoreactivity is increased with neurodegenerative pathologies[91, 92]. Furthermore, neurovascular astrocyte reactivity is increased with cerebrovascular injury and cerebral amyloid angiopathy (CAA)[238, 239]. It can be hypothesized that increased plasma GFAP originates from hypertrophic, reactive astrocytes in the brain as neurodegenerative and cerebrovascular pathologies accumulate, however, future studies will be needed to fully evaluate this hypothesis[100, 240].

In contrast to GFAP, NfL is a protein found in axons of neurons, and plasma NfL has been shown to originate from extracellular release by neurons undergoing neurodegeneration[83]. As neurodegeneration is a key component of dementia, CSF and plasma NfL have been studied for their association with the development of AD and have shown that NfL is elevated in patients with AD compared to controls[38, 59].

However, as neurodegeneration is not specific to AD, NfL is also hypothesized to be a non-specific marker of neurodegeneration[59].

IL-10 is considered an anti-inflammatory cytokine produced by glial cells within the CNS[241]. IL-10 acts to dampen the inflammatory response after being upregulated during periods of inflammation[242]. IL-10 has also been found to associate with cognitive impairment, albeit from a genetic perspective. Previous studies of IL-10 have shown that participants with mutations causing decreased production of IL-10 are at an increased risk of having dementia[110, 111]. Those findings are supported by the observations in this study which identify a positive association between IL-10 at baseline and both 3- and 6-year post-baseline verbal memory and verbal fluency scores. Further analyses are needed to determine if this relationship is maintained after adjusting for an individual's IL-10 polymorphism.

While some of these findings lacked statistical significance after FDR, we believe that this is likely due to our study being underpowered as a result of using a convenience sample of participant data available to us from the UK ADRC. This may explain the lack of statistical association between GFAP and verbal fluency and NfL and verbal memory, which may be seen in a much larger cohort designed to elucidate these effects. Moving forward, these biomarkers need to be validated in multiple large cohorts before they can be brought to the clinic.

In the future, the goal for these biomarkers is to use them individually or in combination to create a low-cost and minimally invasive biomarker panel which can help clinicians better prognosticate the onset of verbal memory and verbal fluency

decline in at-risk patients. These techniques can also be used to develop additional biomarkers which may be more specific to particular types of dementia which can help physicians distinguish between different courses of disease.



Table 4.1 Simoa Biomarker Dilutions

| Assay | Dilution | Catalog Number | LLOQ       | LOD         | Dynamic Range |
|-------|----------|----------------|------------|-------------|---------------|
| NfL   | 1:25     | 103186         | .174 pg/ml | .038 pg/ml  | 0-1800 pg/ml  |
| GFAP  | 1:10     | 102336         | .686 pg/ml | .221 pg/ml  | 0-4000 pg/ml  |
| IL10  | 1:2      | 101643         | .021 pg/ml | .0038 pg/ml | 0-120 pg/ml   |

Dilutions required for quantification for SiMoA biomarkers. Lower limit of quantification

(LLOQ) and limit of detection (LOD) used to determine dilution.

Table 4.2 Cognitive Tests Evaluating Cognitive Domains

| <b>Cognitive Domain</b>   | <b>UDS2 Cognitive Tests</b>                     | <b>UDS3 Cognitive Tests</b>   |
|---------------------------|---|---|
| <b>Language</b>           | Animal Naming, Vegetable Naming, Boston Naming  | Animal Naming, Vegetable Naming, Total F- and L- Words Naming, MINT |
| <b>Verbal Fluency</b>     | Animal Naming, Vegetable Naming                 | Animal Naming, Vegetable Naming                                     |
| <b>Processing Speed</b>   | Trails A, WAIS-R                                | Trails A, WAIS-R  |
| <b>Executive Function</b> | Trails B  | Trails B  |
| <b>Attention</b>          | Digit Span Forward, Digit Span Backward         | Number Span Forward, Number Span Backward                           |
| <b>Verbal Memory</b>      | Logical Memory IA, Logical Memory IIA – Delayed | Craft Story 21 Recall (Immediate), Craft Story 21 Recall (Delayed)  |
| <b>Global</b>             | MMSE  | MoCA  |

Cognitive tests comprising each cognitive domain evaluated by UDS2 or UDS3 cognitive assessment guidelines.

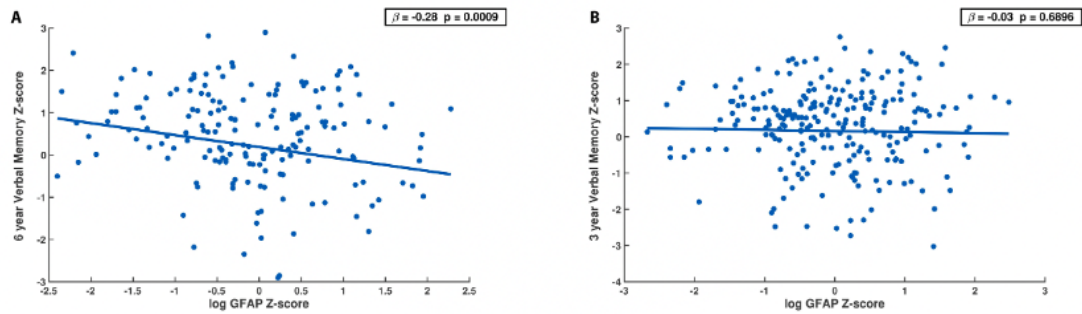
Table 4.3 Participant Characteristics

| Characteristic         | 3-year Cohort Summary* (N = 278) | 6-year Cohort Summary* (N = 205) |
|------------------------|----------------------------------|----------------------------------|
| Age at Baseline, years | 75.7 ± 6.4                       | 75.7 ± 6.4                       |
| MMSE at Baseline       | 28.8 ± 1.8                       | 28.9 ± 1.7                       |
| Female Sex, %          | 62.6%                            | 62.0%                            |
| ≥ 1 APOE e4 allele     | 33.5%                            | 29.3%                            |
| Education, years       | 16.7 ± 2.6                       | 16.7 ± 2.7                       |

Characteristics of included participants from the UK-ADRC cohort. \*All results are mean

± SD or proportion

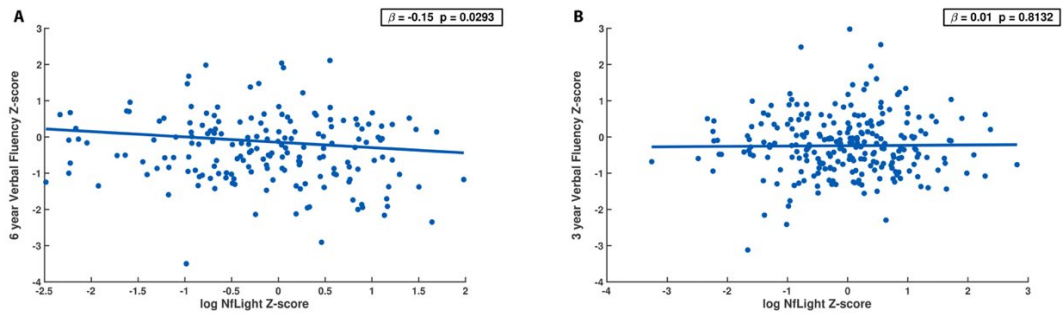
Figure 4.1 Baseline Plasma GFAP Association with Future Verbal Memory



**Baseline plasma GFAP association with verbal memory at 6 years (A) and at 3 years (B)**

**post-baseline.** (A,B)  $\beta$  represents the mean change of verbal memory, in units of standard deviation, for a 1-standard deviation increase in log GFAP.  $\beta$  was calculated using OLS adjusting for baseline verbal memory z-score, age at baseline, sex, years of education, and presence of an ApoE4 allele. P-values shown are nominal. Q-values calculated for FDR were (A) 0.014 and (B) 0.85.

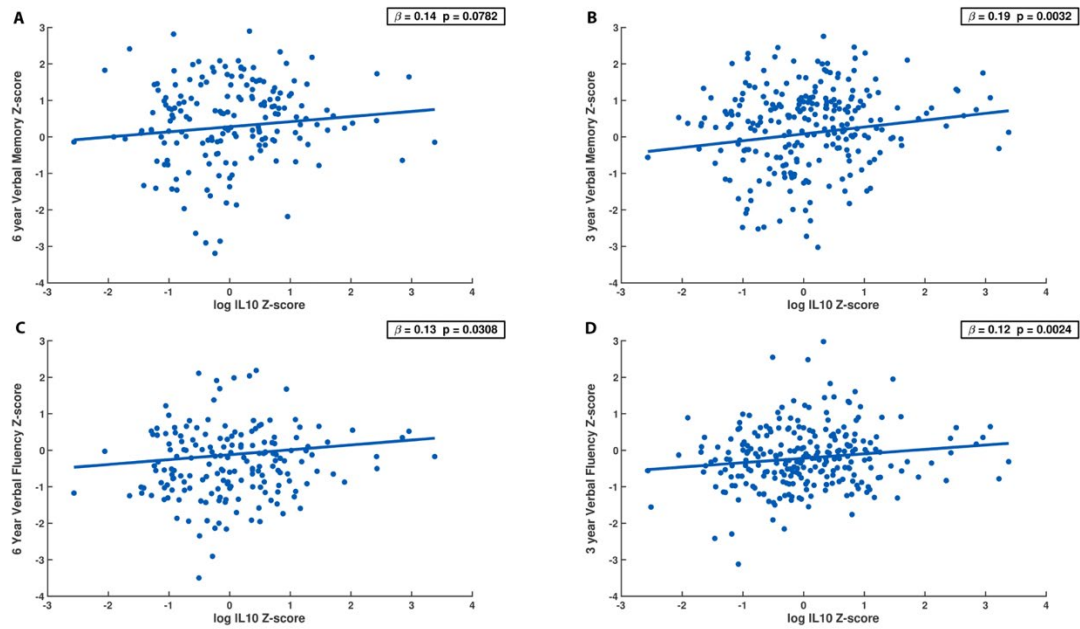
Figure 4.2 Baseline Plasma NfL Association with Future Verbal Fluency



**Baseline plasma NfL association with verbal fluency at 6 years (A) and at 3 years (B)**

**post-baseline.** (A,B)  $\beta$  represents the mean change of verbal memory, in units of standard deviation, for a 1-standard deviation increase in log NfL.  $\beta$  was calculated using OLS adjusting for baseline verbal memory z-score, age at baseline, sex, years of education, and presence of an ApoE4 allele. P-values shown are nominal. Q-values calculated for FDR were (A) 0.25 and (B) 0.93.

Figure 4.3 Baseline Plasma IL-10 Association with Future Verbal Memory and Verbal Fluency



**Baseline plasma IL-10 association with verbal memory (A,B) and verbal fluency (C,D) at 6 years (A,C) and at 3 years (B,D) post-baseline. (A-D)  $\beta$  represents the mean change of verbal memory and verbal fluency, in units of standard deviation, for a 1-standard deviation increase in log IL-10.  $\beta$  was calculated using OLS adjusting for baseline verbal memory z-score, age at baseline, sex, years of education, and presence of an ApoE4 allele. P-values shown are nominal. Q-values calculated for FDR were (A) 0.56, (B) 0.052, (C) 0.25, and (D) 0.0388.**

## 5 Discussion

### 5.1 Overview

In this section of my dissertation, I will briefly discuss the results from chapters 2-4 individually and then focus on evaluating them together in the context of the current field of plasma biomarker usage in dementia. Additionally, I will discuss future studies which can be used to further our current understanding of the utility of plasma biomarkers in the diagnosis and treatment of AD and VCID.

### 5.2 Chapter 2 Review

Chapter 2 asks the question of whether there are identifiable blood-based biomarker profiles in a cohort of patients with MCI due to cerebrovascular disease. This was accomplished using hierarchical clustering analyses (HCA) on plasma samples collected from participants in a cross-sectional fashion from a clinical cohort called the MCI-CVD cohort. The MCI-CVD cohort included participants who were clinically diagnosed with MCI and had at least one risk factor of cerebrovascular disease. Plasma samples were collected from each participant's annual visit and candidate plasma biomarkers were assessed for their intra- and inter-plate variability. Establishing the reliability of our protein quantification is of the utmost importance as any variability in the assay will make it harder to evaluate significant differences between groups of participants within our cohort. Plasma markers were subsequently log-transformed and clustered using two HCA. Two HCA were used to compare how the different algorithms cluster our dataset to reduce the bias associated with using one hierarchical clustering

technique versus another as the results of an HCA are often sensitive to the parameters of the algorithm in datasets where expected clusters are overlapping. We first evaluated how the two HCA algorithms perform in various datasets and found that in the dataset that most closely represented our human plasma biomarker dataset, there was no significant difference in how accurate they were (Chapter 2.4.2, Chapter 2.4.3). We then applied both HCA algorithms to our dataset and found that both algorithms identified a similar group of participants (Cluster 1) who shared a common plasma biomarker profile (Chapter 2.4.4). We then investigated the differences between the groups and identified multiple angiogenic and inflammatory biomarkers (FGF, VEGFA, MMP1, MMP9, IL-8) which were significantly elevated in cluster 1 in both HCA models (Chapter 2.4.5).

These results led us to propose a subsequent hypothesis that participants with a plasma biomarker profile similar to cluster 1 were more likely to be undergoing pathogenic angiogenesis and have a proinflammatory response resulting in increased neurovascular pathology. Previous studies have already identified a positive association between VEGF-A and cerebral microbleeds in patients with dementia[243], as well as increased CSF levels in both patients with AD and VCID[113]. IL-8 is a proinflammatory cytokine seen upregulated in AD patients with a SNP associated with AD as well[244, 245]. While individual markers have often been evaluated for their association with both AD and VCID pathologies, in this study we sought to evaluate a profile of angiogenesis and inflammation which in the future may provide more specificity for specific neurovascular pathologies than any one marker could do alone.



Together, the proteins upregulated in cluster 1 point to a high inflammatory state with IL-8 signaling to activate microglia and VEGF-A potentially acting to open access to the blood brain barrier alongside MMPs to the activated microglia, enhancing inflammation within the brain. IL-8 has already been found to increase cytokine production in in-vitro microglia, strengthening an effect seen with A $\beta$  42[246]. While, VEGF-A can be beneficial at promoting vasculature growth in physiological situations, it also has been found, along with MMPs, to downregulate key tight junction proteins in maintaining the blood barrier[247, 248], which combined with the activation of microglia creates a chronic neuroinflammatory response in the brain.

Future studies on this work would need to focus how these plasma profiles change within an individual over different periods of time and how correlated they are to different stages of pathology. Ideally, multiple participants would have plasma samples collected at baseline, one week post-baseline, one month post-baseline, three months post-baseline, six months post-baseline, and one year post-baseline. These samples would allow us to study how stable these biomarkers are within an individual over time, as it is likely that biomarkers with a significant association with pathology would have a consistent relationship with the pathology over short periods of time. Alternatively, it is possible that longitudinal fluctuations in biomarkers correlate to neuropathology. This relationship is already seen in a biomarker for cardiovascular disease, blood pressure. Blood pressure at cross-sectional time points has been found to be associated with increased risk of cardiovascular disease, and it has also been shown that blood pressure variability over time is also positively associated with cardiovascular disease and all-

cause mortality at long-, mid-, and short-term time points[249]. A similar finding may be seen when evaluating the relationship between angiogenic and inflammatory biomarker variability with neurovascular pathology.

A second follow-up study from this experiment should be to examine if neurovascular pathology differs between clusters derived from participants plasma biomarker profile. As this study was conducted using an observational cohort of individuals who are living, a future study would require in-vivo pathology assessments, ideally using MRI for vascular pathology to compare between clusters. We can hypothesize that participants with an increased angiogenic and pro-inflammatory profile would have increased levels of pathology either cross-sectionally or longitudinally. If future studies supported a longitudinal pathological development based on a novel plasma biomarker profile, then the profile could potentially act as a screening tool for clinicians to use to determine which patients require further neuroimaging evaluations. Given that this data was unavailable for these studies, we decided to evaluate the association of plasma biomarkers and neuropathological findings using an autopsy cohort and plasma samples from within two years antemortem in Chapter 3.

### 5.3 Chapter 3 Review

In chapter 3, we sought to continue from what we learned in chapter 2 and evaluate how not only angiogenic and inflammatory biomarkers correlate with neuropathological findings but also AD and neurodegenerative biomarkers as well. We accomplished this goal using an autopsy cohort of patients from the UK ADRC who had a plasma sample within two years prior to autopsy. A two-year maximum was chosen as we wanted the

plasma findings to be as representative of the neuropathology as possible. Previous studies have shown that a 1 standard deviation reduction in global cognition takes roughly three years to occur during the most rapid phase of decline[3]. This time point also afforded us an ample sample size to evaluate the point estimate of the relationships between pathology and plasma biomarkers. We also acknowledge that this sample does have a larger percentage of cognitively normal individuals and fewer patients diagnosed with dementia than our greater autopsy cohort. We believe that this is likely due to a falloff in clinic visits as cognitive impairment worsens. Many times, annual assessments are done in-home for advanced dementia patients precluding the collection of blood. Two different linear models were used depending on whether the neuropathological variables had a binary (neuritic plaque score and neurofibrillary tangle stage because the two highest and two lowest scores were grouped together because of limited sample size) or ordinal (amyloid plaque, AD neuropathologic change, CAA, arteriolosclerosis, and chronic vascular grade) structure. Logistic regression was used for binary variables while a proportional odds model was used for ordinal variables. With these models we were able to determine the association of each log-transformed biomarker with each neuropathology using odds ratios.

We used an odds ratio to indicate the odds of having a more severe pathology for every one-unit change in the log-transformed biomarker. We found that AD neuropathologic change was inversely associated with the  $A\beta_{42/40}$  ratio (Chapter 3.4.2), which has been widely predicted based on previous studies on the association of CSF  $A\beta_{42/40}$  ratio and amyloid PET imaging[250]. Interestingly, pTau181 showed almost

no association with AD neuropathologic change and a slight positive association with amyloid and neuritic plaque scores (Chapter 3.4.2). This finding varies slightly from previous studies using in-vivo PET imaging that found that pTau181 was associated with early changes to amyloid PET uptake and to a lesser degree with tau PET[213, 251]. We hypothesize that this finding was due to the time frame in which we evaluated AD neuropathology. Since we evaluated patients using post-mortem neuropathology, it could be proposed that while A $\beta$ 42/40 ratio is continually decreased in patients with AD neuropathologic change, pTau181 may only be elevated in the beginning stages of AD neuropathologic change. This hypothesis lends itself to further testing as it is imperative to not only study these biomarkers in cross-sectional cohorts but also in longitudinal cohorts as well to evaluate how these biomarkers change overtime.

In addition to the more typical AD biomarkers, we found that VEGFA, PIGF, and GFAP were positively associated with AD neuropathologic changes (Chapter 3.4.2). While GFAP has previously been shown to positively correlate with AD[101-107], VEGFA and PIGF are more recently beginning to be investigated for their association with AD, but the findings have been inconsistent. Some studies have found that CSF level of VEGFA is increased in patients with AD while another found that higher levels of VEGFA were associated with decreased hippocampal atrophy, increased FDG-PET SUVR and increased longitudinal cognition in patients who are positive for A $\beta$  and Tau[113-115]. Our findings support the positive association of GFAP with AD neuropathology as both are linked pathologically to chronic neuroinflammation. We also provide additional evidence for the positive association between VEGFA/PIGF and AD neuropathology

through an elusive mechanism that may involve mediating the blood brain barrier as previously discussed.

The studies in chapter 3 were some of the first in the field to evaluate the association of plasma biomarkers with autopsy confirmed neuropathological evaluation and generally support what was previously described in the literature, with all three candidate biomarkers of AD (A $\beta$ 42/40, pTau181, NfL) being significantly increased in participants with AD compared to cognitively normal controls[73, 74, 82-86].

We also evaluated the association of plasma AD-related, angiogenic, and inflammatory biomarkers on cerebrovascular neuropathology and found that PlGF had a significant positive association with CAA but had an inverse association with chronic vascular pathology and arteriolosclerosis (Chapter 3.4.3). This finding is interesting because it suggests that the induction of pathogenic angiogenesis via PlGF may be vessel dependent, with CAA predominantly affecting leptomeningeal and cortical arteries and arterioles, while arteriolosclerosis affects penetrating arterioles[123, 137]. The differentiating anatomy may play a role in how the vessels respond to inflammation and vessel stiffening and thereby the resultant upregulation of PlGF. Preliminary findings of PlGF run contrary to this association and show a positive relationship with WMHs, which are a known neuroimaging finding in chronic vascular disease. Pro-inflammatory IL-6 was also found to have a significantly inverse association with chronic vascular grade (Chapter 3.4.3). This was surprising given that VCID is characterized by chronic inflammation and IL-6 has been found to be elevated in patients with VCID and associated with WMHs[178, 252]. We predict that this discrepancy derives from the fact

that WMHs are an in-vivo neuroimaging measure of VCID, while chronic vascular grade is a post-mortem evaluation of various vascular and parenchymal pathologies associated with VCID. While both entities are seen in VCID patients, it is still not clear what the relationship is between WMHs and the vascular pathologies that we evaluated within our novel measure of chronic vascular grade.

Future studies associated with this project would need to focus on the longitudinal relationship of plasma biomarkers and neuropathology. One potential study could look at how biomarker changes over time coincide with neuropathological changes in the future. This would again require a prospective longitudinal cohort with yearly plasma draws and neuropathological evaluations. Currently, the only method of evaluating neuropathology in the living person requires the usage of MRI and PET scans. While our prospective ADRC cohort does conduct annual plasma draws, the number of participants with comparable longitudinal neuroimaging remains substantially less. As this dataset continues to grow now that the UK-ADRC is performing more longitudinal MRI of the cohort the ability to perform such analyses will be enhanced. For chapter 4, we were able to gather comprehensive annual neurocognitive evaluations along with plasma biomarker measures.

#### 5.4 Chapter 4 Review

Here, we sought to clarify the relationship between baseline plasma biomarkers and longitudinal cognitive change. We hypothesized that biomarkers related to neurodegeneration would have an inverse association with future cognition. To test this hypothesis, we used the prospective longitudinal ADRC cohort where we utilized a

baseline plasma sample along with cognitive evaluations at baseline, as well as three- and six-years post baseline. These time points were selected as they represented both middle- and long-term cognitive change over time. One study found that cognition begins to decline at a faster rate at 7.5 years prior to diagnosis of dementia[3]. Given this information and sample size limitations within our cohort we felt confident that if a participant was to be diagnosed with dementia, a six-year longitudinal cognitive change would show significant cognitive changes. Three years was chosen as a half-way point to evaluate if cognitive impairment associated with plasma biomarkers could be seen at a middle-term time point as well. Some cognitive tests performed at baseline were not performed at future time points and vice versa due to the updating of the UDS neurocognitive evaluations from UDS2 to UDS3 in 2015[253]. In order to maintain fluid usage of all cognitive tests, a crosswalk was created by the National Alzheimer's Coordinating Center (NACC) to convert UDS3 score to their UDS2 equivalent[237]. While this method is not 100% accurate it does allow for us to assess cognitive changes across the UDS standardizations. Each cognitive test was then translated into an age, sex, and education adjusted z-score using data supplied by NACC. Assessments of cognitive domains were then established by averaging the z-scores for all tests associated with each domain. Baseline cognitive domain scores and plasma biomarker levels were then included in an ordinary least squares linear regression model along with age at baseline, sex, education level, and presence of an *APOEε4* allele to model longitudinal cognitive domain scores at three- and six-years post-baseline.

The results of this study highlighted three plasma biomarkers that had significant relationships with cognition. Two plasma biomarkers (NfL and GFAP) showed a negative association with cognition at six years post-baseline but not at three years (Chapter 4.4.2). Both NfL and GFAP have been studied previously for their association with AD and neurodegeneration[83, 84, 86, 87, 101-107]. In the current study we found that GFAP was negatively associated with verbal memory scores six years post-baseline but not at three years, while NfL was negatively associated with verbal fluency scores six years post-baseline but not at three years. While this finding is supported by previous studies in the literature, it is interesting to note that the markers were specific for two distinct but related cognitive domains. It is possible that both GFAP and NfL are associated with both verbal fluency and verbal memory, but our sample size was not robust enough to detect such associations. This possibility would have to be tested in a larger prospective cohort to ensure that there is sufficient statistical power to identify this relationship.

We found that the typically anti-inflammatory cytokine IL-10 was positively associated with both verbal fluency and verbal memory at both three- and six-year time points post-baseline (Chapter 4.4.3). Interestingly, patients with IL-10 polymorphisms associated with decreased IL-10 production were found to be at an increased risk of developing AD[110, 111]. Our study supports the hypothesis that IL-10 upregulation can help to reduce cognitive decline in patients at risk of developing AD. This finding lends itself to further studies about using IL-10 as a potential disease modifying agent. However, two studies using mouse models of AD found that IL-10 upregulation



contributed to increase A $\beta$  deposition, while knocking out IL-10 reduces AD pathology[254, 255]. While contrary to our findings and other human based studies, these findings indicate that in a genetically induced model of A $\beta$  deposition, IL-10 prevents microglial activation to clear A $\beta$ . However, sporadic AD is not caused by a genetic mutation causing A $\beta$  deposition, and it is hypothesized that chronic neuroinflammation plays a large role in the development of AD neuropathology[256]. Therefore, it is still likely that upregulating anti-inflammatory IL-10 may be beneficial in sporadic AD.

One aspect of this project that could be further evaluated in future studies is the mediating effect of neurodegenerative and inflammatory biomarkers on the relationship between AD related biomarkers such as A $\beta$ 42/40 ratio and pTau181, and cognition. While both A $\beta$ 42/40 ratio and pTau181 are associated with amyloid PET positivity and with conversion from MCI to dementia[213, 250, 251], the effect of neurodegenerative and inflammatory biomarkers on this relationship has not been studied. We hypothesize that there will be a significant interaction between AD related biomarkers and NfL/GFAP on longitudinal cognitive changes, with higher levels of NfL and GFAP increasing the effect of A $\beta$ 42/40 ratio and pTau181 on cognitive decline. Conversely, we hypothesize that IL-10 may lessen the effect of A $\beta$ 42/40 ratio and pTau181 on cognitive decline. In order to identify this statistical interaction a significantly larger sample size will be required and will likely need to include patients from multiple centers. While multi-center trials are necessary to evaluate the generalizability of the scientific findings, they also present significant challenges in ensuring that protocols are uniform across multiple

locations. The ADRC network and the NACC steering committees are ideally suited to collaborate to test these broader hypotheses.

## 5.5 Limitations

While these studies have helped us to understand the relationships between plasma biomarkers and dementia, they are not without their limitations. One major limitation is the use of observational cohorts for these analyses. All the studies in this dissertation utilized previously collected samples from participants and statistical analyses to better appreciate the correlations between plasma biomarkers and various aspects of dementia. In conducting these analyses, we are limited to the sample sizes which have previously been collected and are therefore often underpowered to detect small effect sizes. As seen in our results, most of our relationships have small effect sizes which ultimately led to a lack of statistically significant findings in chapters 2 and 3. However, we were still able to interpret the relationships between our plasma biomarkers and dementia by focusing on the 95% confidence intervals and point estimates of the correlations. These confidence intervals provide us with a range which, we have high confidence, contain the true value of the correlation and can be used as a basis for future studies to further elucidate the relationship between plasma biomarkers and dementia.

## 5.6 Current Research Focus

Currently, there is a concerted effort within the AD and related dementia field to both identify and validate novel biomarkers to aid physicians in both diagnostic and prognostic aspects of dementia[41, 59, 256, 257]. While AD has established biologically

relevant proteins that have been determined to be associated with neuroimaging hallmarks (MRI and PET), VCID is still lacking fluid biomarkers[41, 169, 257]. The NINDS and NIA have recognized the need for novel biomarkers for VCID and created MarkVCID, a consortium of centers who are seeking to identify and cross-validate imaging and fluid biomarkers for VCID[258]. While this consortium is just beginning to pay dividends after the lengthy patient accrual and protocol development processes, their work will help to expedite the process of biomarker discovery to clinical usage.

While neuroimaging has been the standard in-vivo neuropathological evaluation tool in clinic, there is a growing need for a more easily accessible and minimally invasive screening tool to determine which patients are at an increased risk of developing dementia[59]. This is vital to the ultimate goal of developing treatments for dementia as they are likely to be most beneficial during pre-clinical and pre-dementia stages. Therefore, identifying patients who are likely to progress to symptomatic stages of the disease process is a necessary component of clinical trials. Currently, trials for AD use PET imaging and/or CSF protein biomarkers to evaluate patients for inclusion/exclusion criteria[41]. However, these screening tools are costly, often inaccessible to more rural populations, and invasive to patients. Plasma biomarkers fill this niche of a widely available, minimally invasive, and cost-efficient screening tool for inclusion in clinical trials as well as a tool which can be translated for clinical usage to inform patients of their risk of developing dementia in the future[40, 59]. While the AD field is beginning to transition to plasma biomarker usage with the FDA approved PrecivityAD test, VCID and other ADRDs are in need of a plasma biomarker to help in its diagnosis[169]. These

projects contribute to this growing body of work in the dementia field in demonstrating the utility of plasma biomarkers for in-vivo assessment of AD and VCID.

## REFERENCES

1. Association, A.P., *Neurocognitive Disorders*, in *Diagnostic and statistical manual of mental disorders (5th ed.)*. 2013.
2. Elahi, F.M. and B.L. Miller, *A clinicopathological approach to the diagnosis of dementia*. *Nat Rev Neurol*, 2017. **13**(8): p. 457-476.
3. Wilson, R.S., et al., *The natural history of cognitive decline in Alzheimer's disease*. *Psychol Aging*, 2012. **27**(4): p. 1008-17.
4. Sperling, R.A., et al., *Toward defining the preclinical stages of Alzheimer's disease: recommendations from the National Institute on Aging-Alzheimer's Association workgroups on diagnostic guidelines for Alzheimer's disease*. *Alzheimers Dement*, 2011. **7**(3): p. 280-92.
5. Bondi, M.W., E.C. Edmonds, and D.P. Salmon, *Alzheimer's Disease: Past, Present, and Future*. *J Int Neuropsychol Soc*, 2017. **23**(9-10): p. 818-831.
6. Dubois, B., et al., *Preclinical Alzheimer's disease: Definition, natural history, and diagnostic criteria*. *Alzheimers Dement*, 2016. **12**(3): p. 292-323.
7. Kapasi, A., C. DeCarli, and J.A. Schneider, *Impact of multiple pathologies on the threshold for clinically overt dementia*. *Acta Neuropathol*, 2017. **134**(2): p. 171-186.
8. Schneider, J.A., et al., *Mixed brain pathologies account for most dementia cases in community-dwelling older persons*. *Neurology*, 2007. **69**(24): p. 2197-204.
9. *2021 Alzheimer's disease facts and figures*. *Alzheimers Dement*, 2021. **17**(3): p. 327-406.
10. Brenowitz, W.D., et al., *Mixed neuropathologies and estimated rates of clinical progression in a large autopsy sample*. *Alzheimers Dement*, 2017. **13**(6): p. 654-662.
11. Kawas, C.H., et al., *Multiple pathologies are common and related to dementia in the oldest-old: The 90+ Study*. *Neurology*, 2015. **85**(6): p. 535-42.
12. Cortes-Canteli, M. and C. Iadecola, *Alzheimer's Disease and Vascular Aging: JACC Focus Seminar*. *J Am Coll Cardiol*, 2020. **75**(8): p. 942-951.
13. Drachman, D.A., *The amyloid hypothesis, time to move on: Amyloid is the downstream result, not cause, of Alzheimer's disease*. *Alzheimers Dement*, 2014. **10**(3): p. 372-80.
14. Hyman, B.T., et al., *National Institute on Aging-Alzheimer's Association guidelines for the neuropathologic assessment of Alzheimer's disease*. *Alzheimers Dement*, 2012. **8**(1): p. 1-13.
15. Dickson, D.W., *The pathogenesis of senile plaques*. *J Neuropathol Exp Neurol*, 1997. **56**(4): p. 321-39.
16. Gravina, S.A., et al., *Amyloid beta protein (A beta) in Alzheimer's disease brain. Biochemical and immunocytochemical analysis with antibodies specific for forms ending at A beta 40 or A beta 42(43)*. *J Biol Chem*, 1995. **270**(13): p. 7013-6.

17. Iwatsubo, T., et al., *Visualization of A beta 42(43) and A beta 40 in senile plaques with end-specific A beta monoclonals: evidence that an initially deposited species is A beta 42(43)*. *Neuron*, 1994. **13**(1): p. 45-53.
18. Borchelt, D.R., et al., *Familial Alzheimer's disease-linked presenilin 1 variants elevate Abeta1-42/1-40 ratio in vitro and in vivo*. *Neuron*, 1996. **17**(5): p. 1005-13.
19. Cai, X.D., T.E. Golde, and S.G. Younkin, *Release of excess amyloid beta protein from a mutant amyloid beta protein precursor*. *Science*, 1993. **259**(5094): p. 514-6.
20. Citron, M., et al., *Mutation of the beta-amyloid precursor protein in familial Alzheimer's disease increases beta-protein production*. *Nature*, 1992. **360**(6405): p. 672-4.
21. Scheuner, D., et al., *Secreted amyloid beta-protein similar to that in the senile plaques of Alzheimer's disease is increased in vivo by the presenilin 1 and 2 and APP mutations linked to familial Alzheimer's disease*. *Nat Med*, 1996. **2**(8): p. 864-70.
22. Suzuki, N., et al., *An increased percentage of long amyloid beta protein secreted by familial amyloid beta protein precursor (beta APP717) mutants*. *Science*, 1994. **264**(5163): p. 1336-40.
23. Thal, D.R., et al., *Phases of A beta-deposition in the human brain and its relevance for the development of AD*. *Neurology*, 2002. **58**(12): p. 1791-800.
24. Golde, T.E., *Alzheimer's disease - the journey of a healthy brain into organ failure*. *Mol Neurodegener*, 2022. **17**(1): p. 18.
25. Castellani, R.J., G. Plascencia-Villa, and G. Perry, *The amyloid cascade and Alzheimer's disease therapeutics: theory versus observation*. *Lab Invest*, 2019. **99**(7): p. 958-970.
26. Bancher, C., et al., *Accumulation of abnormally phosphorylated tau precedes the formation of neurofibrillary tangles in Alzheimer's disease*. *Brain Res*, 1989. **477**(1-2): p. 90-9.
27. Grundke-Iqbal, I., et al., *Abnormal phosphorylation of the microtubule-associated protein tau (tau) in Alzheimer cytoskeletal pathology*. *Proc Natl Acad Sci U S A*, 1986. **83**(13): p. 4913-7.
28. Iqbal, K., et al., *Mechanism of neurofibrillary degeneration and pharmacologic therapeutic approach*. *J Neural Transm Suppl*, 2000. **59**: p. 213-22.
29. Braak, E., H. Braak, and E.M. Mandelkow, *A sequence of cytoskeleton changes related to the formation of neurofibrillary tangles and neuropil threads*. *Acta Neuropathol*, 1994. **87**(6): p. 554-67.
30. Bennett, D.A., et al., *Neurofibrillary tangles mediate the association of amyloid load with clinical Alzheimer disease and level of cognitive function*. *Arch Neurol*, 2004. **61**(3): p. 378-84.
31. Braak, H. and E. Braak, *Neuropathological staging of Alzheimer-related changes*. *Acta Neuropathol*, 1991. **82**(4): p. 239-59.

32. Braak, H., et al., *Staging of Alzheimer disease-associated neurofibrillary pathology using paraffin sections and immunocytochemistry*. Acta Neuropathol, 2006. **112**(4): p. 389-404.
33. Congdon, E.E. and E.M. Sigurdsson, *Tau-targeting therapies for Alzheimer disease*. Nat Rev Neurol, 2018. **14**(7): p. 399-415.
34. Masliah, E., et al., *Re-evaluation of the structural organization of neuritic plaques in Alzheimer's disease*. J Neuropathol Exp Neurol, 1993. **52**(6): p. 619-32.
35. Terry, R.D., et al., *Physical basis of cognitive alterations in Alzheimer's disease: synapse loss is the major correlate of cognitive impairment*. Ann Neurol, 1991. **30**(4): p. 572-80.
36. DeKosky, S.T. and S.W. Scheff, *Synapse loss in frontal cortex biopsies in Alzheimer's disease: correlation with cognitive severity*. Ann Neurol, 1990. **27**(5): p. 457-64.
37. Mirra, S.S., et al., *The Consortium to Establish a Registry for Alzheimer's Disease (CERAD). Part II. Standardization of the neuropathologic assessment of Alzheimer's disease*. Neurology, 1991. **41**(4): p. 479-86.
38. Jack, C.R., Jr., et al., *NIA-AA Research Framework: Toward a biological definition of Alzheimer's disease*. Alzheimers Dement, 2018. **14**(4): p. 535-562.
39. Masters, C.L., et al., *Alzheimer's disease*. Nat Rev Dis Primers, 2015. **1**: p. 15056.
40. Winder, Z., D. Wilcock, and G.A. Jicha, *Diagnostic and Prognostic Laboratory Testing for Alzheimer Disease*. Clin Lab Med, 2020. **40**(3): p. 289-303.
41. Jack, C.R., Jr., et al., *A/T/N: An unbiased descriptive classification scheme for Alzheimer disease biomarkers*. Neurology, 2016. **87**(5): p. 539-47.
42. Dickerson, B.C., et al., *The cortical signature of Alzheimer's disease: regionally specific cortical thinning relates to symptom severity in very mild to mild AD dementia and is detectable in asymptomatic amyloid-positive individuals*. Cereb Cortex, 2009. **19**(3): p. 497-510.
43. Fox, N.C., et al., *Imaging of onset and progression of Alzheimer's disease with voxel-compression mapping of serial magnetic resonance images*. Lancet, 2001. **358**(9277): p. 201-5.
44. Besson, F.L., et al., *Cognitive and Brain Profiles Associated with Current Neuroimaging Biomarkers of Preclinical Alzheimer's Disease*. J Neurosci, 2015. **35**(29): p. 10402-11.
45. Fotuhi, M., D. Do, and C. Jack, *Modifiable factors that alter the size of the hippocampus with ageing*. Nat Rev Neurol, 2012. **8**(4): p. 189-202.
46. Jack, C.R., Jr., et al., *An operational approach to National Institute on Aging-Alzheimer's Association criteria for preclinical Alzheimer disease*. Ann Neurol, 2012. **71**(6): p. 765-75.
47. Klunk, W.E., et al., *Imaging brain amyloid in Alzheimer's disease with Pittsburgh Compound-B*. Ann Neurol, 2004. **55**(3): p. 306-19.
48. Rowe, C.C., et al., *Predicting Alzheimer disease with beta-amyloid imaging: results from the Australian imaging, biomarkers, and lifestyle study of ageing*. Ann Neurol, 2013. **74**(6): p. 905-13.

49. Clark, C.M., et al., *Cerebral PET with florbetapir compared with neuropathology at autopsy for detection of neuritic amyloid-beta plaques: a prospective cohort study*. *Lancet Neurol*, 2012. **11**(8): p. 669-78.
50. Curtis, C., et al., *Phase 3 trial of flutemetamol labeled with radioactive fluorine 18 imaging and neuritic plaque density*. *JAMA Neurol*, 2015. **72**(3): p. 287-94.
51. Sabri, O., et al., *Beta-amyloid imaging with florbetaben*. *Clin Transl Imaging*, 2015. **3**(1): p. 13-26.
52. Villemagne, V.L., et al., *Tau imaging: early progress and future directions*. *Lancet Neurol*, 2015. **14**(1): p. 114-24.
53. Cho, H., et al., *In vivo cortical spreading pattern of tau and amyloid in the Alzheimer disease spectrum*. *Ann Neurol*, 2016. **80**(2): p. 247-58.
54. Schwarz, A.J., et al., *Regional profiles of the candidate tau PET ligand 18F-AV-1451 recapitulate key features of Braak histopathological stages*. *Brain*, 2016. **139**(Pt 5): p. 1539-50.
55. Scholl, M., et al., *PET Imaging of Tau Deposition in the Aging Human Brain*. *Neuron*, 2016. **89**(5): p. 971-982.
56. Johnson, K.A., et al., *Tau positron emission tomographic imaging in aging and early Alzheimer disease*. *Ann Neurol*, 2016. **79**(1): p. 110-9.
57. Minoshima, S., et al., *Metabolic reduction in the posterior cingulate cortex in very early Alzheimer's disease*. *Ann Neurol*, 1997. **42**(1): p. 85-94.
58. Landau, S.M., et al., *Associations between cognitive, functional, and FDG-PET measures of decline in AD and MCI*. *Neurobiol Aging*, 2011. **32**(7): p. 1207-18.
59. Blennow, K. and H. Zetterberg, *Biomarkers for Alzheimer's disease: current status and prospects for the future*. *J Intern Med*, 2018. **284**(6): p. 643-663.
60. *Plasma A $\beta$  Test Wins Approval—Are p-Tau Tests Far Behind?* 2020; Available from: <https://www.alzforum.org/news/research-news/plasma-av-test-wins-approval-are-p-tau-tests-far-behind>.
61. Lewczuk, P., et al., *Cerebrospinal fluid and blood biomarkers for neurodegenerative dementias: An update of the Consensus of the Task Force on Biological Markers in Psychiatry of the World Federation of Societies of Biological Psychiatry*. *World J Biol Psychiatry*, 2018. **19**(4): p. 244-328.
62. Lashley, T., et al., *Molecular biomarkers of Alzheimer's disease: progress and prospects*. *Dis Model Mech*, 2018. **11**(5).
63. Alexopoulos, P., et al., *Mapping CSF biomarker profiles onto NIA-AA guidelines for Alzheimer's disease*. *Eur Arch Psychiatry Clin Neurosci*, 2016. **266**(7): p. 587-97.
64. Janelidze, S., et al., *CSF Abeta42/Abeta40 and Abeta42/Abeta38 ratios: better diagnostic markers of Alzheimer disease*. *Ann Clin Transl Neurol*, 2016. **3**(3): p. 154-65.
65. O'Brien, R.J. and P.C. Wong, *Amyloid precursor protein processing and Alzheimer's disease*. *Annu Rev Neurosci*, 2011. **34**: p. 185-204.
66. Van Nostrand, W.E., et al., *Pathogenic effects of cerebral amyloid angiopathy mutations in the amyloid beta-protein precursor*. *Ann N Y Acad Sci*, 2002. **977**: p. 258-65.



67. Greenberg, S.M., et al., *Cerebral amyloid angiopathy and Alzheimer disease - one peptide, two pathways*. Nat Rev Neurol, 2020. **16**(1): p. 30-42.
68. Motter, R., et al., *Reduction of beta-amyloid peptide42 in the cerebrospinal fluid of patients with Alzheimer's disease*. Ann Neurol, 1995. **38**(4): p. 643-8.
69. Olsson, B., et al., *CSF and blood biomarkers for the diagnosis of Alzheimer's disease: a systematic review and meta-analysis*. Lancet Neurol, 2016. **15**(7): p. 673-684.
70. Strozyk, D., et al., *CSF Abeta 42 levels correlate with amyloid-neuropathology in a population-based autopsy study*. Neurology, 2003. **60**(4): p. 652-6.
71. Tapiola, T., et al., *Cerebrospinal fluid {beta}-amyloid 42 and tau proteins as biomarkers of Alzheimer-type pathologic changes in the brain*. Arch Neurol, 2009. **66**(3): p. 382-9.
72. Vogelgsang, J., et al., *Multiplex immunoassay measurement of amyloid-beta42 to amyloid-beta40 ratio in plasma discriminates between dementia due to Alzheimer's disease and dementia not due to Alzheimer's disease*. Exp Brain Res, 2018. **236**(5): p. 1241-1250.
73. Kim, H.J., et al., *Elevation of the Plasma Abeta40/Abeta42 Ratio as a Diagnostic Marker of Sporadic Early-Onset Alzheimer's Disease*. J Alzheimers Dis, 2015. **48**(4): p. 1043-50.
74. Shahpasand-Kroner, H., et al., *A two-step immunoassay for the simultaneous assessment of Abeta38, Abeta40 and Abeta42 in human blood plasma supports the Abeta42/Abeta40 ratio as a promising biomarker candidate of Alzheimer's disease*. Alzheimers Res Ther, 2018. **10**(1): p. 121.
75. Verberk, I.M.W., et al., *Plasma Amyloid as Prescreener for the Earliest Alzheimer Pathological Changes*. Ann Neurol, 2018. **84**(5): p. 648-658.
76. Avila, J., et al., *Role of tau protein in both physiological and pathological conditions*. Physiol Rev, 2004. **84**(2): p. 361-84.
77. Lindwall, G. and R.D. Cole, *Phosphorylation affects the ability of tau protein to promote microtubule assembly*. J Biol Chem, 1984. **259**(8): p. 5301-5.
78. Selden, S.C. and T.D. Pollard, *Phosphorylation of microtubule-associated proteins regulates their interaction with actin filaments*. J Biol Chem, 1983. **258**(11): p. 7064-71.
79. Blennow, K., et al., *Tau protein in cerebrospinal fluid: a biochemical marker for axonal degeneration in Alzheimer disease?* Mol Chem Neuropathol, 1995. **26**(3): p. 231-45.
80. Blennow, K. and H. Hampel, *CSF markers for incipient Alzheimer's disease*. Lancet Neurol, 2003. **2**(10): p. 605-13.
81. Vanmechelen, E., et al., *Quantification of tau phosphorylated at threonine 181 in human cerebrospinal fluid: a sandwich ELISA with a synthetic phosphopeptide for standardization*. Neurosci Lett, 2000. **285**(1): p. 49-52.
82. Tatebe, H., et al., *Quantification of plasma phosphorylated tau to use as a biomarker for brain Alzheimer pathology: pilot case-control studies including patients with Alzheimer's disease and down syndrome*. Mol Neurodegener, 2017. **12**(1): p. 63.

83. Lewczuk, P., et al., *Plasma neurofilament light as a potential biomarker of neurodegeneration in Alzheimer's disease*. *Alzheimers Res Ther*, 2018. **10**(1): p. 71.
84. Mattsson, N., et al., *Association of Plasma Neurofilament Light With Neurodegeneration in Patients With Alzheimer Disease*. *JAMA Neurol*, 2017. **74**(5): p. 557-566.
85. Sanchez-Valle, R., et al., *Serum neurofilament light levels correlate with severity measures and neurodegeneration markers in autosomal dominant Alzheimer's disease*. *Alzheimers Res Ther*, 2018. **10**(1): p. 113.
86. Zhou, W., et al., *Plasma neurofilament light chain levels in Alzheimer's disease*. *Neurosci Lett*, 2017. **650**: p. 60-64.
87. Preische, O., et al., *Serum neurofilament dynamics predicts neurodegeneration and clinical progression in presymptomatic Alzheimer's disease*. *Nat Med*, 2019. **25**(2): p. 277-283.
88. Rohrer, J.D., et al., *Serum neurofilament light chain protein is a measure of disease intensity in frontotemporal dementia*. *Neurology*, 2016. **87**(13): p. 1329-36.
89. Rojas, J.C., et al., *Plasma neurofilament light chain predicts progression in progressive supranuclear palsy*. *Ann Clin Transl Neurol*, 2016. **3**(3): p. 216-25.
90. Brun, A., X. Liu, and C. Erikson, *Synapse loss and gliosis in the molecular layer of the cerebral cortex in Alzheimer's disease and in frontal lobe degeneration*. *Neurodegeneration*, 1995. **4**(2): p. 171-7.
91. Serrano-Pozo, A., et al., *Neuropathological alterations in Alzheimer disease*. *Cold Spring Harb Perspect Med*, 2011. **1**(1): p. a006189.
92. Glass, C.K., et al., *Mechanisms underlying inflammation in neurodegeneration*. *Cell*, 2010. **140**(6): p. 918-34.
93. Torres-Acosta, N., et al., *Therapeutic Potential of TNF-alpha Inhibition for Alzheimer's Disease Prevention*. *J Alzheimers Dis*, 2020. **78**(2): p. 619-626.
94. Clark, I.A. and B. Vissel, *Broader Insights into Understanding Tumor Necrosis Factor and Neurodegenerative Disease Pathogenesis Infer New Therapeutic Approaches*. *J Alzheimers Dis*, 2021. **79**(3): p. 931-948.
95. Decourt, B., D.K. Lahiri, and M.N. Sabbagh, *Targeting Tumor Necrosis Factor Alpha for Alzheimer's Disease*. *Curr Alzheimer Res*, 2017. **14**(4): p. 412-425.
96. Swardfager, W., et al., *A meta-analysis of cytokines in Alzheimer's disease*. *Biol Psychiatry*, 2010. **68**(10): p. 930-41.
97. Ramos, E.M., et al., *Tumor necrosis factor alpha and interleukin 10 promoter region polymorphisms and risk of late-onset Alzheimer disease*. *Arch Neurol*, 2006. **63**(8): p. 1165-9.
98. Lio, D., et al., *Tumor necrosis factor-alpha -308A/G polymorphism is associated with age at onset of Alzheimer's disease*. *Mech Ageing Dev*, 2006. **127**(6): p. 567-71.
99. Pekny, M. and M. Nilsson, *Astrocyte activation and reactive gliosis*. *Glia*, 2005. **50**(4): p. 427-34.

100. Wharton, S.B., et al., *Population variation in glial fibrillary acidic protein levels in brain ageing: relationship to Alzheimer-type pathology and dementia*. Dement Geriatr Cogn Disord, 2009. **27**(5): p. 465-73.
101. Benedet, A.L., et al., *Differences Between Plasma and Cerebrospinal Fluid Glial Fibrillary Acidic Protein Levels Across the Alzheimer Disease Continuum*. JAMA Neurol, 2021. **78**(12): p. 1471-1483.
102. Cicognola, C., et al., *Plasma glial fibrillary acidic protein detects Alzheimer pathology and predicts future conversion to Alzheimer dementia in patients with mild cognitive impairment*. Alzheimers Res Ther, 2021. **13**(1): p. 68.
103. Chatterjee, P., et al., *Plasma glial fibrillary acidic protein is elevated in cognitively normal older adults at risk of Alzheimer's disease*. Transl Psychiatry, 2021. **11**(1): p. 27.
104. Oeckl, P., et al., *Glial Fibrillary Acidic Protein in Serum is Increased in Alzheimer's Disease and Correlates with Cognitive Impairment*. J Alzheimers Dis, 2019. **67**(2): p. 481-488.
105. Asken, B.M., et al., *Plasma Glial Fibrillary Acidic Protein Levels Differ Along the Spectra of Amyloid Burden and Clinical Disease Stage*. J Alzheimers Dis, 2020. **78**(1): p. 265-276.
106. Pereira, J.B., et al., *Plasma GFAP is an early marker of amyloid-beta but not tau pathology in Alzheimer's disease*. Brain, 2021. **144**(11): p. 3505-3516.
107. Verberk, I.M.W., et al., *Combination of plasma amyloid beta(1-42/1-40) and glial fibrillary acidic protein strongly associates with cerebral amyloid pathology*. Alzheimers Res Ther, 2020. **12**(1): p. 118.
108. Akiyama, H., et al., *Inflammation and Alzheimer's disease*. Neurobiol Aging, 2000. **21**(3): p. 383-421.
109. Asselineau, D., et al., *Interleukin-10 Production in Response to Amyloid-beta Differs between Slow and Fast Decliners in Patients with Alzheimer's Disease*. J Alzheimers Dis, 2015. **46**(4): p. 837-42.
110. Di Bona, D., et al., *Association between interleukin-10 polymorphisms and Alzheimer's disease: a systematic review and meta-analysis*. J Alzheimers Dis, 2012. **29**(4): p. 751-9.
111. Vargas-Alarcon, G., et al., *Association of interleukin-10 polymorphisms with risk factors of Alzheimer's disease and other dementias (SADEM study)*. Immunol Lett, 2016. **177**: p. 47-52.
112. Gangishetti, U., et al., *Non-beta-amyloid/tau cerebrospinal fluid markers inform staging and progression in Alzheimer's disease*. Alzheimers Res Ther, 2018. **10**(1): p. 98.
113. Tarkowski, E., et al., *Increased intrathecal levels of the angiogenic factors VEGF and TGF-beta in Alzheimer's disease and vascular dementia*. Neurobiol Aging, 2002. **23**(2): p. 237-43.
114. Tubi, M.A., et al., *Regional relationships between CSF VEGF levels and Alzheimer's disease brain biomarkers and cognition*. Neurobiol Aging, 2021. **105**: p. 241-251.

115. Hohman, T.J., et al., *The role of vascular endothelial growth factor in neurodegeneration and cognitive decline: exploring interactions with biomarkers of Alzheimer disease*. JAMA Neurol, 2015. **72**(5): p. 520-9.
116. Otrrock, Z.K., J.A. Makarem, and A.I. Shamseddine, *Vascular endothelial growth factor family of ligands and receptors: review*. Blood Cells Mol Dis, 2007. **38**(3): p. 258-68.
117. Mahoney, E.R., et al., *Brain expression of the vascular endothelial growth factor gene family in cognitive aging and alzheimer's disease*. Mol Psychiatry, 2021. **26**(3): p. 888-896.
118. Jack, C.R., Jr., et al., *Introduction to the recommendations from the National Institute on Aging-Alzheimer's Association workgroups on diagnostic guidelines for Alzheimer's disease*. Alzheimers Dement, 2011. **7**(3): p. 257-62.
119. Brookmeyer, R. and N. Abdalla, *Estimation of lifetime risks of Alzheimer's disease dementia using biomarkers for preclinical disease*. Alzheimers Dement, 2018. **14**(8): p. 981-988.
120. Dubois, B., et al., *Clinical diagnosis of Alzheimer's disease: recommendations of the International Working Group*. Lancet Neurol, 2021. **20**(6): p. 484-496.
121. Albert, M.S., et al., *The diagnosis of mild cognitive impairment due to Alzheimer's disease: recommendations from the National Institute on Aging-Alzheimer's Association workgroups on diagnostic guidelines for Alzheimer's disease*. Alzheimers Dement, 2011. **7**(3): p. 270-9.
122. McKhann, G.M., et al., *The diagnosis of dementia due to Alzheimer's disease: recommendations from the National Institute on Aging-Alzheimer's Association workgroups on diagnostic guidelines for Alzheimer's disease*. Alzheimers Dement, 2011. **7**(3): p. 263-9.
123. Dichgans, M. and D. Leys, *Vascular Cognitive Impairment*. Circ Res, 2017. **120**(3): p. 573-591.
124. van der Flier, W.M., et al., *Vascular cognitive impairment*. Nat Rev Dis Primers, 2018. **4**: p. 18003.
125. Gorelick, P.B., et al., *Vascular contributions to cognitive impairment and dementia: a statement for healthcare professionals from the american heart association/american stroke association*. Stroke, 2011. **42**(9): p. 2672-713.
126. Hachinski, V., et al., *National Institute of Neurological Disorders and Stroke-Canadian Stroke Network vascular cognitive impairment harmonization standards*. Stroke, 2006. **37**(9): p. 2220-41.
127. Skrobot, O.A., et al., *Progress toward standardized diagnosis of vascular cognitive impairment: Guidelines from the Vascular Impairment of Cognition Classification Consensus Study*. Alzheimers Dement, 2018. **14**(3): p. 280-292.
128. Iadecola, C., et al., *Vascular Cognitive Impairment and Dementia: JACC Scientific Expert Panel*. J Am Coll Cardiol, 2019. **73**(25): p. 3326-3344.
129. Looi, J.C. and P.S. Sachdev, *Differentiation of vascular dementia from AD on neuropsychological tests*. Neurology, 1999. **53**(4): p. 670-8.
130. Canning, S.J., et al., *Diagnostic utility of abbreviated fluency measures in Alzheimer disease and vascular dementia*. Neurology, 2004. **62**(4): p. 556-62.

131. Kalaria, R.N., *The pathology and pathophysiology of vascular dementia*. Neuropharmacology, 2018. **134**(Pt B): p. 226-239.
132. Cannistraro, R.J., et al., *CNS small vessel disease: A clinical review*. Neurology, 2019. **92**(24): p. 1146-1156.
133. Sachdev, P., et al., *Diagnostic criteria for vascular cognitive disorders: a VASCOG statement*. Alzheimer Dis Assoc Disord, 2014. **28**(3): p. 206-18.
134. Pantoni, L., *Cerebral small vessel disease: from pathogenesis and clinical characteristics to therapeutic challenges*. Lancet Neurol, 2010. **9**(7): p. 689-701.
135. Skrobot, O.A., et al., *Vascular cognitive impairment neuropathology guidelines (VCING): the contribution of cerebrovascular pathology to cognitive impairment*. Brain, 2016. **139**(11): p. 2957-2969.
136. Deramecourt, V., et al., *Staging and natural history of cerebrovascular pathology in dementia*. Neurology, 2012. **78**(14): p. 1043-50.
137. Blevins, B.L., et al., *Brain arteriolosclerosis*. Acta Neuropathol, 2021. **141**(1): p. 1-24.
138. Iadecola, C., *The pathobiology of vascular dementia*. Neuron, 2013. **80**(4): p. 844-66.
139. Brown, W.R. and C.R. Thore, *Review: cerebral microvascular pathology in ageing and neurodegeneration*. Neuropathol Appl Neurobiol, 2011. **37**(1): p. 56-74.
140. Arvanitakis, Z., et al., *Relation of cerebral vessel disease to Alzheimer's disease dementia and cognitive function in elderly people: a cross-sectional study*. Lancet Neurol, 2016. **15**(9): p. 934-943.
141. Arvanitakis, Z., et al., *The Relationship of Cerebral Vessel Pathology to Brain Microinfarcts*. Brain Pathol, 2017. **27**(1): p. 77-85.
142. Smith, E.E., et al., *Cerebral microinfarcts: the invisible lesions*. Lancet Neurol, 2012. **11**(3): p. 272-82.
143. Soontornniyomkij, V., et al., *Cerebral microinfarcts associated with severe cerebral beta-amyloid angiopathy*. Brain Pathol, 2010. **20**(2): p. 459-67.
144. Haglund, M., et al., *Cerebral amyloid angiopathy and cortical microinfarcts as putative substrates of vascular dementia*. Int J Geriatr Psychiatry, 2006. **21**(7): p. 681-7.
145. De Reuck, J., et al., *The impact of cerebral amyloid angiopathy on the occurrence of cerebrovascular lesions in demented patients with Alzheimer features: a neuropathological study*. Eur J Neurol, 2011. **18**(6): p. 913-8.
146. Okamoto, Y., et al., *Cortical microinfarcts in Alzheimer's disease and subcortical vascular dementia*. Neuroreport, 2009. **20**(11): p. 990-6.
147. White, L., et al., *Cerebrovascular pathology and dementia in autopsied Honolulu-Asia Aging Study participants*. Ann N Y Acad Sci, 2002. **977**: p. 9-23.
148. Kovari, E., et al., *Cortical microinfarcts and demyelination significantly affect cognition in brain aging*. Stroke, 2004. **35**(2): p. 410-4.
149. del Ser, T., et al., *Vascular dementia. A clinicopathological study*. J Neurol Sci, 1990. **96**(1): p. 1-17.
150. Sonnen, J.A., et al., *Pathological correlates of dementia in a longitudinal, population-based sample of aging*. Ann Neurol, 2007. **62**(4): p. 406-13.

151. Arvanitakis, Z., et al., *Microinfarct pathology, dementia, and cognitive systems*. Stroke, 2011. **42**(3): p. 722-7.
152. Schneider, J.A., et al., *Subcortical infarcts, Alzheimer's disease pathology, and memory function in older persons*. Ann Neurol, 2007. **62**(1): p. 59-66.
153. Troncoso, J.C., et al., *Effect of infarcts on dementia in the Baltimore longitudinal study of aging*. Ann Neurol, 2008. **64**(2): p. 168-76.
154. Westover, M.B., et al., *Estimating cerebral microinfarct burden from autopsy samples*. Neurology, 2013. **80**(15): p. 1365-9.
155. Wardlaw, J.M., et al., *Neuroimaging standards for research into small vessel disease and its contribution to ageing and neurodegeneration*. Lancet Neurol, 2013. **12**(8): p. 822-38.
156. Gouw, A.A., et al., *Heterogeneity of small vessel disease: a systematic review of MRI and histopathology correlations*. J Neurol Neurosurg Psychiatry, 2011. **82**(2): p. 126-35.
157. Fazekas, F., et al., *Histopathologic analysis of foci of signal loss on gradient-echo T2\*-weighted MR images in patients with spontaneous intracerebral hemorrhage: evidence of microangiopathy-related microbleeds*. AJNR Am J Neuroradiol, 1999. **20**(4): p. 637-42.
158. Shoamanesh, A., C.S. Kwok, and O. Benavente, *Cerebral microbleeds: histopathological correlation of neuroimaging*. Cerebrovasc Dis, 2011. **32**(6): p. 528-34.
159. Alber, J., et al., *White matter hyperintensities in vascular contributions to cognitive impairment and dementia (VCID): Knowledge gaps and opportunities*. Alzheimers Dement (N Y), 2019. **5**: p. 107-117.
160. Marshall, V.G., et al., *Deep white matter infarction: correlation of MR imaging and histopathologic findings*. Radiology, 1988. **167**(2): p. 517-22.
161. Simpson, J.E., et al., *White matter lesions in an unselected cohort of the elderly: astrocytic, microglial and oligodendrocyte precursor cell responses*. Neuropathol Appl Neurobiol, 2007. **33**(4): p. 410-9.
162. Young, V.G., G.M. Halliday, and J.J. Kril, *Neuropathologic correlates of white matter hyperintensities*. Neurology, 2008. **71**(11): p. 804-11.
163. Schmidt, R., et al., *Heterogeneity in age-related white matter changes*. Acta Neuropathol, 2011. **122**(2): p. 171-85.
164. Fernando, M.S., et al., *White matter lesions in an unselected cohort of the elderly: molecular pathology suggests origin from chronic hypoperfusion injury*. Stroke, 2006. **37**(6): p. 1391-8.
165. Debette, S. and H.S. Markus, *The clinical importance of white matter hyperintensities on brain magnetic resonance imaging: systematic review and meta-analysis*. BMJ, 2010. **341**: p. c3666.
166. Hu, H.Y., et al., *White matter hyperintensities and risks of cognitive impairment and dementia: A systematic review and meta-analysis of 36 prospective studies*. Neurosci Biobehav Rev, 2021. **120**: p. 16-27.

167. Lee, S., et al., *White matter hyperintensities are a core feature of Alzheimer's disease: Evidence from the dominantly inherited Alzheimer network*. *Ann Neurol*, 2016. **79**(6): p. 929-39.
168. Marnane, M., et al., *Periventricular hyperintensities are associated with elevated cerebral amyloid*. *Neurology*, 2016. **86**(6): p. 535-43.
169. Cipollini, V., F. Troili, and F. Giubilei, *Emerging Biomarkers in Vascular Cognitive Impairment and Dementia: From Pathophysiological Pathways to Clinical Application*. *Int J Mol Sci*, 2019. **20**(11).
170. Wardlaw, J.M., C. Smith, and M. Dichgans, *Small vessel disease: mechanisms and clinical implications*. *Lancet Neurol*, 2019. **18**(7): p. 684-696.
171. Poggesi, A., et al., *Circulating biologic markers of endothelial dysfunction in cerebral small vessel disease: A review*. *J Cereb Blood Flow Metab*, 2016. **36**(1): p. 72-94.
172. Forsythe, J.A., et al., *Activation of vascular endothelial growth factor gene transcription by hypoxia-inducible factor 1*. *Mol Cell Biol*, 1996. **16**(9): p. 4604-13.
173. Carmeliet, P. and R.K. Jain, *Molecular mechanisms and clinical applications of angiogenesis*. *Nature*, 2011. **473**(7347): p. 298-307.
174. Dewerchin, M. and P. Carmeliet, *PlGF: a multitasking cytokine with disease-restricted activity*. *Cold Spring Harb Perspect Med*, 2012. **2**(8).
175. Chau, K., A. Hennessy, and A. Makris, *Placental growth factor and pre-eclampsia*. *J Hum Hypertens*, 2017. **31**(12): p. 782-786.
176. Ren, Z., et al., *Placental growth factor reverses decreased vascular and uteroplacental MMP-2 and MMP-9 and increased MMP-1 and MMP-7 and collagen types I and IV in hypertensive pregnancy*. *Am J Physiol Heart Circ Physiol*, 2018. **315**(1): p. H33-H47.
177. Sudduth, T.L., et al., *Induction of hyperhomocysteinemia models vascular dementia by induction of cerebral microhemorrhages and neuroinflammation*. *J Cereb Blood Flow Metab*, 2013. **33**(5): p. 708-15.
178. Nagai, K., et al., *Relationship between interleukin-6 and cerebral deep white matter and periventricular hyperintensity in elderly women*. *Geriatr Gerontol Int*, 2011. **11**(3): p. 328-32.
179. West, P.K., et al., *Microglia responses to interleukin-6 and type I interferons in neuroinflammatory disease*. *Glia*, 2019. **67**(10): p. 1821-1841.
180. Ribeiro Xavier, A.L., et al., *A Distinct Population of Microglia Supports Adult Neurogenesis in the Subventricular Zone*. *J Neurosci*, 2015. **35**(34): p. 11848-61.
181. Hilal, S., et al., *C-Reactive Protein, Plasma Amyloid-beta Levels, and Their Interaction With Magnetic Resonance Imaging Markers*. *Stroke*, 2018. **49**(11): p. 2692-2698.
182. Wada-Isoe, K., et al., *Elevated interleukin-6 levels in cerebrospinal fluid of vascular dementia patients*. *Acta Neurol Scand*, 2004. **110**(2): p. 124-7.
183. Zuliani, G., et al., *High interleukin-6 plasma levels are associated with functional impairment in older patients with vascular dementia*. *Int J Geriatr Psychiatry*, 2007. **22**(4): p. 305-11.

184. Kim, Y.S., K.J. Lee, and H. Kim, *Serum tumour necrosis factor-alpha and interleukin-6 levels in Alzheimer's disease and mild cognitive impairment*. Psychogeriatrics, 2017. **17**(4): p. 224-230.
185. Rissin, D.M., et al., *Single-molecule enzyme-linked immunosorbent assay detects serum proteins at subfemtomolar concentrations*. Nat Biotechnol, 2010. **28**(6): p. 595-9.
186. Wilson, D.H., et al., *The Simoa HD-1 Analyzer: A Novel Fully Automated Digital Immunoassay Analyzer with Single-Molecule Sensitivity and Multiplexing*. J Lab Autom, 2016. **21**(4): p. 533-47.
187. Murphy, M.P., R.A. Corriveau, and D.M. Wilcock, *Vascular contributions to cognitive impairment and dementia (VCID)*. Biochim Biophys Acta, 2016. **1862**(5): p. 857-9.
188. Rizzi, L., I. Rosset, and M. Roriz-Cruz, *Global epidemiology of dementia: Alzheimer's and vascular types*. Biomed Res Int, 2014. **2014**: p. 908915.
189. Corriveau, R.A., et al., *The Science of Vascular Contributions to Cognitive Impairment and Dementia (VCID): A Framework for Advancing Research Priorities in the Cerebrovascular Biology of Cognitive Decline*. Cell Mol Neurobiol, 2016. **36**(2): p. 281-8.
190. Harrison, S.L., et al., *A Systematic Review of the Definitions of Vascular Cognitive Impairment, No Dementia in Cohort Studies*. Dement Geriatr Cogn Disord, 2016. **42**(1-2): p. 69-79.
191. Kapasi, A. and J.A. Schneider, *Vascular contributions to cognitive impairment, clinical Alzheimer's disease, and dementia in older persons*. Biochim Biophys Acta, 2016. **1862**(5): p. 878-86.
192. Abner, E.L., et al., *Outcomes after diagnosis of mild cognitive impairment in a large autopsy series*. Ann Neurol, 2017. **81**(4): p. 549-559.
193. Dodge, H.H., et al., *Risk of incident clinical diagnosis of Alzheimer's disease-type dementia attributable to pathology-confirmed vascular disease*. Alzheimers Dement, 2017. **13**(6): p. 613-623.
194. Winblad, B., et al., *Mild cognitive impairment--beyond controversies, towards a consensus: report of the International Working Group on Mild Cognitive Impairment*. J Intern Med, 2004. **256**(3): p. 240-6.
195. Petersen, R.C., et al., *Mild cognitive impairment: clinical characterization and outcome*. Arch Neurol, 1999. **56**(3): p. 303-8.
196. Mahoney, E.R., et al., *Brain expression of the vascular endothelial growth factor gene family in cognitive aging and alzheimer's disease*. Mol Psychiatry, 2019.
197. Xu, R. and D.C. Wunsch, 2nd, *Clustering algorithms in biomedical research: a review*. IEEE Rev Biomed Eng, 2010. **3**: p. 120-54.
198. Damian, M., et al., *Single-domain amnesic mild cognitive impairment identified by cluster analysis predicts Alzheimer's disease in the european prospective DESCRIPA study*. Dement Geriatr Cogn Disord, 2013. **36**(1-2): p. 1-19.
199. Racine, A.M., et al., *Biomarker clusters are differentially associated with longitudinal cognitive decline in late midlife*. Brain, 2016. **139**(Pt 8): p. 2261-74.



200. Wallin, A.K., et al., *CSF biomarkers predict a more malignant outcome in Alzheimer disease*. *Neurology*, 2010. **74**(19): p. 1531-7.
201. Nettiksimmons, J., et al., *Biological heterogeneity in ADNI amnesic mild cognitive impairment*. *Alzheimers Dement*, 2014. **10**(5): p. 511-521 e1.
202. Grubbs, F.E., *Sample Criteria for Testing Outlying Observations*. *Ann. Math. Statist.*, 1950. **21**(1): p. 27-58.
203. Fred, A. and A.K. Jain. *Data Clustering Using Evidence Accumulation*. in *Internat. Conf. Pattern Recognition*. 2002.
204. Maaten, L., *Visualizing data using t-SNE*. *Journal of machine learning research : JMLR*, 2008. **9**(Nov): p. 2579.
205. McComb, C., *Adjusted Rand Index*. 2015: MATLAB Central File Exchange.
206. Snyder, H.M., et al., *Vascular contributions to cognitive impairment and dementia including Alzheimer's disease*. *Alzheimers Dement*, 2015. **11**(6): p. 710-7.
207. Hanseeuw, B.J., et al., *Association of Amyloid and Tau With Cognition in Preclinical Alzheimer Disease: A Longitudinal Study*. *JAMA Neurol*, 2019. **76**(8): p. 915-924.
208. Barro, C. and H. Zetterberg, *The blood biomarkers puzzle - A review of protein biomarkers in neurodegenerative diseases*. *J Neurosci Methods*, 2021. **361**: p. 109281.
209. Nagy, Z., et al., *Assessment of the pathological stages of Alzheimer's disease in thin paraffin sections: a comparative study*. *Dement Geriatr Cogn Disord*, 1998. **9**(3): p. 140-4.
210. McMahan, P.M., et al., *Cost-effectiveness of PET in the diagnosis of Alzheimer disease*. *Radiology*, 2003. **228**(2): p. 515-22.
211. Montine, T.J., et al., *National Institute on Aging-Alzheimer's Association guidelines for the neuropathologic assessment of Alzheimer's disease: a practical approach*. *Acta Neuropathol*, 2012. **123**(1): p. 1-11.
212. Zetterberg, H. and S.C. Burnham, *Blood-based molecular biomarkers for Alzheimer's disease*. *Mol Brain*, 2019. **12**(1): p. 26.
213. Mielke, M.M., et al., *Plasma phospho-tau181 increases with Alzheimer's disease clinical severity and is associated with tau- and amyloid-positron emission tomography*. *Alzheimers Dement*, 2018. **14**(8): p. 989-997.
214. Wilcock, D., et al., *MarkVCID cerebral small vessel consortium: I. Enrollment, clinical, fluid protocols*. *Alzheimers Dement*, 2021. **17**(4): p. 704-715.
215. Schmitt, F.A., et al., *University of Kentucky Sanders-Brown healthy brain aging volunteers: donor characteristics, procedures and neuropathology*. *Curr Alzheimer Res*, 2012. **9**(6): p. 724-33.
216. Benjamini, Y. and Y. Hochberg, *Controlling the False Discovery Rate: A Practical and Powerful Approach to Multiple Testing*. *Journal of the Royal Statistical Society: Series B (Methodological)*, 1995. **57**(1): p. 289-300.
217. Ahtiluoto, S., et al., *Diabetes, Alzheimer disease, and vascular dementia: a population-based neuropathologic study*. *Neurology*, 2010. **75**(13): p. 1195-202.

218. Iadecola, C., et al., *Impact of Hypertension on Cognitive Function: A Scientific Statement From the American Heart Association*. Hypertension, 2016. **68**(6): p. e67-e94.
219. Argaw, A.T., et al., *IL-1beta regulates blood-brain barrier permeability via reactivation of the hypoxia-angiogenesis program*. J Immunol, 2006. **177**(8): p. 5574-84.
220. Ng, A., et al., *IL-1beta, IL-6, TNF- alpha and CRP in Elderly Patients with Depression or Alzheimer's disease: Systematic Review and Meta-Analysis*. Sci Rep, 2018. **8**(1): p. 12050.
221. Patterson, C., *The state of the art of dementia research: new frontiers*, in *World Alzheimer report 2018*. 2018: Alzheimer's Disease International.
222. Schwarzingler, M. and C. Dufouil, *Forecasting the prevalence of dementia*. Lancet Public Health, 2022. **7**(2): p. e94-e95.
223. Jack, C.R., Jr., et al., *Tracking pathophysiological processes in Alzheimer's disease: an updated hypothetical model of dynamic biomarkers*. Lancet Neurol, 2013. **12**(2): p. 207-16.
224. Weintraub, S., et al., *Version 3 of the Alzheimer Disease Centers' Neuropsychological Test Battery in the Uniform Data Set (UDS)*. Alzheimer Dis Assoc Disord, 2018. **32**(1): p. 10-17.
225. Weintraub, S., et al., *The Alzheimer's Disease Centers' Uniform Data Set (UDS): the neuropsychologic test battery*. Alzheimer Dis Assoc Disord, 2009. **23**(2): p. 91-101.
226. Tatsumi, I.F. and M. Watanabe, *Verbal Memory*, in *Encyclopedia of Neuroscience*, M.D. Binder, N. Hirokawa, and U. Windhorst, Editors. 2009, Springer Berlin Heidelberg: Berlin, Heidelberg. p. 4176-4178.
227. Sutin, A.R., Y. Stephan, and A. Terracciano, *Verbal fluency and risk of dementia*. Int J Geriatr Psychiatry, 2019. **34**(6): p. 863-867.
228. Shao, Z., et al., *What do verbal fluency tasks measure? Predictors of verbal fluency performance in older adults*. Front Psychol, 2014. **5**: p. 772.
229. Henry, J.D., J.R. Crawford, and L.H. Phillips, *Verbal fluency performance in dementia of the Alzheimer's type: a meta-analysis*. Neuropsychologia, 2004. **42**(9): p. 1212-22.
230. Gallucci, M., et al., *Neuropsychological tools to predict conversion from amnesic mild cognitive impairment to dementia. The TREDEM Registry*. Neuropsychol Dev Cogn B Aging Neuropsychol Cogn, 2018. **25**(4): p. 550-560.
231. Lu, M., et al., *Blood rheology biomarkers in sickle cell disease*. Exp Biol Med (Maywood), 2020. **245**(2): p. 155-165.
232. Kamtchum-Tatuene, J. and G.C. Jickling, *Blood Biomarkers for Stroke Diagnosis and Management*. Neuromolecular Med, 2019. **21**(4): p. 344-368.
233. Salamanna, F., et al., *Blood factors as biomarkers in osteoporosis: points from the COVID-19 era*. Trends Endocrinol Metab, 2021. **32**(9): p. 672-679.
234. Jacquemont, L., J.P. Souillou, and N. Degauque, *Blood biomarkers of kidney transplant rejection, an endless search?* Expert Rev Mol Diagn, 2017. **17**(7): p. 687-697.

235. Wallin, A., et al., *Biochemical markers in vascular cognitive impairment associated with subcortical small vessel disease - A consensus report*. BMC Neurol, 2017. **17**(1): p. 102.
236. Shirk, S.D., et al., *A web-based normative calculator for the uniform data set (UDS) neuropsychological test battery*. Alzheimers Res Ther, 2011. **3**(6): p. 32.
237. Monsell, S.E., et al., *Results From the NACC Uniform Data Set Neuropsychological Battery Crosswalk Study*. Alzheimer Dis Assoc Disord, 2016. **30**(2): p. 134-9.
238. Giannoni, P., et al., *Cerebrovascular pathology during the progression of experimental Alzheimer's disease*. Neurobiol Dis, 2016. **88**: p. 107-17.
239. Pekny, M., et al., *Astrocyte activation and reactive gliosis-A new target in stroke?* Neurosci Lett, 2019. **689**: p. 45-55.
240. Simpson, J.E., et al., *Astrocyte phenotype in relation to Alzheimer-type pathology in the ageing brain*. Neurobiol Aging, 2010. **31**(4): p. 578-90.
241. Rasley, A., et al., *Murine glia express the immunosuppressive cytokine, interleukin-10, following exposure to Borrelia burgdorferi or Neisseria meningitidis*. Glia, 2006. **53**(6): p. 583-92.
242. Burmeister, A.R. and I. Marriott, *The Interleukin-10 Family of Cytokines and Their Role in the CNS*. Front Cell Neurosci, 2018. **12**: p. 458.
243. Zhang, J.B., et al., *Association of serum vascular endothelial growth factor levels and cerebral microbleeds in patients with Alzheimer's disease*. Eur J Neurol, 2016. **23**(8): p. 1337-42.
244. Galimberti, D., et al., *Intrathecal chemokine synthesis in mild cognitive impairment and Alzheimer disease*. Arch Neurol, 2006. **63**(4): p. 538-43.
245. Qin, B., et al., *Interleukin-8 gene polymorphism -251T>A contributes to Alzheimer's disease susceptibility*. Medicine (Baltimore), 2016. **95**(39): p. e5039.
246. Franciosi, S., et al., *IL-8 enhancement of amyloid-beta (Abeta 1-42)-induced expression and production of pro-inflammatory cytokines and COX-2 in cultured human microglia*. J Neuroimmunol, 2005. **159**(1-2): p. 66-74.
247. Morin-Brureau, M., et al., *Epileptiform activity induces vascular remodeling and zonula occludens 1 downregulation in organotypic hippocampal cultures: role of VEGF signaling pathways*. J Neurosci, 2011. **31**(29): p. 10677-88.
248. Gu, Y., et al., *Caveolin-1 regulates nitric oxide-mediated matrix metalloproteinases activity and blood-brain barrier permeability in focal cerebral ischemia and reperfusion injury*. J Neurochem, 2012. **120**(1): p. 147-56.
249. Stevens, S.L., et al., *Blood pressure variability and cardiovascular disease: systematic review and meta-analysis*. BMJ, 2016. **354**: p. i4098.
250. Pannee, J., et al., *Reference measurement procedure for CSF amyloid beta (Abeta)1-42 and the CSF Abeta1-42 /Abeta1-40 ratio - a cross-validation study against amyloid PET*. J Neurochem, 2016. **139**(4): p. 651-658.
251. Brickman, A.M., et al., *Plasma p-tau181, p-tau217, and other blood-based Alzheimer's disease biomarkers in a multi-ethnic, community study*. Alzheimers Dement, 2021. **17**(8): p. 1353-1364.

252. Noz, M.P., et al., *Pro-inflammatory Monocyte Phenotype During Acute Progression of Cerebral Small Vessel Disease*. *Front Cardiovasc Med*, 2021. **8**: p. 639361.
253. Besser, L., et al., *Version 3 of the National Alzheimer's Coordinating Center's Uniform Data Set*. *Alzheimer Dis Assoc Disord*, 2018. **32**(4): p. 351-358.
254. Guillot-Sestier, M.V., et al., *Il10 deficiency rebalances innate immunity to mitigate Alzheimer-like pathology*. *Neuron*, 2015. **85**(3): p. 534-48.
255. Chakrabarty, P., et al., *IL-10 alters immunoproteostasis in APP mice, increasing plaque burden and worsening cognitive behavior*. *Neuron*, 2015. **85**(3): p. 519-33.
256. Scheltens, P., et al., *Alzheimer's disease*. *Lancet*, 2021. **397**(10284): p. 1577-1590.
257. Rosenberg, G.A., *Binswanger's disease: biomarkers in the inflammatory form of vascular cognitive impairment and dementia*. *J Neurochem*, 2018. **144**(5): p. 634-643.
258. Gladman, J.T., et al., *Vascular contributions to cognitive impairment and dementia: Research consortia that focus on etiology and treatable targets to lessen the burden of dementia worldwide*. *Alzheimers Dement (N Y)*, 2019. **5**: p. 789-796.

## VITA

### Zachary S. Winder

Doctoral Candidate  
Department of Physiology  
Sanders-Brown Center on Aging  
University of Kentucky College of Medicine

### Educational Institutions

University of Florida, Gainesville, FL  
Bachelor of Science: Chemistry  
Specialization: Biochemistry May 2015  
Bachelor of Science: Finance May 2015

### Professional Positions

- UK MD-PhD Program Admissions Committee, Chair, August 2021 – August 2022
- UK MD-PhD Program Admissions Committee, Member, August 2020 – Present
- Kentucky Hillel, Treasurer, May 2019 – May 2020
- Society for Neuroscience, Member, April 2019 – Present
- UK Physiology/Neuroscience Grant Writing Workshop, Member, January 2019 – May 2019
- UK MD-PhD Program Retreat Committee, Member, December 2018 – June 2019
- Student Interest Group in Neurology, Treasurer, August 2017 – May 2018
- American Medical Association, Member, August 2016 – Present

### Scholastic and Professional Honors

- NIH F30 Ruth L. Kirschstein Individual Predoctoral NRSA for MD/PhD Fellowship (F30 NS118777-01A1), May 2021 – Present
- NIH T32 Fellowship Program “Training in Translational Research in Alzheimer’s and Related Dementias” (T32 AG057461), August 2020 – May 2021
- University of Kentucky College of Medicine Fellowship for Excellence in Graduate Research, August 2019 – August 2020
- University of Kentucky College of Medicine Professional Student Mentored Research Fellowship, May 2017 – May 2018
- University of Kentucky Physiology Retreat Graduate Student Honorable Mention Poster Award, October 2021
- University of Kentucky Physiology & Neuroscience Grant Writing Workshop Getchell Award for Outstanding Trainees, April 2021
- Markesbery Symposium Predoctoral Student Poster Award Winner, November 2020

- Alzheimer's Association International Conference PIA Day Vascular Cognitive Disorders 3MT Competition Winner, August 2020
- BrightFocus Alzheimer's Fast Track Mock Grant Proposal Winner, October 2019

#### Professional Publications

Colin Sumners, Amy Alleyne, Vermalí Rodríguez, David J. Pioquinto, Jacob A. Ludin, Shormista Kar, **Zachary Winder**, Yuma Ortiz, Meng Liu, Eric G. Krause and Annette D. de Kloet. *Brain angiotensin type-1 and type-2 receptors: cellular locations under normal and hypertensive conditions*. Hypertension Research. 2020 Apr;43(4):281-295. doi: 10.1038/s41440-019-0374-8. Epub 2019 Dec 18. PMID: 31853042; PMCID: PMC7538702.

**Winder, Zachary**, Sudduth, Tiffany L, Fardo, David, Cheng, Qiang, Goldstein, Larry B, Nelson, Peter T, Schmitt, Frederick A, Jicha, Gregory, Wilcock, Donna M. *Hierarchical Clustering Analyses of Plasma Proteins in Subjects with Cardiovascular Risk Factors Identifies Informative Subsets Based on Differential Expression of Angiogenic and Inflammatory Biomarkers*. Frontiers in Neuroscience. 2020 Feb 6;14:84. doi: 10.3389/fnins.2020.00084. PMID: 32116527; PMCID: PMC7016016.

**Winder Z**, Wilcock D, Jicha GA. *Diagnostic and Prognostic Laboratory Testing for Alzheimer Disease*. Clin Lab Med. 2020 Sep;40(3):289-303. doi: 10.1016/j.cll.2020.05.003. PMID: 32718500.

Bahrani AA, Smith CD, Barber JM, Al-Janabi OM, Powell DK, Andersen AH, Ramey BD, Abner EL, Goldstein LB, **Winder Z**, Gold BT, Van Eldik L, Wilcock DM, Jicha GA. *Development of a protocol to assess within-subject, regional white matter hyperintensity changes in aging and dementia*. J Neurosci Methods. 2021 Aug 1;360:109270. doi: 10.1016/j.jneumeth.2021.109270. Epub 2021 Jun 24. PMID: 34171312; PMCID: PMC8513808.

Kloske CM, Dugan AJ, Weekman EM, **Winder Z**, Patel E, Nelson PT, Fardo DW, Wilcock DM. *Inflammatory Pathways Are Impaired in Alzheimer Disease and Differentially Associated With Apolipoprotein E Status*. J Neuropathol Exp Neurol. 2021 Oct 26;80(10):922-932. doi: 10.1093/jnen/nlab085. PMID: 34486652; PMCID: PMC8557334.

**Winder Z**, Sudduth TL, Anderson S, Patel E, Neltner J, Martin BJ, Snyder KE, Abner EL, Jicha GA, Nelson PT, Wilcock DM. Examining the association between blood-based biomarkers and human postmortem neuropathology in the University of Kentucky Alzheimer's Disease Research Center autopsy cohort. Alzheimers Dement. 2022 Mar 10. doi: 10.1002/alz.12639. Epub ahead of print. PMID: 35266629.

Zachary S. Winder